Doctoral Thesis

Photoresponsive self-assembly/disassembly of thermoresponsive macromolecules in azobenzene functionalized ionic liquids

(アゾベンゼン含有イオン液体中における高分子の温度および光応答性自己集合)

Graduate School of Engineering
Yokohama National University
(国立大学法人　横浜国立大学大学院　工学府)

Caihong Wang
(彩虹　王)

September 2017

Photoresponsive self-assembly/disassembly of thermoresponsive macromolecules in azobenzene functionalized ionic liquids

A Dissertation Submitted to Yokohama National University for the Partial Fulfillment of the Requirements for the Degree of Doctor of Engineering

Submitted by

Wang Caihong

14SA592

September 2017

Department of Materials Science and Engineering

Yokohama National University

Yokohama, Japan

Content

Acknowledgement 1
Synopsis 3

Chart 1 General introduction

1.1 Ionic liquids 7
1.1.1 Introduction of ionic liquids 7
1.1.2 Functional ionic liquids 8
1.2 Polymers and ionic liquids.....9
1.3 Thermoresponsive polymers in ionic liquids.....11
1.4 Sol-gel transitions 12
1.5 References.....23

Chart 2 Preparation of azobenzene ionic liquids

and their physical properties.

2.1 Azobenzene functionalized ionic liquid 20
2.1.1 Synthesis of azobenzene ionic liquid.....20
2.1.2 Synthesis of azobenzene ionic liquids with various anions.....22
2.1.3 Synthesis of $[C_1mim][NTf_2]$ 23
2.2 Physical properties of ionic liquid 23
2.2.1 ^{1}H-NMR spectra for ionic liquids.....24
2.2.2 Melting points of each azobenzene ionic liquid 24
2.2.3 Photoisomerization of azobenzene ionic liquid.....26
2.3 Conclusions.....29
2.4 References.....30

Chart 3 Phase transition behaviors for LCST homopolymers

3.1 Materials and experiments.....32
3.1.1 Materials 33
3.1.2 Polymerization of LCST polymers.....33
3.1.3 Sample preparation for transmittance measurements.....35

3.1.4 UV source 35
3.2 Photoresponsive LCST behaviors in ionic liquids 36
3.2.1 Thermoresponsive LCST behaviors 36
3.2.2 Photoswitchable LCST behaviors.....38
3.3 Mechanism of LCST behaviors 40
3.3.1 LCST behaviors by modifying polymer structures 41
3.3.2 LCST behaviors by modifying ionic liquid structures 42
3.3.3. Mechanism of photoresponsive LCST behaviors.....47
3.4 Conclusions.....51
3.5 References.....52

Chart 4 Photo/thermoresponsive micellizations and gelations of the PMP solution

4.1 Synthesis of PMP polymer.....56
4.1.1 Materials 56
4.1.2 Polymerization of PMP.....56
4.2 Photo/thermoresponsive micellization behaviors.....58
4.2.1 Experiments 58
4.2.2 Thermoresponsive micellization behaviors 60
4.2.3 Photoinduced micellization behaviors.....64
4.3 Photo/thermoresponsive sol-gel transitions.....65
4.3.1 Experiments 65
4.3.2 Thermoresponsive sol-gel transitions.....66
4.3.3 Photoinduced sol-gel transitions.....70
4.4 Small-angle X-ray scattering experiments 71
4.4.1 Experiments 71
4.4.2 Results of SAXS measurements 71
4.5 Conclusions.....73
4.6 References.....74

Chart 5 Photo/thermoresponsive micellizations and gelations of the BMB solution

5.1 Synthesis of BMB triblock copolymers.....79
5.2 Photo/thermoresponsive micellization behaviors.....80
5.2.1 Thermoresponsive micellization behaviors 80
5.2.2 Photoresponsive micellization behaviors 82

5.3 Thermoresponsive gelation of BMB polymer 82
5.3.1 Experiments 82
5.3.2 Thermoresponsive sol-gel transitions 83
5.3.3 Photoresponsive gelation behaviors 84
5.4 Small-angle X-ray scattering experiments 85
5.5 Conclusions 86
5.6 References 87

Chart 6 Concluding remarks and future directions

6 Concluding remarks and future directions 89
Publish list 91

Acknowledgement

I would like to express my sincere thanks to all the people who helped me wherever I needed, encouraged me if I was depressed, and taught me within patience. The doctor course itself is a tough work but people in "Watanabe lab" make it sweet and colorful to me.

I clearly remember my first presentation here, I was so nervous that I could not catch the questions asked in English nor answer questions correctly in English. But by now, practicing in seminars and conferences gives me confidence to present my research work in English.

My deepest gratitude is to my supervisor, **Professor Masayoshi Watanabe**, Department of Chemistry and Biotechnology, Yokohama National University, Japan, for his immense knowledge, continuous encouragement, invaluable guidance and infinite support. No words can convey his influence on me, but I believe it is profound and lasting. Although three years for being there is too short, the things learned from him would definitely impact my future life. Honestly speaking, it is my first time to be so close to someone who is so genius, smart and seems to know everything well. He gives me a perfect and vivid image of being professional, which deserves my whole life to fulfill. The most important thing which I have learned in Japan, is not about research, but about being professional.

I would like to acknowledge members of my thesis committee, **Professor Masayoshi Watanabe, Professor Yasushi Yokoyama, Professor Toshiyuki Oyama, Associate Professor Takashi Ubukata and Associate Professor Kazuhide Ueno**, for their constructive and insightful comments on my doctor thesis as well as my research. Their advice on my final defense inspired me a lot, particularly for NMR part. I would always remember the hot discussion in my final defense. Your attitude towards science or research does give me a good example.

I would like to express my sincere gratitude to **Dr. Hisashi Kokubo**, **Dr. Kei Hashimoto, Dr. Shiguo Zhang, Dr. Yuzo Kitazawa, and Ms. Yumi Kobayashi** for their help during my research. Without their help, I could not graduate smoothly on time. Particularly, due to Dr. Kokubo's efficient management of the big lab, I can work efficiently and smoothly. Dr. Hashimoto gave me a lot of help in guiding my

paper writing, I would like to give him a huge hug before I leave japan. Dr. Yuzo and Miss. Yumi were always so kind that they taught me how to use various measuring machines, conduct polymerizations and analysis data. I appreciate their valuable help.

I am also deeply thankful to **Dr. Morgan L. Thomas, Dr. Jiaheng Zhang, Dr. Zhe Li, Dr. Miao Xu, Dr. XiaoFeng Ma, Dr. Yutaro Kamei** and **other group members**, for their kind cooperation to assist me during my research and life. Also, I am indebted to the secretaries, three beautiful ladies, for their warm words. I would also give my respect and thanks to **Dr. Ryota Tamate**. Although he joined the lab just four month ago, his hardworking and brightness impressed me a lot.

I would like to express my thanks to **Prof. Takashi Nakanishi** and **Dr. Fengniu Lu** from National Institute for Materials Science for their kind help in SAXS measurements. I would miss the time in NIMS, which is such an advanced research institute.

I would give my deepest love and gratitude to my dear parents for their unreserved loving and considerate care. Though I have been an adult for over 10 years, I am always a naughty child to them.

I appreciate Yokohama National University for providing me with a chance to pursue my doctor course here. I was so lucky to join such a high-level research group with excellent research training. Meanwhile, I also appreciate the China Scholarship Council for financial support, to allow me to experience oversea life and study for 36 months.

Synopsis

Room temperature ionic liquids (ILs) have been attracting increasing interest from various research fields, due to their infinite combinations of attractive physical properties, with feasibly designable chemical structures. These unique properties, such as high chemical and thermal stability, lower volatility and flammability, and desired ionic conductivity, make ILs valuable for use in emerging technologies. However, to process the ILs for these and other applications, it is essential to create more rigid composites, while retaining the desired attributes. A widely-applied method is to add well-designed ABA triblock copolymers into conventional ILs, producing ion gels or ionogels. Generally, A end blocks are immiscible with the IL, consequently self-assembling into micellar cores, while the well-solvated B midblocks serve as bridges among the micelles, resulting in a percolating network. In particular, thermoresponsive sol-gel transitions, enabled by introducing thermoresponsive polymers as A end blocks, have drawn intense attention as affordable materials of interest in 3D printing, patterning, etc. One unique advantage of the thermoresponsive sol-gel transitions is its ability to process materials from the molecular precursor to the product. Prof. Lodge and his coworkers have reported well-designed ABA triblock copolymers and thermoresponsive poly(N-isopropylacrylamide) (NIPAm) as the A end blocks, with poly(ethylene oxide) as the B midblocks, which form gels at low temperature, while being free-flowing liquids above the gelation temperature (T_{gel}). With a further modification of A end blocks by introducing random copolymers comprised of 4-phenylazophenyl methacrylate and NIPAm, photoinduced sol-gel transitions were obtained due to the photoresponsive self-assembly behavior of A end blocks in certain hydrophobic ILs. The photoresponsive sol-gel transitions enable contactless material processing, controlled by selected wavelengths and intensities. In such research, optimizing the azobenzene content is very important, since azobenzene can easily influence the thermoresponsive temperatures. However, the preparation of the azobenzene-functionalized ABA triblock copolymers with the desired content often involves a laborious process. Moreover, azobenzene located on the side chains can make *cis*-azobenzene isomer unstable because of the steric hindrance effect. These undesirable issues greatly constrain the development of photo/thermoresponsive materials. In order to solve these issues, we have proposed a simple method of constructing a photo/thermoresponsive system, based on an azobenzene-based ionic liquid, inspired by other stimuli located in the solution, such as pH or ionic strength. To the best of our knowledge, no research has been reported on the study of the

photoresponsive self-assembling behaviors of block copolymers in a photoswitchable IL.

In this work, by using an azobenzene containing IL, [Azo][NTf_2] ([Azo] = 1-butyl-3-(4-phenylazobenzyl)imidazolium) as a small molecular trigger, diluted by 1-methyl-3-methylimidazolium bis{(trifluoromethyl)sulfonyl}imide ([C_1mim][NTf_2]), poly(benzyl methacrylate) (PBnMA) and poly(2-phenylethyl methacrylate) (PPhEtMA) have been reported to show photoresponsive lower critical solution temperature (LCST) behavior for the first time in an IL mixture. In this IL mixture, the cloud temperature point (T_{cp}) of PBnMA is higher under UV than in the dark. However, the T_{cp} of PPhEtMA under UV is lower than that in the dark, even though only a tiny structural difference in alkyl chain (n=1, 2) exists between the ester and aromatic rings. Through temperature dependent ^{1}H-NMR, the opposite UV responsive chemical shifts of the acidic proton from [C_1mim]$^+$ were obtained, resembling the opposite UV responsive solvation interaction changes. It is assumed that the polarity change, induced by azobenzene isomerization, influences the affinities between polymers and IL mixtures, resulting in opposite chemical shifts for this proton from [C_1mim]+ cation towards UV, corresponding to opposite photoresponsive LCST behaviors.

Based on photoresponsive LCST behaviors switched by an azobenzene molecular trigger, two well-designed and prepared ABA triblock copolymers, poly(benzyl methacrylate)-b-poly(methyl methacrylate)-b-poly(benzyl methacrylate) (BMB) and poly(2-phenylethyl methacrylate)-b-poly(methyl methacrylate)-b-poly(2-phenylethyl methacrylate) (PMP), underwent a photo/thermoresponsive polymer architecture change in ionic liquid mixtures. Diluted BMB and PMP polymer solutions showed thermoresponsive micellization behaviors in the azobenzene-containing IL mixture, with different micellization temperatures being obtained in the dark and under UV. This range is defined as bi-stable temperature. Under UV, at the bi-stable temperature, the BMB solution underwent a "*micelle to unimer*" transition, while the PMP solution experienced a "*unimer to micelle*" transition. In more concentrated polymer solutions, thermoresponsive sol-gel transitions were observed, while different gelation temperatures were obtained under UV and in the dark. At this bi-stable temperature, the PMP solution underwent a UV-responsive "*sol-to-gel*" transition, while the BMB solution underwent a UV-responsive weaker gelation transition, ascribed to the opposite photoresponsive LCST behaviors.

To the best of our knowledge, it is the first time that a photoresponsive system, using the azobenzene ionic liquid as a molecular trigger to drive the self-assembly of

thermoresponsive polymers, has been studied. The photoresponsive sol-gel transitions thus achieved are advantageous for processing the polymer materials in a contactless manner. Moreover, the ionic liquid used as a solvent can be easily removed after the polymer materials have been processed into a product. This unique advantage of making materials soft or hard, based on photoresponsive molecular trigger, has potential for application as a novel industrial method to process polymeric materials using light. More importantly, compared with the conventional ways, by adding plasticizers or heating, which are neither environment-friendly, nor economical, using light as stimuli to process materials offers some unique advantages, such as being more environment-friendly, less toxic, with point-to-point operation.

Therefore, this study provides a novel way to develop photo/thermoresponsive "*unimer-micelle*" and "*sol-gel*" transitions through a photoresponsive IL, rather than azobenzene functionalized polymers. More generally, it may create a new path to make polymeric materials soft or hard based on a molecular switch, instead of a photochromic reaction of azobenzene polymers.

Chapter One

General introduction

1.1 Ionic liquids

1.1.1 Introduction of ionic liquids

In 1914, Walden reported the presence of a molten salt, ethylammonium nitrate, with a melting point below room temperature, as the first discovery of ionic liquids (ILs) [1]. However, not much attention was paid to the IL at that time. Pyridinium or imidazolium, used as cations, refreshed the interest to study ILs, for their unique properties, such as negligible vapor pressure, low-flammability, desired conductivity, and wide solubility for various materials [2–8]. These very useful properties of ILs have made them popular as a green solvent, which is recyclable, safer and environment-friendly, compared with the materials used currently, which are more volatile, flammable, and toxic organic [9–13].

In terms of IL structures, an organic cation with low flammability, and a weakly coordinating inorganic or organic anion, are combined together through intermolecular interactions to form ILs [14–15]. The common ionic liquid structures are demonstrated in **Figure 1**. Varying the cation and anion combinations produces numerous ILs. An increasing number of studies aim at understanding the relationship between the structure and its properties [16–21]. For example, the low melting point of ILs is due to the asymmetry between the cation and anion, which will lead to poor crystal structure among the ions [20–22]. In addition, a large cohesive energy density from molecular interactions may contribute to low vapor pressure of ILs [20–24]. Meanwhile, by clearing the dominant forces that impact their properties, we can design targeted ILs with desired functionality, to serve rich applications [25–28]. Properties of ILs originate from an infinite number of adjustable combinations

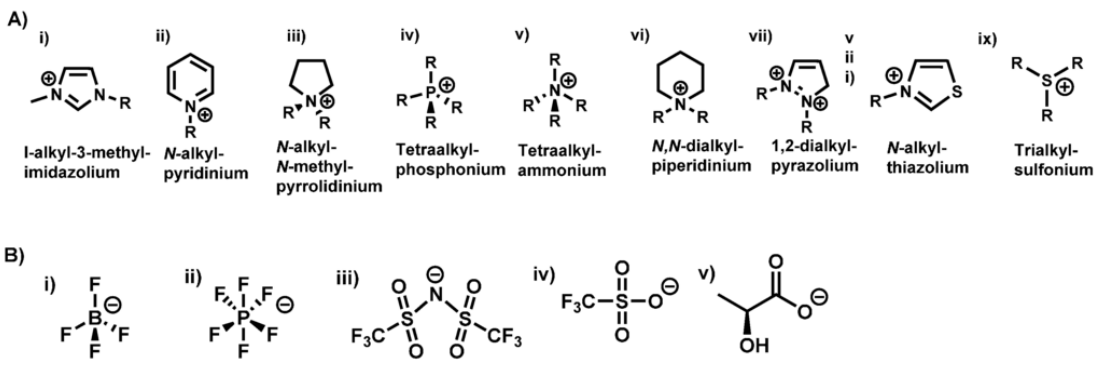

Figure 1. Various structures of cations (A) and anions (B) for ILs.

between cations and anions. For this reason, ILs are known as designer solvents. Carefully modifying the ionic liquid structure provides us a feasible and facile method to obtain an ionic liquid with targeted properties, called task-specific ILs [12,15, 25–28].

1.1.2 Functional ionic liquids

Through chemical functionalization or ion exchange in the ionic groups, some targeted functional groups can be easily incorporated into the IL structure to obtain the desired materials [25–27]. Altering anionic structures with functionalized groups is usually carried out by metal coordinating [16]. To modify the cationic structure, silica or other metal particles connected to the ionic liquid structure have been widely studied, which can be applied in catalytic reactions [27–29]. Meanwhile, imidazolium ILs have been used as solvent and stabilizer to produce metal nanoparticles [29]. In addition, some task-specific ILs have been designed and proven useful in both, synthetic and separation applications[30–31]. One task-specific IL has been reported to react with CO_2, to reversibly sequester the gas as a carbamate salt. Thus, the ionic liquid can be repeatedly recycled to capture CO_2, suitable for lower pressure and higher temperature, with an efficiency comparable to commercial amine[30].

Light, as an external stimulus, is preferred due to its contactless nature with point-to-point control. Azobenzene has always been incorporated as a photoresponsive group into ionic liquid structures to produce photoresponsive functional ionic liquids[32–35]. As shown in **Figure 2,** azobenzene-based ionic liquids can control the function of ion channels [32]. Very recently, azobenzene based ionic liquid crystals have become well-known for their ability to liquify under UV irradiation because

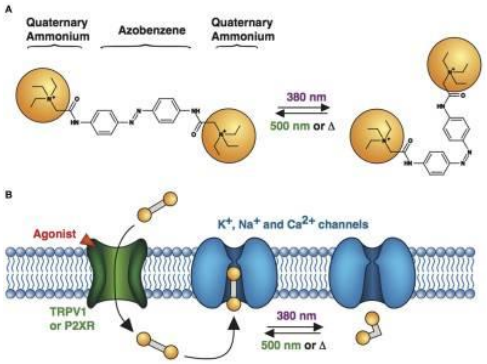

Figure 2. Photoswitchable blockers for voltage-gated K^+, Na^+, and Ca^{2+} channels of azobenzene-based ionic liquids [32].

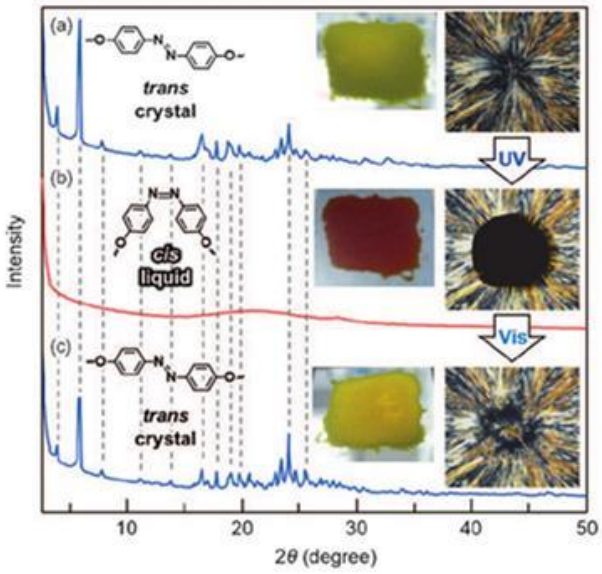

Figure 3. X-ray diffraction patterns obtained for azobenzene ionic liquid prepared on silicon wafer: a) as prepared film, b) after UV irradiation, and c) after Vis irradiation. A picture of each sample is shown as an inset. Optical microscopy images under crossed polarizers are shown on the right side (substrate, glass slide).[32]

the *cis*-isomers of azobenzene disrupt the ordering structure of rigid azobenzene packing [35]. Moreover, Prof. Kimizuka has reported the liquefication of crystalline azobenzene, rather than liquid crystal azobenzene. It appears that *cis*-azobenzene has a lower melting point compared with *trans*-azobenzene, as demonstrated in **Figure 3** [36]. Due to the photoinduced liquefication processes or volume changes, azobenzene compounds have been materials of interest in various fields, such as pattern, image memory, and bending actuator [32–36].

1.2 Polymers and ionic liquids

From the perspective of material science, combining ILs and polymers is promising for exploring novel smart materials with intrinsic properties of ionic liquids as well as polymers. In 1993, Prof. Watanabe published the first report about a polymer-based electrolyte, consisting of a chloroaluminate IL and a polymer, which showed high ionic conductivity [8]. Subsequently, common vinyl monomers were found to be compatible with some common ILs [5–6]. Regarding the desired compatibility between polymers and ILs, free radical polymerization, or living radical polymerization, such as atom transfer radical polymerization and reversible addition fragmentation transfer polymerization, has been conducted in ILs [39–51]. The polymers have a higher molecular weight within a narrower polydispersity,

compared with polymers occurring in conventional solvents. Moreover, good compatibility of certain polymers could be obtained with the ILs, irrespective of temperature and amount of polymer. In addition to the above-mentioned polymers, which are compatible with ILs, certain polymers in ILs experience phase transition behavior within a narrow temperature window, known as thermoresponsive polymers, which we will discuss in **Section 1.3**. However, some polymers are completely insoluble in ILs, regardless of temperature, such as poly(styrene).

As reported in the aqueous phase, introducing hydrophobic and hydrophilic polymers together can form some unique nano-order structures through the self-assembly of block copolymers in ionic liquids or other solvents, as demonstrated in **Figure 4** [52–61]. The insoluble part tends to aggregate to reduce the interface with IL, whereas the soluble part of the polymer is freely in contact with IL. Thus, the self-assembly behavior is motivated by intramolecular phase separation between polymers and ionic liquids. In a polymer solution, a macroscopically homogeneous structure is formed, to the scale of a few nanometers to several micrometers. Such nanostructures show various architectures and formed morphologies, including spherical micelles, cylindrical micelles, vesicles in diluted solutions and packed spheres, hexagonally packed cylinders, cubic phases and lamellae phases in higher concentrations, as shown in **Figure 4**. Moreover, adjusting the molecular weight of each block or ionic liquid mixture can also display various morphologies [62]. The composites thus formed consist of IL-rich and polymer-rich domains. The former retains the intrinsic functionalities of ILs and polymers, while the latter contributes mechanical strength to make it solidified or processable.

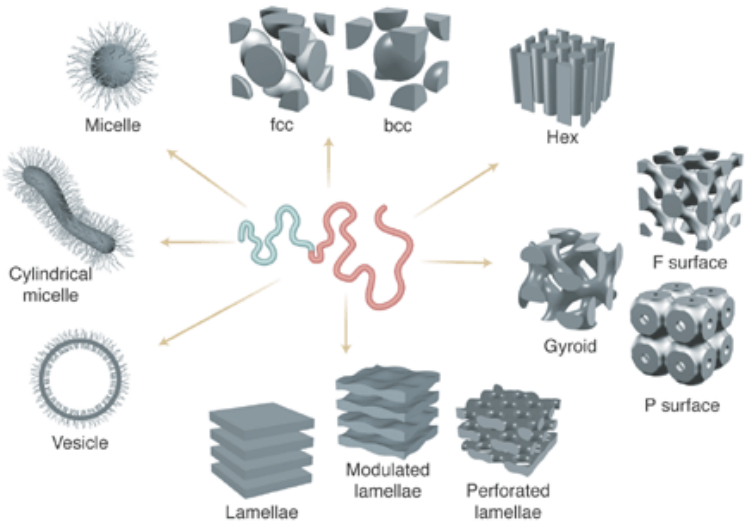

Figure 4. Self-organization structures of block copolymers [52]

In short, the compatibility of polymers with ILs is of interest in determining the ordering of nanostructure or polymeric architecture in ILs. Additionally, thermoresponsive segments are introduced into block copolymer solutions, with temperature as an external stimulus, to achieve the thermoresponsive self-assembling of block copolymers in ILs with changes in morphology.

1.3 Thermoresponsive polymers in ionic liquids

To investigate thermoresponsive polymers across a wide range of temperatures, thermally stable ILs are essential to obtain a better understanding of phase transition behavior. Lower critical solution temperature (LCST) phase behavior is one type of thermoresponsive behavior, which means that the polymer is soluble in ionic liquids at a lower temperature, while being insoluble at a higher temperature [63–71]. LCST type behavior is always observed in water phase [72–76]. However, it is not thermodynamically common in the IL field. Based on the Flory-Huggins lattice model, a positive value of the mixing entropy (S_{mix}) of the solution is assumed, as phase separation occurs. Thus, a more negative G_{mix} is obtained by increasing the temperature. In fact, such a simple model is not suitable to explain the LCST phase behavior. One of the most well-known polymers with LCST phase behavior is Poly(N-isopropylacrylamide) (PNIPAm) [77–78]. The unique advantage of PNIPAm is that its phase transition temperature is close to ambient temperature, which is favorable for real-life applications. Various PNIPAm containing polymers, such as

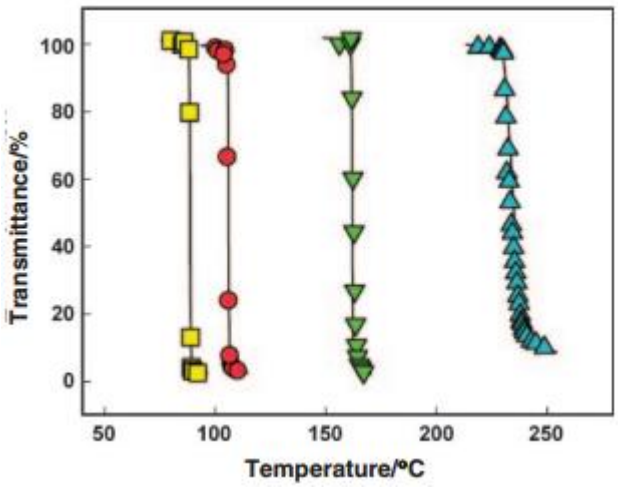

Figure 5. Temperature dependent transmittance for PBnMA polymer solutions in $[C_nmim][NTf_2]$, $[C_1mim][NTf_2]$(yellow), $[C_2mim][NTf_2]$ (red), $[C_4mim][NTf_2]$ (green), and $[C_6mim][NTf_2]$ (blue).[119]

random copolymers and block copolymers have been synthesized, gaining significant interest not only from a fundamental point of view, but also from an application perspective [79–100]. Most of the reported thermoresponsive PNIPAm gels work as a sensor for temperature, with potential application in drug-delivery, actuators, optical and sensing devices [80–100]. Apart from PNIPAm, other polymers such as polyether derivatives, cellulose derivatives, and betaine polymers have also been reported to exhibit LCST phase behavior in aqueous solutions [100–105]. The negative ΔS_{mix} for PNIPAm aqueous solutions corresponds to the formation of a cage-like structure surrounded by hydrogen bonding, while a negative ΔH_{mix} is affected by the hydrogen-bonding interactions among the amide groups with water. Based on this theory, along with increasing reports on the formation of π-cation interaction, structurally ordered aggregates in the mixtures of aromatic compounds and ILs, called "liquid clathrates", are thought to be the cause of the negative ΔS_{mix} [118]. We have assumed that IL solvents can form a structurally ordered solvation shell around the aromatic side chains. Meanwhile, a negative exothermic solvation (ΔH_{mix}) may be ascribed to the interaction between the ester group and IL, particularly anions, to maintain a local electron balance. One strong supporting evidence for the assumption is that, while modifying the PBnMA structure, a series of LCST homopolymers were obtained at different temperatures. This is supplementary evidence to support the strong influence of a nano environment around the aromatic side chain on the polymer phase behavior. As shown in **Figure 5,** the phase separation temperature of PBnMA can be easily influenced by a change in the chemical structure of the IL [119]. It can be seen that even such a small change can induce a significant change in the phase transition temperature. Moreover, 10 times lower entropy and enthalpy changes were observed in the IL phase than in PNIPAm in an aqueous solution, making the systems much more sensitive and smart.

1.4 Sol-gel transitions

To make a material soft or hard, it is essential to process the molecular-level materials to obtain a product. One direct way to soften materials is by heating over the melting points or glass transition temperatures of materials, which is cost- and resource-intensive. Adding various plasticizers is also widely used. However, they are toxic to human beings and other creatures, in addition to being hard to decompose. To solve these issues, a novel method to process materials using light has gradually evoked interest as a contactless method with low toxicity [120–121].

Moreover, the photoinduced liquification of polymer materials has evoked intense interest with respect to energy storage materials and 3D patterning [121].

Reported photoswitchable sol-gel transitions are mostly based on the change in ordering structure of azobenzene liquid crystals [32–35]. When the isomerization of azobenzene occurs in a liquid crystal phase, azobenzene, being a rigid part, could break the ordering structure, leading to an isotropic state, liquid phase. Very recently, Prof. Wu and his group reported the liquification of azobenzene polymers, through the isomerization of azobenzene, based on photoswitchable glass temperatures [121]. However, the isomerization of azobenzene also requires the solvent to assist in the isomerization. Moreover, it occurs only on the surface, due to the high concentration of azobenzene compounds. Therefore, it is urgent and important to explore a novel method to make materials soft or hard with a small amount of azobenzene, for the developing light processing industry.

In our lab, we have reported a photoinduced sol-gel transition, based on the solubility change of azobenzene-functionalized thermoresponsive polymers. Well-designed ABA triblock copolymers, with PNIPAm as A end blocks by introducing functionalized random copolymers comprising of 4-phenylazophenyl methacrylate and PNIPAm, and poly(ethylene oxide) as B midblock, form gels at low temperature, while being free-flowing liquids above the gelation temperature [122-123]. Moreover, different gelation temperatures were obtained in the dark and under UV, defined as bi-stable temperatures. Thus, at the bi-stable temperature, a photoinduced sol-gel transition was achieved due to the photoresponsive self-assembly behavior of A end blocks in certain hydrophobic ILs. The difference in polarities between *cis*-polymer and *trans*-polymer can be attributed to different compatibilities with ILs. *Cis*-polymers possess a higher affinity to the ILs. Meanwhile, photo-healing materials

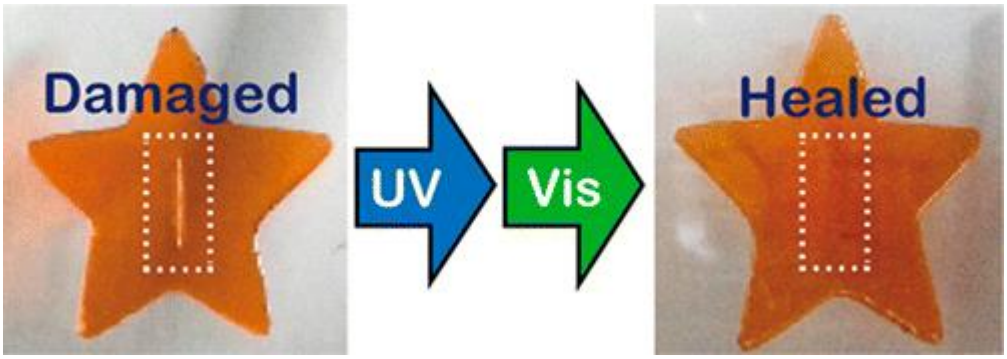

Figure 6. Photo-healing materials based on a ABA triblock copolymers in ionic liquids.[124]

are well-developed in using the photoinduced sol-gel transitions, as shown in **Figure 6** [124]. However, the preparation of these azobenzene functionalized ABA triblock copolymers with a desired content often involves a tedious process. Moreover, azobenzene, located on the side chains, can make *cis*-azobenzene isomers unstable because of the steric hindrance effect. These undesirable issues greatly constrain the development of photo/thermoresponsive materials. Thus, exploring photoreswitchable liquid-solid or sol-gel transitions continues to be challenging and important.

Herein, we have proposed a novel, simple method, to construct a photo/thermoresponsive system based on an azobenzene-based ionic liquid, inspired by other stimuli located in the solution, such as PH or ionic strength. Based on previous research, the thermoresponsive behaviors of polymers are highly dependent on cation and anion combinations, which are very sensitive to any change in solvent, such as the elongation of cations [119]. This means, the isomerization of azobenzene ionic liquid, working as a solvent with an adjustable polarity by light sources, can potentially induce a dramatic change in solubility of the thermoresponsive polymers. The polymer solubility is expected to experience a sudden change, becoming soluble/insoluble under UV. To the best of our knowledge, no research has been reported that studies photoresponsive phase transition behaviors, based on an azobenzene ionic liquid. Furthermore, the amount of azobenzene can be easily controlled since the azobenzene ionic liquid works as a solvent. Additionally, introducing a photoswitchable LCST behavior by using a photoswitchable IL can potentially induce a photo-controlled sol-gel transition.

1.5 References

[1] Walden P, *Bull. Acad. Imp. Sci.* (St. Petersburg) **1914**, 405.
[2] Hurley F H, Wier T P, J. *Electrochem. Soc*. **1951**, 98, 203.
[3] Robinson J, Osteryoung R A. *J. Am. Chem. Soc.* **1979**, 101, 323.
[4] Wilkes J S, Zaworotko M J. J. Chem. Soc., *Chem. Commun*. 1992, 965.
[5] Noda A, Watanabe M, *Electrochim. Acta*. **2000**, 45, 1265.
[6] Susan Md. A. B. H., T. Kaneko, A. Noda, M. Watanabe, *J. Am. Chem. Soc.* **2005**, 127, 4976.
[7] Gale R J, Gilbert B, Osteryoung R A. *Inorg. Chem*. **1978**, 17, 2728.
[8] Watanabe M, Yamada S I, Sanui K, et al. *Chem. Commun*.**1993**, 11, 929.
[9] Pham T P T, Cho C W, Yun Y S. *Water research*, **2010**, 44, 352.

[10] Rogers R D, Seddon K R. *Science*, **2003**, 302, 792.
[11] Sheldon R. *Chem. Commun*. 2001, 23, 2399.
[12] Olivier B H, Magna L, Morvan D. *Appl. Catal. A- Gen.*, **2010**, 373, 1.
[13] Zhao H, Holladay J E, Brown H, et al. *Science*, **2007**, 316, 1597.
[14] Dupont J. *Journal of the Brazilian Chemical Society*, **2004**, 15, 341.
[15] Hunt P A, Gould I R, Kirchner B. *Aust. J. Chem.* **2007**, 60, 9.
[16] Hayashi S, Hamaguchi H. *Chem. Lett.* **2004**, 33, 1590.
[17] Tokuda H, Hayamizu K, Ishii K, Susa M A B H, Watanabe M. *The J. Phys. Chem. B.* **2005**,109, 6103.
[18] Marsh K N, Boxall J A, Lichtenthaler R. *Fluid Phase Equilibria*. **2004**, 219, 93.
[19] Rogers R D, Seddon K R. Ionic Liquids III A: Fundamentals, Progress, Challenges, and Opportunities: Properties and Structure[M]. American Chemical Society, **2005**.
[20] Welton T. *Chem. Rev.* **1999**, 99, 2071.
[21] Huddleston J G, Visser A E, Reichert W M, et al. *Green chem.* **2001**, 3, 156.
[22] Ngo H L, LeCompte K, Hargens L, et al. *Thermochimica Acta*, **2000**, 357, 97.
[23] Anderson J L, Ding J, Welton T, et al. *J. Am. Chem. Soc.* **2002**, 124, 14247.
[24] Rebelo L P N, Canongia Lopes J N, Esperança J M S S, et al. *The J. Phys. Chem. B.* **2005**, 109, 6040.
[25] Armand M, Endres F, MacFarlane D R, et al. *Nature mater*. **2009**, 8, 621.
[26] Kumar A, Gupta G, Srivastava S. *Green chem.* **2011**, 13, 2459.
[27] Bates E D, Mayton R D, Ntai I, et al. *J. Am. Chem. Soc.* **2002**, 124, 926.
[28] Yamaguchi K, Yoshida C, Uchida S, et al. *J. Am. Chem. Soc.* **2005**, 127, 530.
[29] Antonietti M, Kuang D, Smarsly B, et al. *Angew. Chem. Int. Ed.* 2004, 43, 4988.
[30] Bates E D, Mayton R D, Ntai I, et al. *J. Am. Chem. Soc.* **2002**, 124, 926.
[31] Dupont J, de Souza R F, Suarez P A Z. *Chem. Rev.* **2002**, 102, 3667.
[32] Mourot A, Fehrentz T, Le Feuvre Y, Smith CM, Herold C, Dalkara D, Nagy F, Trauner D, Kramer RH. *Nat Methods*. **2012**, 9, 396.
[33] Zhang S, Liu S, Zhang Q, et al. *Chem. Commun.* **2011**, 47, 6641.
[34] Kimura K, Suzuki T, Yokoyama M. *Journal of the Chemical Society, Chem. Commun.***1989**, 20, 1570.
[35] Soberats B, Uchida E, Yoshio M, Kagimoto J, Ohno H, Kato T. *J. Am. Chem. Soc.* **2014**, *136*, 9552.
[36] Ishiba K, Morikawa M, Chikara C, et al. *Angew. Chem. Int. Ed.* **2015,** 54, 1532.
[37] Wu S, Huang J. *RSC Advances* **2012**, 2, 12084.

[38] Zhou H, Xue C, Weis P, Suzuk Y, Huang S, Koynov K, Wu S. *Nature Chemi.* **2017**, *9*, 145.
[39] Kato M, Kamigaito M, Sawamoto M, Higashimura T, *Macromolecules* **1995**, 28, 1721.
[40] Wang J S, Matyjaszewski K. *Macromolecules* **1995**, 28, 7901.
[41] Matyjaszewski K, Xia J. *Chem. Rev.* **2001**, 101, 2921.
[42] Matyjaszewski K, Tsarevsky N V. *Nat. Chem.* **2009**, 1, 276.
[43] Tsarevsky N V, Matyjaszewski K. *Chem. Rev.* **2007**, 107, 2270.
[44] Chiefari J, Chong Y K, Ercole F, Krstina J, Jeffery J, Le T P T, Mayadunne R T A, Meijs G F, Moad C, Moad G, Rizzardo E, Thang S H. *Macromolecules* **1998**, 31, 5559.
[45] Moad G, Rizzardo E, Thang S H. *Aust. J. Chem.* **2005**, 58, 379.
[46] Moad G, Rizzardo E, Thang S H. *Aust. J. Chem.* **2006**, 59, 669.
[47] Moad G, Chiefari J, Chong Y K, Krstina J, Postma A, Mayadunne R T A, Postma A, Rizzardo E, Thang S H. *Polym. Int.* **2000**, 49, 993.
[48] Moad G, Rizzardo E, Solomon D H. *Macromolecules* **1982**, 15, 909.
[49] Benoit D, Chaplinski V, Braslau R, Hawker C J. *J. Am. Chem. Soc.* **1999**, 121, 3904.
[50] Hawker C J. *J. Am. Chem. Soc.* **1994**, 116, 11185.
[51] Kamigaito M, Ando T, Sawamoto M. *Chem. Rev.* **2001**, 101, 3689.
[52] Bucknall D G, Anderson H L. *Science*, **2003**, 302, 1904.
[53] Cheng J Y, Mayes A M, Ross C A. *Nature mater.* **2004**, 3, 823.
[54] Cheng J Y, Ross C A, Smith H I, et al. *Adv. Mater.* **2006**, 18, 2505.
[55] Whitesides G M, Grzybowski B. *Science* **2002**, 295, 2418.
[56] Carrasco P M, Ruiz de Luzuriaga A, Constantinou M, et al. *Macromolecules* **2011**, 44, 4936.
[57] Hao J, Zemb T. *J. Comb. Chem.* **2007**, 12, 129.
[58] Smart T, Lomas H, Massignani M, et al. *Nano Today* **2008**, 3, 38.
[59] Lee J S, Wang X, Luo H, et al. *J. Am. Chem. Soc.* **2009**, 131, 4596.
[60] Moffitt M, Khougaz K, Eisenberg A. *Acc. Chem. Res.* **1996**, 29, 95.
[61] Chen J T, Thomas E L, Ober C K, et al. *Science* **1996**, 273, 343.
[62] He Y, Li Z, Simone P, Lodge T P. *J. Am. Chem. Soc.* **2006**, *128*, 2745
[63] Chiantore O, Costa L, Guaita M. *Chem. Rapid. Commun.* **1982**, 3, 303.
[64] Ahmad H, Macromol J. *J. Sci. Chem.* **1982**, 17, 585.
[65] Brandrup J, Immergut E H, Grulke E A. *Polymer Handbook*, 4th ed. Wiley Interscience, Hoboken, New Jersey, **1999**.
[66] Lutz J F, Akdemir Ö, Hoth A. *J. Am. Chem. Soc.* **2006**, 128, 13046.
[67] Reddy P M, Venkatesu P. *J. Phys. Chem. B.* **2011**, 115, 4752.

[68] Tsuda R, Kodama K, Ueki T, et al. *Chem. Commun.* **2008**, 40, 4939.
[69] Ohno H, Fukumoto K. *Acc. Chem. Res*. **2007**, 40, 1122.
[70] Fujii K, Ueki T, Niitsuma K, et al. *Polymer* **2011**, 52,1589.
[71] He Y, Li Z, Simone P, et al. *J. Am. Chem. Soc.* **2006**, 128, 2745.
[72] Pelton R. *J. Colloid Interface Sci.* **2010**, 348, 673.
[73] Lin S Y, Chen K S, Liang R C. *Polymer* **1999**, 40, 2619.
[74] Luzon M, Boyer C, Peinado C, et al. *J. Polym. Sci., Part A: Polym. Chem.* **2010**, 48, 2783.
[75] Zhang Y, Furyk S, Bergbreiter D E, et al. *J. Am. Chem. Soc.* **2005**, 127,14505.
[76] Zhao Y, Tremblay L, Zhao Y. *Macromolecules* 2011, 44, 4007.
[77] Schild H G, *Prog. Polym. Sci.* **1992**, 17, 163.
[78] Hirokawa Y, Tanaka T, *J. Chem. Phys.* **1984**, 81, 6379.
[79] Makino K, Mack E J, Okano T, Kim S W, J. *J. Controlled Release* **1990**, 12, 235.
[80] Kost J, Horbett T A, Ratner B D, Singh M, J. Biomed. *Mater. Res.* **1985**, 19, 1117.
[81] Ishihara K, Kobayashi M, Shinohara I, *Macromol. Chem. Rapid. Commun.* **1983**, 4, 327.
[82] Ito Y, Casolaro M, Kono K, Imanishi Y. *J. Controlled Release* **1989**, 10, 195.
[83] Kataoka K, Miyazaki H, Bunya M, Okano T, Sakurai Y, *J. Am. Chem. Soc.* **1998**, 120, 12694.
[84] Akashi R, Tsutsui H, Komura A, *Adv. Mater.* **2002**, 14, 1808.
[85] Nayak S, Lee H, Chmielewski J, Lyon L A, *J. Am. Chem. Soc*. **2004**, 126, 10258.
[86] Kim J, Nayak S, Lyon L A, *J. Am. Chem. Soc.* **2005**, 127, 9588.
[87] Kim J, Serpe M J, Lyon L A, *Angew. Chem., Int. Ed.* **2005**, 44, 1333.
[88] Osada Y, Okuzaki H, Hori H, *Nature* **1992**, 355, 242.
[89] Varga Z, Filipcsei G, Zrínyi M, *Polymer* **2006**, 47, 227.
[90] Okuzaki.H, Funasawa K, *Macromolecules* **2000**, 33, 8307.
[91] Takeoka Y, Watanabe M, *Adv. Mater.* **2003**, 15, 199.
[92] Takeoka Y, Watanabe M, *Langmuir* **2002**, 18, 5977.
[93] Takeoka Y, Watanabe M, *Langmuir* **2003**, 19, 9554.
[94] Takeoka Y, Watanabe M, *Langmuir* **2003**, 19, 9104.
[95] Takeoka Y, Watanabe M, Yoshida R, *J. Am. Chem. Soc.* **2003**, 125, 13320.
[96] Saito H, Takeoka Y, Watanabe M, *Chem. Commun*. **2003**, 2126.
[97] Nakayama D, Takeoka Y, Watanabe M, Kataoka K. *Angew. Chem., Int. Ed.* **2003**, 42, 4197.
[98] Matsubara K, Watanabe M, Takeoka Y, *Angew. Chem., Int. Ed.* **2007**, 46, 1688.

[99] Ueno K, Matsubara K, Watanabe M, Takeoka Y, *Adv. Mater.* **2007**, 19, 2807.
[100] Ueno K, Sakamoto J, Takeoka Y, Watanabe M, *J. Mater. Chem.* **2009**, 19, 4778.
[101] Kodama K, Tsuda R, Niitsuma K, et al. *Polym. J.*, **2011**, 43, 242.
[102] Feng L, Chen Z. *J. Mol. Liq.* **2008**, 142, 1.
[103] Fukaya Y, Hayashi K, Wada M, et al. *Green chem.* **2008**, 10, 44.
[104] Fletcher K A, Pandey S. *Langmuir*, **2004**, 20, 33.
[105] Medronho B, Romano A, Miguel M G, et al. *Cellulose* **2012**, 19, 581.
[106] Shiga T, Hirose Y, Okada A, et al. *J. Appl. Polym. Sci.* **1992**, 44, 249.
[107] Kim S J, Kim H I, Park S J, et al. *Smart Mater Struct.* **2005**, 14, 511.
[108] Qiu Y, Park K. *Adv Drug Deliv Rev.* **2001**, 53, 321.
[109] Shiga T, Hirose Y, Okada A, et al. *J. Appl. Polym. Sci.* **1993**, 47, 113.
[110] Tanaka T, Nishio I, Sun S T, et al. *Science* **1982**, 218,467.
[111] Zrinyi M. *Colloid Polym. Sci.* **2000**, 278, 98.
[112] Satarkar N S, Hilt J Z. *J. Controlled Release* **2008**, 130, 246.
[113] Liu T Y, Hu S H, Liu K H, et al. *J. Magn. Magn. Mater.* **2006**, 304, 397.
[114] Xu F, Wu C M, Rengarajan V, et al. *Adv. Mater.* **2011**, 23, 4254.
[115] Gupta P, Vermani K, Garg S. *Drug discovery today*, **2002**, 7, 569.
[116] Dong L, Hoffman A S. *J.Controlled Release* **1991**, 15,141.
[117] Ueki T, Watanabe M, *Langmuir* **2007**, 23, 988.
[118] Fujii K, Ueki T, Niitsuma K, Matsunaga T, Watanabe M, Shibayama M, *Polymer* **2011**, 52, 1589.
[119] Kodama K, Nanashima H, Ueki T, et al. *Langmuir* **2009**, 25, 3820.
[120] Wu S, Huang J. *RSC Advances*, **2012**, 2, 12084.
[121] Zhou H, Xue C, Weis P, Suzuki Y, Huang S, Koynov K, Wu S. *Nature Chem.* **2017**, 9, 145.
[122] Ueki T, Watanabe M. *Chem. Lett.* **2006**, 35, 964.
[123] He Y, Lodge T P. *Chem. Commun*. **2007**, 26, 2732.
[124] Ueki T, Watanabe M. *Angew. Chem. Int. Ed*. **2015**, 54, 3018.

Chapter Two

Preparation of azobenzene ionic liquids

and their physical properties.

2.1 Azobenzene functionalized ionic liquid

Ionic liquids (ILs) are nonflammable, not significantly volatile, and are thermally and electrochemically stable. Owing to these unique and favorable properties, ILs have been widely used in chemical reactions, in electrochemistry as electrolytes, in separations, and so forth [1-5]. The properties of ILs can also be easily tuned by incorporating functional groups to either the cations or anions, or by mixing ILs with functional molecules, for example, azobenzene-based molecules, to achieve properties tailored to a specific task. It was reported that photoresponsive ILs can be obtained by covalent attachment of an azobenzene moiety to either cation or anion [6-9]. The first intrinsically photochromic ILs consisting of a methyl orange anion and appropriate organic cations were reported by Pina et al., while the rate of *cis*-to-*trans* isomerization of methyl orange ILs is too high to detect the *cis*-form at ambient temperature, since methyl orange is an aminoazobenzene derivative in which λ (n-π^*) and λ (π-π^*) exist in comparable barrier height [6]. Furthermore, most of the reported azobenzene ILs are likely solid at room temperature owing to their large molecular volume and strong π-π stacking interactions with the azobenzene moiety [6-11]. Therefore, ILs with bulky anions and longer carbon chains are generally used to maintain low melting points, yielding room temperature ILs [10].

2.1.1 Synthesis of azobenzene ionic liquid

Azobenzene molecule as shown in **Figure 1** is well known for its reversible isomerization, *trans*-isomer in the dark and *cis*-isomer under UV [12-15]. Azobenzene compounds are usually insoluble in common imidazolium based IL due to strong π-π stacking. To solve the issue, connecting azobenzene covalently to ionic liquid perhaps can make azobenzene easily soluble in IL. However, due to stronger rigidity of azobenzene molecules, mostly reported azobenzene containing ILs are solid state, insoluble in ILs. Taken those issues into account, one bigger volume of butyl-

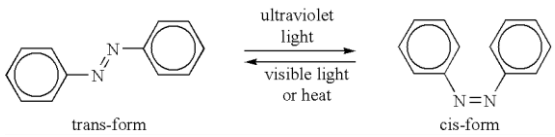

Figure 1. Photo isomerization of azobenzene structure

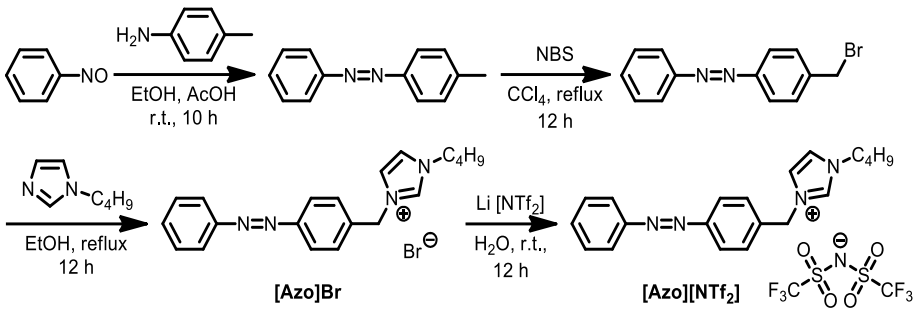

Figure 2. Synthesis of [Azo][NTf_2].

imidazolium was chosen to connect azobenzene by a methylene to increase the compatibility between them. The synthesis was shown in **Figure 2**.

Synthesis of 4-methylazobenzene

A solution of *p*-toluidine (5.03 g, 4.70mmol) in ethanol (12 mL) was added dropwise to a magnetically stirred solution of nitrosobenzene (5.06 g, 4.70mmol) in acetic acid (12 mL) at 45 °C in the dark. After 3 h, mixture was allowed to cool to room temperature and stirred for 10 h. The brown solid was washed with hydrochloric acid (1mol/L, 100ml), excess amount of NaOH aqueous solution (1mol/L, 100ml) and water. The crude product was purified by recrystallization twice from ethanol/water to give 4-methylazobenzene (5.54 g, 60%).^{1}H NMR (500 MHz, $CDCl_3$) δ 7.87 (m, 4H), 7.55-7.60 (m, 4H), 7.34 (s, 1H), 2.41 (s, 3H).

Synthesis of 4-(bromomethyl)azobenzene

Carbon tetrachloride (150 mL), 4-methylazobenzene (6.67 g, 3.40 mmol), peroxidation benzoin formyl (0.35 g, 0.21 mmol) and 1-bromopyrrolidine-2,5-dione (6.48 g, 3.60 mmol) were mixed at 85 °C under UV irradiation overnight. After filter, the crude product was recrystallized three times from ethanol, yielding organic solid (6.39 g, 69%). ^{1}H NMR (500 MHz, $CDCl_3$) δ 7.87 (m, 4H), 7.55-7.34 (m, 5H), 4.50 (s, 2H).

Synthesis of 1-butyl-3-(4-phenylazobenzyl)imidazolium bromide ([Azo]Br)

A solution of 4-(bromomethyl)azobenzene (3.61 g, 131 mmol), 1-butylimidazole (1.81mL, 138 mmol) in ethanol (120 mL) was heated at 70 ℃ under reflux for 12 h. After evaporation, the product was obtained by recrystallization three times from 2-propanol/ethyl acetate, yielding orange solid (3.65 g, 75%). ^{1}H NMR (500 MHz,

$CDCl_3$) δ 10.75 (s, 1H), 7.87 (d, 4H), 7.75-7.70 (m, 2H), 7.65-7.60 (m, H), 7.52-7.43 (m, 4H), 5.80 (s, 2H), 4.30 (s, 2H), 1.86-1.30 (m, 4H), 0.89 (s, 3H).

Synthesis of 1-butyl-3-(4-phenylazobenzyl)imidazolium bis(trifluoromethane-sulfonyl)imide ([Azo][NTf_2])

The solution of Li[NTf_2] (3.45 g, 12.00 mmol) in water was added dropwise into the mixture of [Azo]Br (3.99 g, 10. 00 mmol) in water (100 mL) at room temperature. After 36 h, chloroform was used for extracting crude product from water for eight times, then dry the orange product to obtain [Azo][NTf_2] (4.51 g, 75%). ^{1}H NMR (500 MHz, $CDCl_3$): δ 9.13 (s,1H), 7.97 (m, 4H), 7.60-7.42 (m, 5H), 7.35-7.20 (m, 2H), 5.41 (s, 2H), 4.20 (s, 2H), 1.85-1.30 (m, 4H), 0.89 (s, 3H).

2.1.2 Synthesis of azobenzene ionic liquids with various anions

Synthesis of 1-butyl-3-(4-phenylazobenzyl)imidazolium bis(trifluoromethane-sulfonyl)imide ([Azo][BF_4])

The solution of Li[BF_4] (1.12 g, 12 mmol) in water was added dropwise into the mixture of [Azo]Br (3.99 g, 10 mmol) in water (100 mL) at room temperature. After 36 h, chloroform was used for extracting crude product from water for eight times, then dry the orange product to obtain [Azo][BF_4] (4.51 g, 75%). ^{1}H NMR (500 MHz, $CDCl_3$): δ 8.90 (s,1H), 7.88 (d, 4H), 7.79-7.66 (m, 2H), 7.55-7.32 (m, 5H), 5.45 (s, 2H), 4.10 (s, 2H), 1.85-1.30 (m, 4H), 0.89 (s, 3H).

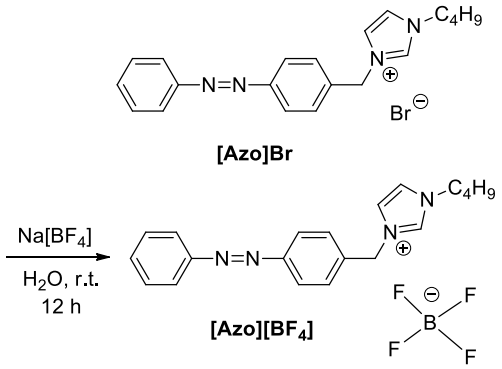

Figure 2. synthesis of [Azo][BF_4]

Synthesis of 1-butyl-3-(4-phenylazobenzyl)imidazolium bis(trifluoromethane-sulfonyl)imide ([Azo][PF_6])

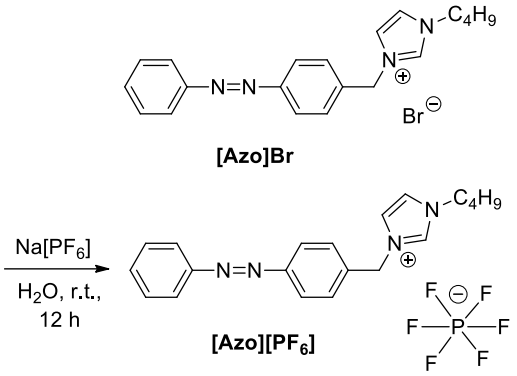

Figure 3. synthesis of [Azo][PF_6]

The solution of Li[PF_6] (1.82g, 12.00 mmol) in water was added dropwise into the mixture of [Azo]Br (3.99 g, 10.00 mmol) in water (100 mL) at room temperature. After 36 h, chloroform was used for extracting crude product from water for eight times, then dry the orange product to obtain [Azo][PF_6] (4.51 g, 75%). ^{1}H NMR (500 MHz, $CDCl_3$): δ 8.60 (s,1H), 7.87 (d, 4H), 7.69-7.66 (m, 2H), 7.45-7.52 (m, 4H), 7.34 (s, 1H), 5.45 (s, 2H), 4.02 (s, 2H), 1.80-1.30 (m, 4sH), 0.89 (s, 3H).

2.1.3 Synthesis of [C_1mim][NTf_2]

A solution of iodomethane (8.28 ml, 134 mmol), 1-methylimidazole (9.65 ml, 122 mmol) in cyclohexane (100 mL) was stirred strongly at ice water bath for 24 h. After evaporating, the product was obtained by recrystallization three times from 2-propanol/ethyl acetate, yielding white solid (22 g, 75%). ^{1}H NMR (500 MHz, $CDCl_3$): δ 9.05 (s, 1H), 7.69 (s, 2H), 3.86(s, 6H).

The solution of Li[NTf_2] (14.16 g, 49.3 mmol) in water (70 mL) was added dropwise into the mixture of [C_1mim][I](10 g, 44.8 mmol) in water (100 mL) at room temperature. After 36 h, chloroform was used for extracting crude product from water for eight times, then dry the orange product to obtain [C_1mim][NTf_2] (14.9 g, 86%). ^{1}H NMR (500 MHz, $CDCl_3$): δ 9.02 (s, 1H), 7.69 (s, 2H), 3.86(s, 6H).

2.2 Physical properties of ionic liquids

2.2.1 ^{1}H-NMR spectra for ionic liquids

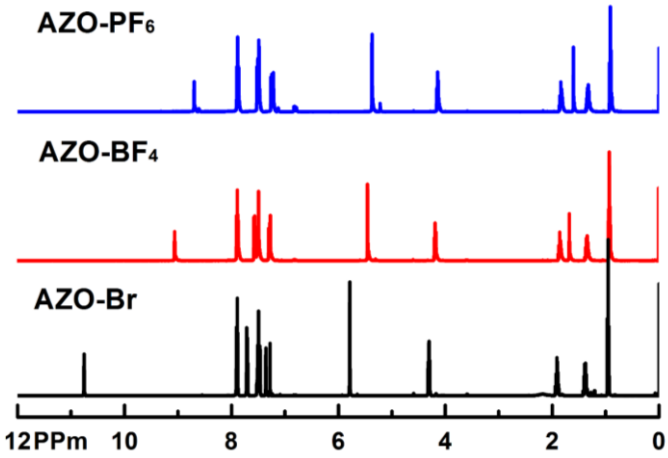

Figure 4. ^{1}H NMR spectra of azobenzene ionic liquids with various anions in $CDCl_s$ in the dark.

Figure 4 shows the ^{1}H NMR spectra of azobenzene ionic liquids with different anions in $CDCl_3$. Different chemical-shifts of acidic proton in cations were observed dependent on anion structures. Introducing azobenzene as an electron withdrawing groups can make the protons of cations more naked, increasing sensitivity to Lewis anions. Thus, changing anions can induce different chemical-shifts of the proton from imidazolium cation based on the Lewis acidity as following order, PF_6 <BF_4<Br.

2.2.2 Melting points of each azobenzene ionic liquid

Melting points of those azobenzene ILs with various anions were measured through DSC measurements on second heating as shown in **Figure 5**. Different heating

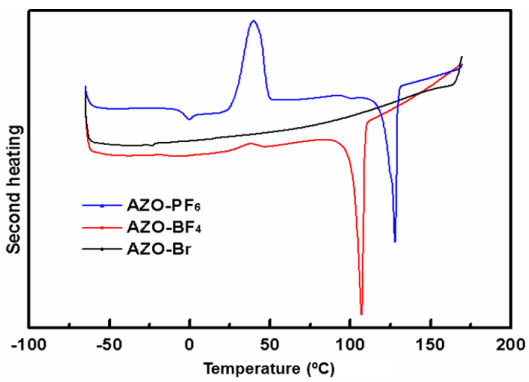

Figure 5. DSC curves of various ionic liquids on second heating at 3ºC/min.

Table 1. Thermo-physical properties of various azobenzene ILs.

Anions	T_g °C	K °C	T_m °C
Br	-	-	>150
PF_6	-4.5	40.3	127.6
BF_4	-	38.1	107.5
NTf_2	-37	-	-

T_g glass temperature; K crystalline temperature; T_m melting temperature; - means no related data. Measured range: -50 to 150 °C

behaviors were observed on heating process of azobenzene compounds. Taken [Azo][PF_6] as an example, the glass temperature (T_g) was observed at -4.5 °C, and by further heating, a new peak appeared, related to a crystalline transition process, at 127.6 °C, a sharp peak was observed, corresponding to a melting peak. Melting points, T_gs and crystalline temperatures (K) for various anions are listed in **Table 1**. It seems that bulky anions was efficient to lower the melting points (T_ms) of azobenzene compounds. Azobenzene ionic liquid with bearing bromide anions gives the highest melting point yet without any crystalline process, showing supercooled liquid property on cooling process as reported eleswhere [9].

Moreover, we have conducted photoresponsive liquification experiments for azobenzene compounds. A tiny amount of [Azo][BF_4] was putting on a glass under polarized optical microscope (POM). By heating the sample above 150 °C above

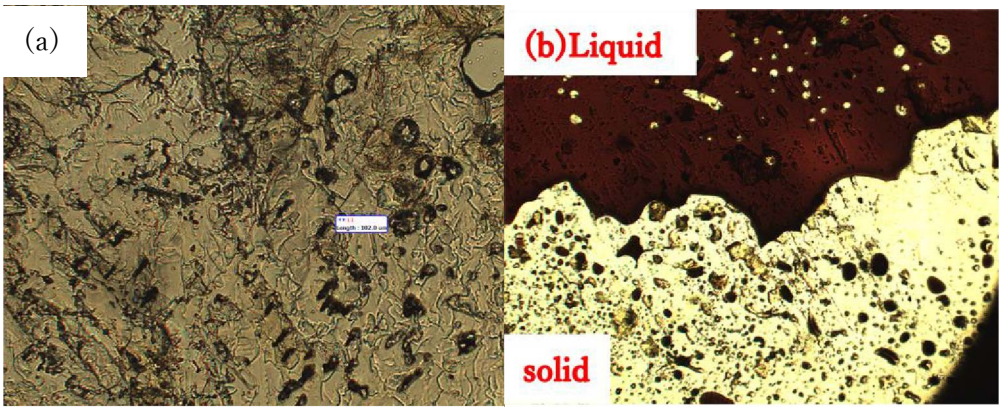

Figure 6. phase texture of *trans*-[Azo][BF_4] (a) and *cis*-[Azo][BF_4] (brown part) and *trans*-[Azo][BF_4] (yellow part) (b) under POM by cooling to room temperature.

melting points, we have observed the liquification process of [Azo][BF_4], and then cool down to room temperature to form a thin film, we have observed crystalline phase under POM as shown in **Figure 6(a)**. Then UV light was employed to irradiate the sample partly, while the other part was covered by aluminum foil to stop light getting through. We have observed the *cis*-[Azo][BF_4] (UV irradiated area) shows an isotropic state at a lower temperature in **Figure 6(b)**, dark brown part while unirradiated area, *trans*-[Azo][BF_4] shows a solid state at the same temperature. *Cis*-[Azo][BF_4] as liquid state can allow light to get through the sample, transparent color. It suggested that *cis*-[Azo][BF_4] can retain liquid state under UV irradiation at room temperature, while yellow part, *trans*-[Azo][BF_4], keeps crystalline state at the same temperature. After removing UV light source, the *cis*-[Azo][BF_4] can survive for 8 hours in the dark due to thermal reverse of azobenzene isomers. To conclude, by changing anions, we can observe various ILs with tunable thermal properties. And photo isomerization of the azobenzene IL can show a liquefication process of azobenzene compounds.

2.2.3 Photoisomerization of azobenzene ionic liquid

Next, we demonstrated the ^{1}H-NMR experiments to calculate the *trans* and *cis* ratio

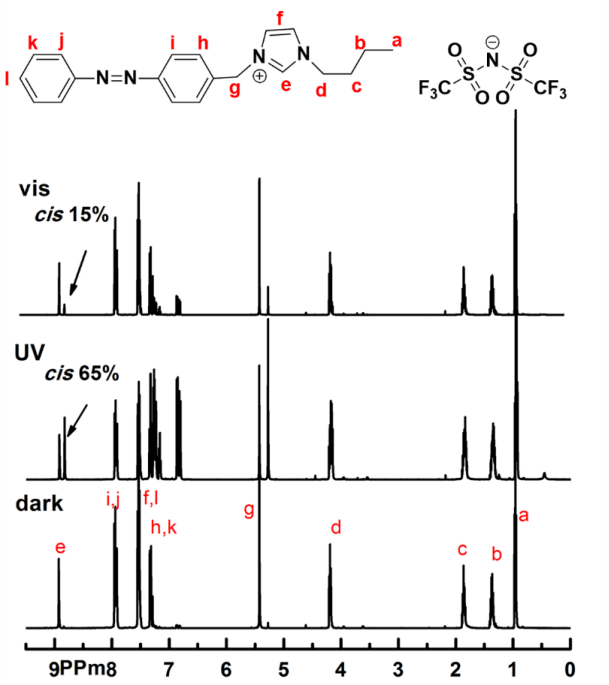

Figure 7. ^{1}H NMR spectra of [Azo][NTf_2] in $CDCl_3$ in the dark, UV and visible light irradiation at room temperature.

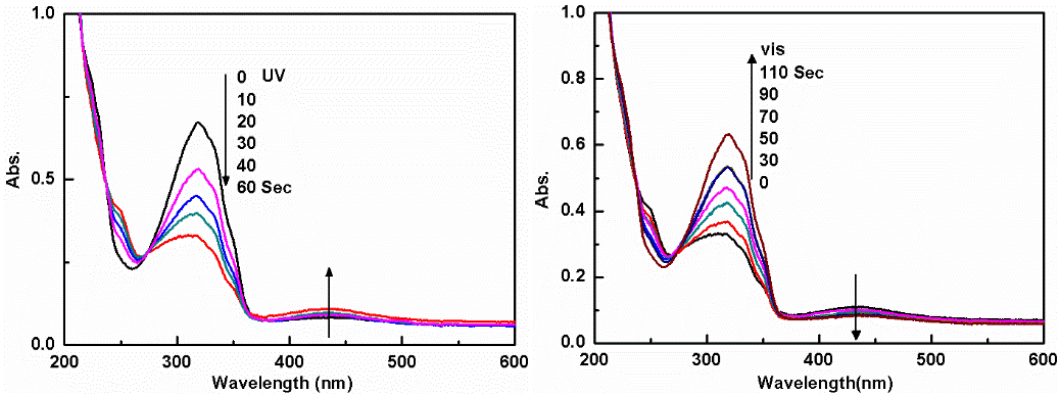

Figure 8. UV-vis spectra of [Azo][NTf_2] in [C_1mim][NTf_2] under UV and under visible light illumination at room temperature.

in the dark, under UV and visible light illuminations in **Figure 7**. The sample solution has been stored in dark for 12 hours to gain 100% *trans*-[Azo][NTf_2] by isomerzation of *cis*-[Azo][NTf_2] in $CDCl_3$. For the sample under UV, the sample solution has been irradiated under UV for 12 hours to achieve *cis*-[Azo][NTf_2] as much as possible. As indicated in **Figure 7**, 65% *cis*-[Azo][NTf_2] was obtained. Again, under visible light for 12 hours, *cis*-[Azo][NTf_2] transfers to *trans*-[Azo][NTf_2] and still 15% *cis*-[Azo][NTf_2] can survive under visible light illumination.

It is noticeable that *cis*-azobenzene is unstable at a higher temperature since *cis*-isomer can transfer to *trans*-isomer in the dark or by heating [12-15]. Here, UV-Vis spectra were used to show the photoresponsive isomerization of [Azo][NTf_2] in [C_1mim][NTf_2] as well as thermal isomerization of *cis*-azobenzene at various temperatures. A lower concentration of [Azo][NTf_2] in [C_1mim][NTf_2] (~10^{-3}

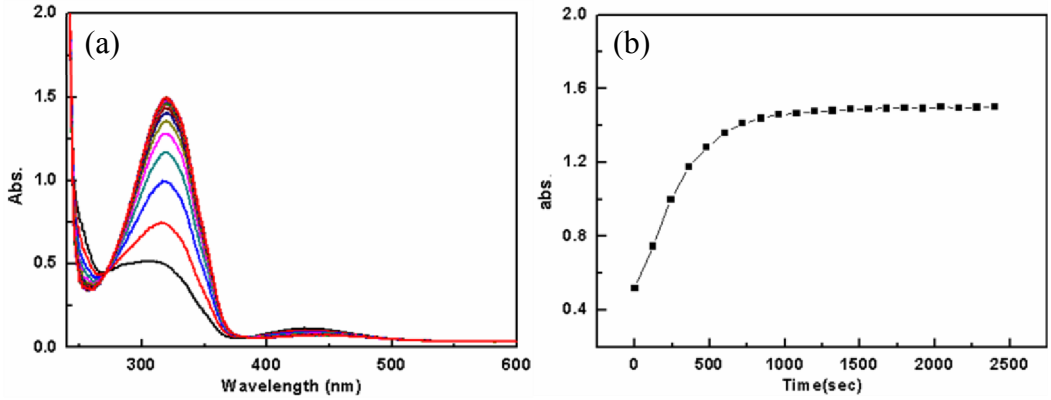

Figure 9. Thermal isomerization of [Azo][NTf_2] in [C_1mim][NTf_2] at 90 ºC in the dark (a) and plotted values of abs. dependent of time (b).

mol/L) was prepared by a co-solvent method. Photoresponsive reversible isomerization of [Azo][NTf_2] in [C_1mim][NTf_2] under UV and visible illuminations at room temperature was demonstrated in **Figure 8**. The wavelength at 310 nm is ascribed to *trans* isomer, ascribed to π-π* transition and another notable weak peak at 440 nm, is mainly belonging to *cis* form, n-π* transition with a small amount of π-π* transition [12, 16-17]. Under UV irradiation, it takes about 1 mins for *trans*-form to transfer to *cis*-form to reach a dynamic balance. Again, upon visible light illumination, the *cis*-form undergoes the isomerization to a *trans*-form within 2 minutes. That is to say, reversible photoisomerizations of [Azo][NTf_2] in [C_1mim][NTf_2] was achieved at room temperature.

Regarding the thermal isomerization of *cis*-[Azo][NTf_2] at a higher temperature, thermal isomerization speed at a higher temperature is important to consider *cis*-isomer life length. Thermal isomerization of [Azo][NTf_2] in [C_1mim][NTf_2] at various temperatures was conducted in the dark. Here, **Figure 9(a)** shows *cis* to *trans* isomerization of [Azo][NTf_2] in [C_1mim][NTf_2] in the dark at 90 ºC dependent on time. Apparently, *cis*-[Azo][NTf_2] survived less than 20minutes in the dark as indicated in **Figure 9(b)**. It is obvious that increasing temperature can accelerate the thermal isomerization as indicated in **Figure 10**. It seems that temperature lower than 50 ºC offers relatively friendly circumstances for *cis*-azobenzene with a long-lived time. And at room temperature, the *cis* form can survive at least for one days. Above 70 ºC, temperature appears to be a critical factor for the thermal isomerization. At 70 ℃ , without UV irradiation, *cis*-isomer can transfer to *trans*-isomer in 25 minutes. At 110℃ , it only takes less than 10 mins to transfer *cis*-isomer. In another hand, the light sensitivity is improved at a higher temperature.

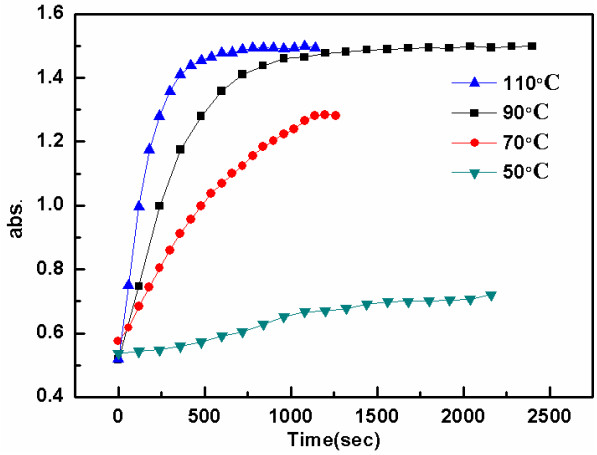

Figure 10. Thermal isomerization of [Azo][NTf_2] in [C_1mim][NTf_2] at various temperatures was conducted in the dark.

Then, thermal *cis* to *trans* isomerization speed was roughly calculated based on Beer length law without considering second rate k_2 for the *trans* to *cis* isomerization. Thus, according to **Equation1**, we can roughly calculate the first-order isomerization rate, k, 1.05X10^9/s.

$$-kt = \ln\left(\frac{A_t - A_\infty}{A_0 - A_\infty}\right) \qquad \textbf{Equation 1}$$

The time-dependent thermal isomerization of [Azo][NTf_2] in [C_1mim][NTf_2] were shown in **Figure 11**. Thus, the activation energy calculated from Arrhenius laws **Equation 2.** At a relatively mild temperature range from 40 to 70 ºC, the activation energy is around 86.2 kJ/mol, similar values as reported elsewhere [17-20].

$$ln\, k = \ln A - \frac{E_a}{RT} \qquad \textbf{Equation 2}$$

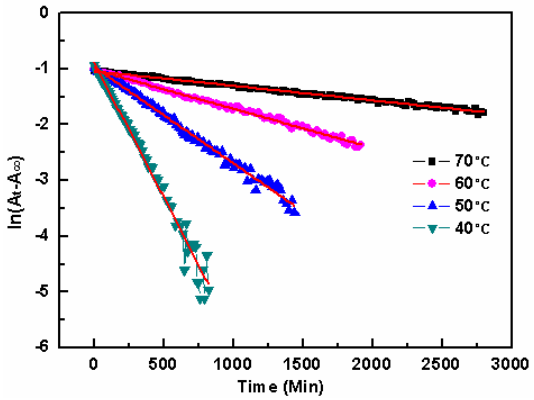

Figure 11. Time dependent of thermal isomerization of [Azo][NTf_2] in [C_1mim][NTf_2] at various temperatures from 40, 50, 60 and 70 ºC.

2.3 Conclusions

A series of novel azobenzene compounds covalently connected imidazolium ionic liquid were prepared and only [NTf_2] anion offers a room temperature ionic liquid ([Azo][NTf_2]). It shows photoresponsive reversible isomerization in ionic liquid under light irradiations. At various temperatures, the thermal isomerization speed in the dark was studied that *cis*-azobenzene have a short life above 70 ºC within 30 mins while at room temperature, it can survive at least for 1 day. Thermal isomerization enthalpy below 70 ºC is 86.2 kJ/mol, similar to reported azobenzene systems. Besides, tuning anions or cations with a longer alky chain and bigger anion size enables to produce room temperature azobenzene-based ILs. Also, azobenzene

IL with [BF_4] anion shows a liquefication process under UV irradiation based on a photochromic reaction of azobenzene compounds.

2.4 References

[1] Pham T P T, Cho C W, Yun Y S. *Water research* **2010**, 44, 352.
[2] Rogers R D, Seddon K R. *Science* **2003**, 302, 792.
[3] Sheldon R. *Chem. Commun*. **2001**, 23, 2399.
[4] Olivier B H, Magna L, Morvan D. *Appl. Catal. A- Gen.* **2010**, 373, 1.
[5] Zhao H, Holladay J E, Brown H, et al. *Science* **2007**, 316, 1597.
[6] Branco L C, Pina F, *Chem. Commun.* **2009**, 41, 6204.
[7] Coleman S, Byrne R, Alhashimy N, Frase K J, MacFarlane D R, Diamond D, *Phys. Chem. Chem. Phys.* **2010**, 12, 7009.
[8] Ishiba K, Morikawa M, Chikara C, Yamada T, Iwase K, Kawakita M, Kimizuka N, *Angew. Chem. Int. Ed*. **2015**, 127, 1552.
[9] Zhang S, Liu S, Zhang Q, Deng Y, *Chem. Commun.* **2011**, 47, 6641.
[10] Zhang Q, Shan C, Wang X, et al. *Liq. Cryst.* **2008**, 35, 1299.
[11] Zakrevskyy Y, Stumpe J, Smarsly B, et al. *Physical Review E*, **2007**, 75, 31703.
[12] Kumar G S, Neckers D C. *Chem. Rev.* **1989**, 8, 1915.
[13] Liu Z F, Hashimoto K, Fujishima A. *Nature*, **1990**, 347. 658.
[14] Bandara H M D, Burdette S C. *Chem. Soc. Rev.* **2012**, 41, 1809.
[15] Ikeda T, Nakano M, Yu Y, et al. *Adv. Mater.* **2003**, 15, 201.
[16] Eisenbach C D. *Macromol. Chem. Phys*. **1978**, 179, 2489.
[17] Jiang W, Wang G, He Y, et al. *Chem. Commun*. **2005**, 28, 3550.
[18] Takeshita K, Hirota N, Terazima M. *J. Photochem. Photobiol. A Chem*. **2000**, 134, 103.
[19] Halicioğlu T, Sinanoğlu O. *Ann. N.Y. Acad. Sci.* **1969**, 158, 308.
[20] Dias A R, Da Piedade M E M, Simoes J A M, et al. *J. Chem. Thermodyn.* **1992**, 24, 439.

Chapter Three

Phase transition behaviors for LCST homopolymers

Recently, growing interest was attracted by the phase transition behavior of stimuli responsive polymers in ILs. Our group previously reported that poly(benzyl methacrylate) (PBnMA) and its derivatives showed lower critical solution temperature (LCST) phase transition behaviors in 1-ethyl-3-methylimidazolium bis(trifluoromethanesulfonyl)imide ([C_2mim][NTf_2]) [1]. By introducing 4-phenylazophenyl methacrylate to the side chain of PBnMA, the obtained random copolymer (P(AzoMA-*r*-BnMA)) showed a LCST phase transition behavior in [C_2mim][NTf_2], and the LCST temperature difference (ΔT_{cp}) between the *trans*- and *cis*-forms was as large as 22 °C [2]. At a given temperature, P(AzoMA-*r*-BnMA) also showed a photoresponsive phase transition in [C_2mim][NTf_2]: it is insoluble in the absence of light but soluble under UV irradiation. These results suggested that random polymers containing an azobenzene moiety exhibited photoresponsive phase transition behaviors in ILs. The *cis*-rich azobenzene-based polymers appeared to be much more compatible with ILs than the *trans*-rich azobenzene-based polymers [2-5]. Most of the reported photoresponsive phase transition behaviors were owing to functional polymers like those containing azobenzene [2-11]. However, the content of azobenzene should be carefully controlled because the incorporation of azobenzene often results in the change in the phase transition temperature of the polymers. Also, the presence of azobenzene in polymers may sometimes widen the polydispersity index [12-14].

In this chapter, we have developed a new photoresponsive phase transition of nonfunctional thermoresponsive polymers (PBnMA and poly(2-phenylethyl methacrylate) (PPhEtMA)) in 1,3-dimethylimidazolium bis(trifluoromethanesulfonyl)amide ([C_1mim][NTf_2]) assisted by a photoresponsive IL comprising an azobenzene moiety (1-butyl-3-(4-phenylazobenzyl)imidazolium bis(trifluoromethanesulfonyl)amide; [Azo][NTf_2]). The [Azo][NTf_2], IL synthesized in this work, is a novel photoresponsive room temperature IL, which has a glass transition temperature of -39 °C (no melting temperature). By simply mixing polymers with [C_1mim][NTf_2] and [Azo][NTf_2] in different weight ratios, the obtained ternary system exhibited photoresponsive LCST behaviors. Particularly, a transparent solution of PBnMA in ILs containing *cis*-rich [Azo][NTf_2] became opaque under visible light irradiation. In contrast, PPhEtMA under the same conditions gave rise to an opposite trend where the transparent solution in ILs containing *trans*-rich [Azo][NTf_2] became turbid under UV light irradiation.

3.1 Materials and experiments

3.1.1 Materials

2-Cyanoprop-2-yl 1-dithionaphthalate (CTA), 2-phenylethyl methacrylate (PhEtMA), and 3-phenylpropyl methacrylate (PhPrMA) were synthesized and purified according to previously reported procedures [15-20]. 2,2′-Azobis(2-methylpropionitrile) (AIBN) was purchased from Wako Pure Chemical Industries and recrystallized from methanol prior to use. 1-Butylimidazole and 1-methylimidazole were purchased from TCI and distilled at reduced pressure before use. *N*,*N*,*N*′,*N*″,*N*″-Pentamethyldiethylenetriamine (PMDETA) was purchased from TCI, and PBnMA (M_n = 74 kDa, PDI = 1.47) was purchased from Aldrich and distilled at reduced pressure before use. CuBr and $CuBr_2$ were dried for 12 h at 60 °C under vacuum. All other chemical reagents were used as received, unless otherwise noted.

3.1.2 Polymerization of LCST polymers

Polymerization of PhEtMA

PPhEtMA was synthesized using reversible addition-fragmentation chain-transfer (RAFT) polymerization according to the reported procedure [16]. The polymerization was performed under argon atmosphere. CTA (0.54 g, 1.97 mmol) was placed in three neck flask, and then dehydrated anisole (80 mL) and PhEtMA (100 mL, 0.51 mol) were added to the flask. The nitrogen gas was bubbled into the solution with stirring for 30 min. AIBN (109 mg, 0.65 mmol) was dissolved in dehydrated anisole (20 mL) in another flask, and the argon gas was bubbled into the solution with stirring for 30 min. After bubbling, the AIBN solution was added to the monomer solution. RAFT polymerization was carried out at 60 °C for 9 h and was terminated by quenching the solution with dry ice/methanol. The product was purified twice by reprecipitation using THF and methanol as a good solvent and a poor solvent, respectively. CTA was removed by further reaction as reported. The product was dried for 24 h at room temperature under vacuum. PPhEtMA was characterized by using ^{1}H NMR spectroscopy and size exclusion chromatography (SEC). The number-average molecular weight (M_n) was calculated from the monomer conversion in the reaction solution determined by ^{1}H NMR, and the polydispersity (M_w/M_n, where M_w is the weight-average molecular weight) was determined by SEC

calibrated with polystyrene standards using THF as the eluent. The date was summarized in **Table 1**.

Polymerization of PhPrMA

PhPrMA was synthesized similar to PhEtMA monomer and polymerized by atom transfer radical polymerization (ATRP) according to the reported procedure [15-18]. CuBr (100 mg, 0.70 mmol), $CuBr_2$ (1.56 mg, 0.07 mmol) and PMDETA (147 μL, 0.71 mmol) were dissolved in anisole (50 mL). After stirring for 30 min at room temperature, the solution of monomer (10 mL, 0.05 mmol) and the functional initiator ethyl 2-bromoisobutyrate (49 mg, 0.025 mmol) were added. The solution was degassed three times using freeze-pump-thaw cycles. Polymerization were carried out at 60 °C for 14 h and terminated by quenching the solution with dry ice/methanol. The product was precipitated by ethyl acetate and methanol as a good solvent and a pour solvent, respectively. M_n: 22,000 and M_w/M_n: 1.35 obtained in similar method as PPhEtMA.

Polymerization of PhMeOBnMA

PhMeOBnMA was synthesized similar to PhEtMA monomer and polymerized by ATRP method. CuBr (100 mg, 0.70 mmol), $CuBr_2$ (1.56 mg, 0.07 mmol) and PMDETA (147 μL, 0.71 mmol) were dissolved in anisole (50 mL). After stirring for 30 min at room temperature, the solution of monomer (10 mL, 0.05 mmol) and the functional initiator ethyl 2-bromoisobutyrate (49 mg, 0.025 mmol) were added. The solution was degassed three times using freeze-pump-thaw cycles. Polymerization were carried out at 60 °C for 14 h and terminated by quenching the solution with liquid nitrogen. The product was precipitated by ethyl acetate and methanol as a

Table 1 Physical and molecular properties of the polymers used in this study.

Polymer	T_g / °C	T_d [a] / °C	M_n / *k*Da	M_w/M_n	Solubility[b] in $[C_1mim][NTf_2]$	Solubility in $[Azo][NTf_2]$
PBnMA	38.5	273.0	74	1.45	LCST	soluble
PMeOBnMA	51.2	289.4	31	1.12	LCST	soluble
PPhEtMA	35.2	293.3	29	1.31	insoluble	soluble
PPhPrMA	24.3	283.4	22	1.35	insoluble	soluble

T_d [a]: decomposition temperature of 5% weight loss; Solubility[b]: measured temperature range is from 30 to 200 ºC.

good solvent and a pour solvent, respectively. M_n: 22,000 and M_w/M_n: 1.35 measured in similar method as PPhEtMA.

3.1.3 Sample preparation for transmittance measurements

The ILs and polymers were prepared by a coslovent method using THF. A homogeneous polymer solution in THF was obtained after being stirred for 4 h and then proper ionic liquid amount was added at room temperature with a strong stirring for 24 h. Then the polymer solution was stirring at 40 °C for 24 h and excess THF was removed under vacuum for 48 h at 40 °C.

A drop of 7 wt% polymer solution was placed on a concave slide glass and covered with another glass. The samples were sandwiched between two glass plates in which one plate has a circle hole in depth of 30 μm-hollow. The slide glass was placed on a hot stage (Imoto, Japan) that enabled temperature control up to 400 °C. The temperature was increased from ambient temperature to 200 °C by 0.1 °C/min (0.3 °C/3min), and the transmittance of polymer/ILs was monitored at 612 nm with a USB fiber optic spectrometer (Ocean Optics). The upper-limit temperature was determined taking into account the possiblity of decomposition of the polymethacrylates up to 200 ℃ . The samples were heated to (T_{cp} – 10) ℃ in dark or under UV for 12 h and then phase-seperated samples were heated to (T_{cp} + 10) °C. For T_{cp} under UV irradiation, the sample was heated to (T_{cp} – 10) ℃ under light irradiation for12 h. For these measurements, a transmittance value of 50% at 612 nm was defined as the phase separation temperature, and the temperature difference (ΔT_{cp}) of samples under UV irradiation and in the absence of light was defined as the bistable temperature window.

3.1.4 UV source

A 500-W high-pressure mercury lamp using (Ushio Optical Modulex BA-H500) was used to irradiate the sample at a tuned intensity and wavelength by glass filters (UV light: 366 nm, Δλ 30nm, 8 mWcm-2; visible light: 437 nm, Δλ 23nm, 4 mWcm-2). The intensity of UV light was shown as in **Figure 1**. All the photoirradiation measurements were using a heat-absorbing filter to dissipate the heat generated by the mercury lamp. Furthermore, all the samples were put in the dark or under UV irradiation for 12 h before the transmittance experiments.

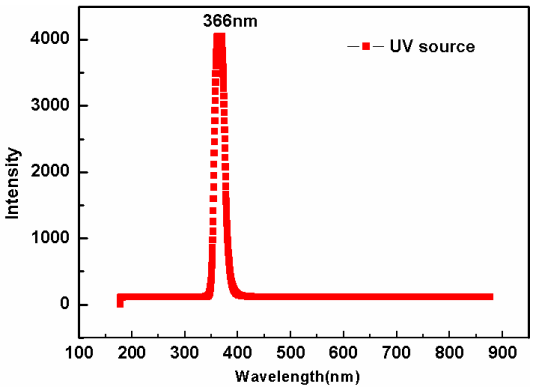

Figure 1. Intensity of UV source of UV lamp.

3.2 Photoresponsive LCST behaviors in ionic liquids

3.2.1 Thermoresponsive LCST behaviors

In this work, we first reported the photoresponsive phase transition of nonfunctional thermoresponsive polymers in 1,3-dimethylimidazolium bis(trifluoromethanesulfonyl)amide ([C_1mim][NTf_2]) assisted by an IL containing azobenzene moiety (1-butyl-3-(4-phenylazobenzyl)imidazolium bis(trifluoromethanesulfonyl)amide; [Azo][NTf_2]). Here we took 7 wt% polymer solutions of PPhEtMA as an example to describe the photoswitchable LCST behaviors by simply mixing polymers with [C_1mim][NTf_2] and [Azo][NTf_2] together in different weight ratios, that is, even 4wt% of [Azo][NTf_2] in

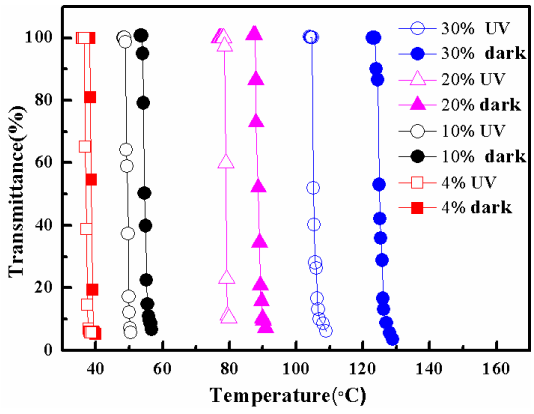

Figure 2. Temperature dependence of transmittance at 612 nm for 7wt% PPhEtMA solutions in [Azo][NTf_2]/[C_1mim][NTf_2] blends measured at a heating rate of 0.1 °C/min in the dark (closed) or under UV light irradiation (open). The weight fraction of [Azo][NTf_2] in the ILs is indicated. “4wt%” means the weight ratio of [Azo][NTf_2]/[C_1mim][NTf_2] is 4 / 96.

[C_1mim][NTf_2] ensured the completed dissolution of PPhEtMA at 30 °C, thus making it possible to measure the photoresponsive properties by examining the solubility and clouding temperature (T_{cp}). The results of turbidity measurements for 7wt% of PPhEtMA dissolved in a series of the IL mixtures with variable content of [Azo][NTf_2] were given in **Figure 2**. Clearly, for all the obtained composite systems, the transmittance drastically decreased from 100% to nearly 0% with increasing the temperature in a very narrow range, demonstrating the obvious LCST type phase behavior. Interestingly, T_{cp} values in the dark were generally higher than those obtained under UV irradiation induced by photoisomerization of azobenzene moieties in IL mixture. Furthermore, the content of [Azo][NTf_2] is found to significantly affect the photo-induced LCST phase behavior. Both the T_{cp} value and the difference of T_{cp} between *trans*-IL (dark) and *cis*-IL (UV) tend to increase as the content of [Azo][NTf_2] in IL mixtures increases. For example, PPhEtMA in mixed ILs containing 4wt% [Azo][NTf_2] showed a T_{cp} of 38 °C, which increased to 125 °C when 30wt% [Azo][NTf_2] was doped. A more detailed analysis given in **Figure 3** suggests that the T_{cp} for PPhEtMA ystem increased linearly with the content of [Azo][NTf_2] in the dark or under UV light irradiation. These results are consistent with the phase transition behavior of poly(ethylene oxide) in mixed aqueous media. Correspondingly, the ΔT_{cp} increased from 2 to 20 °C with increasing the [Azo][NTf_2] from 4 wt% to 30 wt% as shown in **Figure 3**. The linearly increasing of T_{cp} suggests that *cis*-[Azo][NTf_2] can work as third solvent in the solution, as a cooperative solvent. By increasing [Azo][NTf_2] content, the influence of *cis*-[Azo][NTf_2] is much more obvious, as increasing values of ΔT_{cp} ($\Delta T_{cp} = trans\text{-}T_{cp} - cis\text{-}T_{cp}$).

Similar measurements have also been conducted for PBnMA. PBnMA, which has a very similar structure to PPhEtMA but has a methylene spacer between the ester and

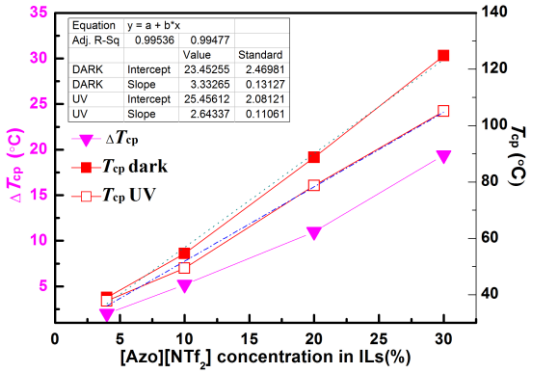

Figure 3. T_{cp} of 7 wt% PPhEtMA solutions independence of various [Azo][NTf_2] contents in [C_1mim][NTf_2] under UV light irradiation or in the dark and related bistable temperature window of ΔT_{cp}.

benzene ring instead of an ethylene spacer, was also used to assess the photoresponsive LCST phase behaviors in the [Azo][NTf_2]/[C_1mim][NTf_2] mixed medium. It should be noted that PBnMA is soluble in pure [C_1mim][NTf_2] as well as the IL mixtures containing [Azo][NTf_2] at 30 ℃ . PBnMA exhibited a LCST phase transition behavior for 7 wt% PBnMA in [C_1mim][NTf_2] (T_{cp} = 102 °C), as well as in the mixed ILs. As observed in the case of the PPhEtMA solution, both the T_{cp} and the absolute value of ΔT_{cp} for PBnMA significantly increased by increasing the content of [Azo][NTf_2] (**Figure 4**). Specifically, the *trans*-T_{cp} increased from 113 °C to 174 °C when the content of [Azo][NTf_2] increased from 4wt% to 20 wt%. Oddly, a slight increase in transmittance from 40% to 50% was observed for PBnMA in mixed ILs containing 20 wt% [Azo][NTf_2] when irradiated by UV light above 174 °C. This increase in transmittance at such a higher temperature was possibly owing to rubbery state of the polymer. When T_{cp} was lower than T_g, the aggregated particle scattered the light, and the transmittance decreased completely. However, when the T_{cp} was much higher than T_g, the aggregated melting polymer might allow light to pass through the solution. Interestingly, ΔT_{cp} for PBnMA was negative despite its small absolute value, meaning that the mixtures containing *cis*-[Azo][NTf_2] have a higher T_{cp} than those containing *trans*-[Azo][NTf_2]; this contrasts the results observed for PPhEtMA but agrees with the reported random copolymers comprising an azobenzene moiety [5].

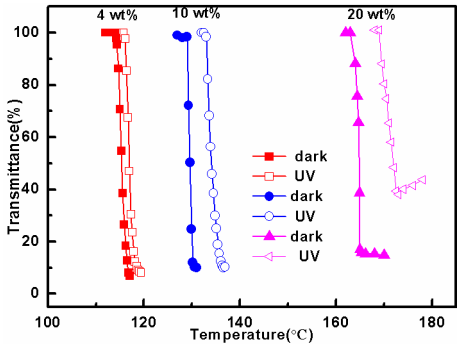

Figure 4. Temperature dependence of transmittance at 612 nm for 7wt% PBnMA solutions in [Azo][NTf_2]/[C_1mim][NTf_2] blends measured at a heating rate of 0.1 °C/min in the dark (closed) or under UV light irradiation (open).The weight fraction of [Azo][NTf_2] in the IL mixture is indicated. “4wt%” means the weight ratio of [Azo][NTf_2]/[C_1mim][NTf_2] is 4 / 96.

3.2.2 Photoswitchable LCST behaviors

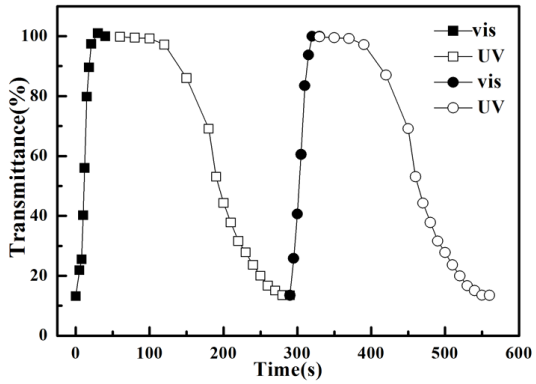

Figure 5. Reversible process of 7 wt% PPhEtMA in the mixed IL from a turbid to a transparent solution by irradiation with visible light (filled) and from a transparent to a turbid solution with UV (hollow) irradiation at 112 °C. And the weight ratio of [Azo][NTf_2]/[C_1mim][NTf_2] is 30 / 70.

Based on the LCST phase behaviors of the *trans*- and *cis*-isomers of [Azo][NTf_2]-containing IL mixtures, one can easily achieve a photoinduced phase separation of PPhEtMA in IL blends at a given bistable temperature window. As seen in **Figure 5**, the mixture containing 30 wt% [Azo][NTf_2] demonstrated a reversible phase separation and dissolution at 112 ºC under alternating UV and visible-light irradiation. Before the first measurement, the sample was irradiated with UV light for 12 h to achieve a turbid mixture (phase separation), which is rich in *cis*-[Azo][NTf_2]. Under visible-light irradiation, the turbid polymer mixture became transparent after only 30 s, increasing the transmittance dramatically from 11.9% to 100%. The response speed is comparable to popular azobenzene-based responsive materials [24]. Subsequent UV irradiation to isomerize the *trans*-[Azo][NTf_2] and revert to the phase-separated state, however, required an induction period of 60 s

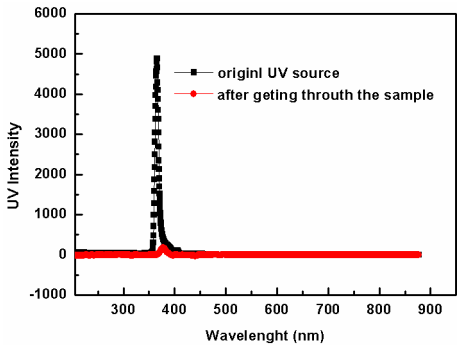

Figure 6. Transmittance of UV intensity with or without getting through the sample of ionic liquid mixture at room temperature. And the weight ratio of [Azo][NTf_2]/[C_1mim][NTf_2] is 30 / 70.

and the isomerization rate was lower (240 s) than the rate of dissolution. The difference in response time can be explained by the high azobenzene content present in the mixture. Under UV light irradiation, most of the light was presumably

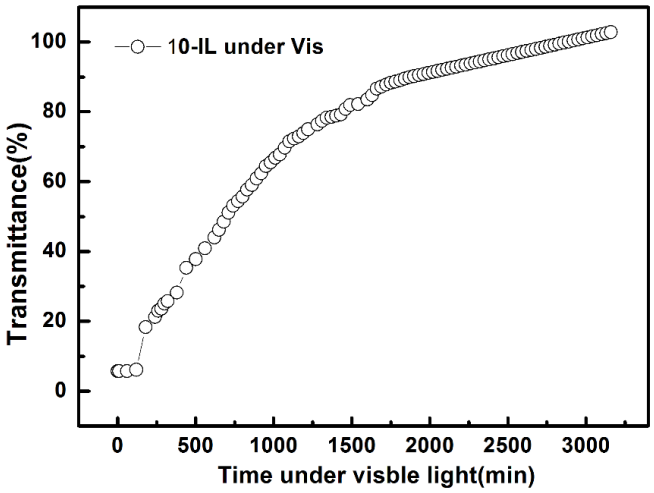

Figure 7. Reversible process of 7 wt% PPhEtMA in the IL mixture from a turbid to a transparent solution by irradiation with visible light (filled) at 52 °C. And the weight ratio of [Azo][NTf_2]/[C_1mim][NTf_2] is 10 / 90.

absorbed by the azobenzene molecules on the surface of a glass cell facing the light source owing to the high extinction coefficient of the azobenzene moieties (π-π* transition of *trans*-[Azo][NTf_2]) as shown in **Figure 6**, where UV light can barely get through the membrane at room temperature. The isomerization of *trans*-[Azo][NTf_2] resulted in a phase separation primarily on that surface; therefore, light scattering also occurred on that surface and only a small portion of the UV light penetrated the sample. A *cis*-rich IL layer was formed at the cell's surface rather than through the bulk of the sample. Next, dissolution under visible light irradiation, which led to an increased transmittance due to the low extinction coefficient of n-π* transition of *cis*-[Azo][NTf_2], allowed light to penetrate the sample. Therefore, the *cis*-[Azo][NTf_2] was quickly isomerized, leading to a fast rate of dissolution. Similar reversible phase transition behavior has also been observed in a lower content of [Azo][NTf_2] ([Azo][NTf_2]/[C_1mim][NTf_2] is 10 wt%), a slower process was obtained, taking around 5 h to fulfill the whole phase transition behavior.

3.3 Mechanism of LCST behaviors

3.3.1 LCST behaviors by modifying polymer structures

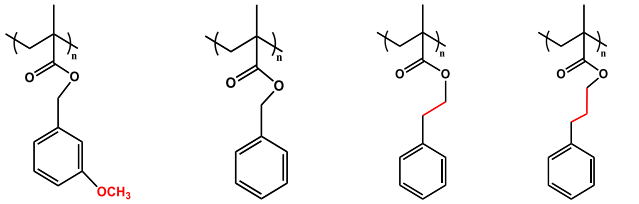

PMeOBnMA **PBnMA** **PPhEtMA** **PPhPrMA**

Figure 8. Polymer structures of LCST polymers used in study.

As shown in **Figure 8**, polymers, PMeOBnMA and PPhPrMA with similar structures of PBnMA and PPhEtMA have also been used to display the photoswitchable LCST behavior triggered by a small molecular trigger, azobenzene based ionic liquid. Firstly, PMeOBnMA with electron donating group ‘‘CH_3O” has shown photoresponsive LCST behaviors in various concentrations of azobenzene ionic liquid as indicated in the **Figure 9**. It shows similar photoresponsive LCST behaviors to PBnMA systems that in *cis*-ILs, higher T_{cp}s were observed than those containing *trans*-[Azo][NTf_2].

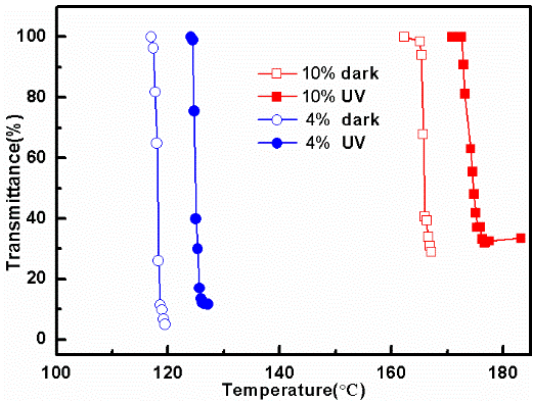

Figure 9. Temperature dependence of transmittance at 612 nm for 7wt% PMeOBnMA solutions in [Azo][NTf_2]/[C_1mim][NTf_2] blends measured at a heating rate of 0.1 °C/min in the dark (open) or under UV light irradiation (closed).The weight fraction of [Azo][NTf_2] in the ILs is indicated. “4 %” means the weight ratio of [Azo][NTf_2]/[C_1mim][NTf_2] is 4 / 96.

To investigate the effect of the alkyl linker, poly(3-phenylpropyl methacrylate) (PPhPrMA), which has a longer alkyl linker, was prepared and exhibited a LCST phase transition behavior in ILs with 4 wt% [Azo][NTf_2], but the temperature response was prolonged as shown in **Figure 10**. It seems the polymer solutions

became very viscous which made it difficult for polymer aggregating together. PPhPrMA in *cis*-rich ILs exhibited lower T_{cp} than in *trans*-rich ILs in **Figure 9**, similar photoresponsive behaviors to PPhEtMA. Thus, we can not only tune the T_{cp} but also control the photoresponsive LCST behaviors by a small modifying of polymer structures. It seems that polymer structures greatly affected the photoresponsive LCST behaviors.

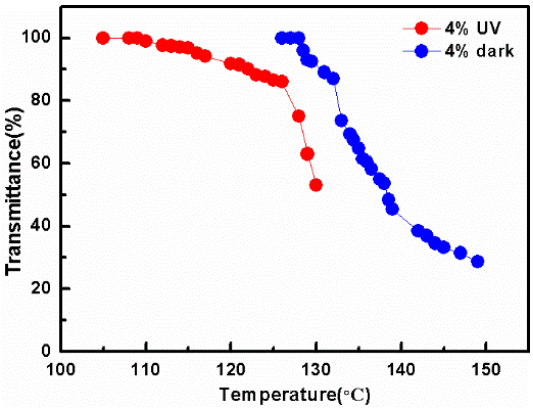

Figure 10. Turbidity measurements of 7 wt% PPhPrMA in ionic liquid blends under UV light (red) or in the dark(blue). "4%" means the weight ratio of [Azo][NTf_2]/[C_1mim][NTf_2] is 4 / 96.

3.3.2 LCST behaviors by modifying ionic liquid structures

Synthesis of [C_2mim][NTf_2]

A solution of ethyl bromide (15.6mL, 201 mmol), 1-methylimidazole (14.5 mL,183 mmol) in cyclohexane (100 mL) was stirred strongly at ice water bath for 24 h. After evaporation, the product was obtained by recrystallization three times from 2-propanol/ethyl acetate, yielding white solid [C_2mim][Br] (22 g, 75%). ^{1}H NMR (500 MHz, DMSO) δ 9.35 (s, 1H), 7.69-7.89 (m, 2H), 4.18 (m, 2H), 3.89(s, 3H), 1.42(m, 3H).

The solution of Li[NTf_2] (14.16 g, 49.3 mmol) in water (70 mL) was added dropwise into the mixture of [C_2mim][Br] (15.3 g, 44.8 mmol) in water (100 mL) at room temperature. After 36 h, chloroform was used for extracting crude product from water for eight times, then dry the orange product to obtain [C_2mim][NTf_2] (21.9g, 90%). ^{1}H NMR (500 MHz, DMSO) δ 9.22 (s, 1H), 7.69-7.89 (m, 2H), 4.18 (m, 2H), 3.89(s, 3H), 1.42(m, 3H).

Synthesis of new [Azo-1][NTf_2] ionic liquid.

4-phenolazophenol (10g, 50mmol) after being dried at 60 ºC, was soluble in anhydrous THF (100ml) with dropwise of triethylamine (10mL), then drop the 6-bromohexanoyldiloride (9.26ml, 60mmol) in THF solution (50mL). After stirring strongly at 45 ºC for 36 h, evaporate excess THF, and adding water to remove salt and by filtration with methylene chloride three times. Then the raw product was purified by crystalline in use of methanol twice, obtaining yellow product (13.1g, 70%). ^{1}H NMR (500 MHz, $CDCl_3$) δ 8.03-7.86 (m, 4H), 7.61-7.44 (m, 3H), 7.21-7.28 (m, 2H), 3.50-3.39(m, 2H), 2.67-2.58 (m, 2H), 1.96 (s, 2H), 1.77-1.86 (m, 2H), 1.56-1.66 (m, 2H).

1-butylimidazole solution in ethanol (30 mL) was dropped into bromohexanoyl phenolazophenol (8g, 23mmol) solution in anhydrous ethanol (50ml) at 60 ºC for 36 h under water reflux. Followed by evaporation of ethanol, the raw product was purified by crystalline in use of propanol/ethyl acetate, obtaining yellow product (13.1g, 70%). ^{1}H NMR (500 MHz, DMSO) δ 10.31 (s, 1H), 8.02-7.80 (m, 6H), 7.68-7.44 (m, 3H), 7.41-7.29 (m, 2H), 4.27-4.13 (m, 4H), 2.74-2.62 (m, 2H), 1.94-1.86 (m, 6H), 1.42-1.23 (m, 4H), 0.89 (s, 3H).

The solution of Li[NTf_2] (14.16 g, 49.3 mmol) in water (70 mL) was added dropwise into the mixture of [Azo-1][Br] (15.3 g, 44.8 mmol) in water (100 mL) at room temperature. After 36 h, chloroform was used for extracting crude product from water for eight times, then dry the orange product to obtain [Azo-1][NTf_2] (21.9g, 90%). ^{1}H NMR (500 MHz, DMSO) δ 9.21 (s, 1H), 8.05-7.81 (m, 6H), 7.70-7.46 (m, 3H), 7.45-7.31 (m, 2H), 4.30-4.19 (m, 4H), 2.84-2.65 (m, 2H), 1.98-1.86 (m, 6H), 1.45-1.23 (m, 4H), 0.89 (s, 3H).

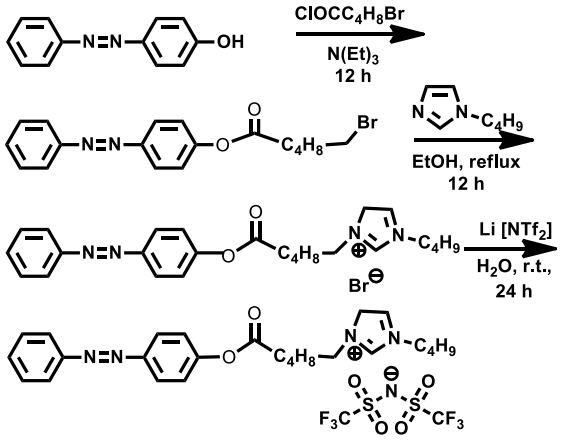

Figure 11. Synthesis of new [Azo-1][NTf_2] ionic liquid.

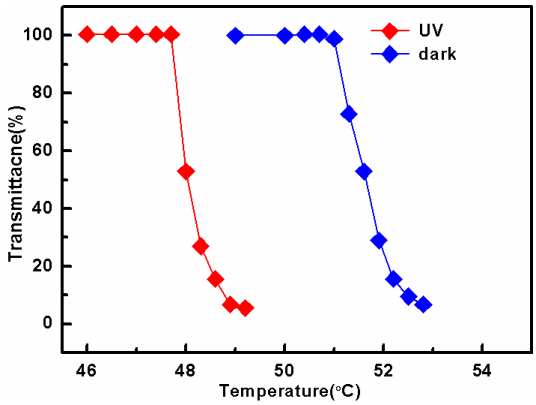

Figure 12. Turbidity measurements of 7 wt% PPhEtMA in ionic liquid blends and the ratio of [Azo][NTf_2]/[C_2mim][NTf_2] is 4/96 under UV light (red) or in the dark(blue).

To further investigate the photoresponsive LCST phase behavior involved IL structure, similar experiments were conducted by using [C_2mim][NTf_2] rather than its analog [C_1mim][NTf_2] as well as a newly synthesized azobenzene ionic liquid [Azo-1][NTf_2] (**Figure 11**).

By replacing [C_1mim][NTf_2] with [C_2mim][NTf_2], the results shown in **Figure 12** also demonstrated very similar photoinduced LCST phase transition behaviors with [C_1mim][NTf_2], suggesting that the observed phenomena originated perhaps from the interplay between the thermoresponsive polymers and [Azo][NTf_2], while much less affected by the main solvent ([C_1mim][NTf_2] or [C_2mim][NTf_2]). The observable difference between the two ILs is the slightly higher T_{cp} as well as wider ΔT_{cp} in [C_2mim][NTf_2]. A pronounced increase in *trans*-T_{cp} for [C_2mim][NTf_2] is a plausible explanation because an increase in the alkyl chain length on the imidazolium ring gives rise to strong interactions between the polymer chain and

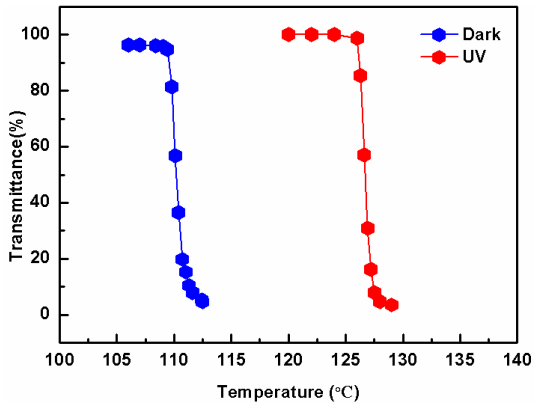

Figure 13. Turbidity measurements of 7 wt% PBnMA in ionic liquid blends and the ratio of [Azo][NTf_2]/[C_2mim][NTf_2] is 4/96 under UV light (red) or in the dark(blue).

ILs.[21] In addition, for PBnMA case, similar phase traisition behavior was also measured by similar method as shown in **Figure 13**. Also a wide ΔT_{cp} was observed, given rise to increasing alkyl chain lenghth of [C_2mim][NTf_2] with enhancing the intermolecular interactions when comparing with corresponding [C_1mim][NTf_2] system.

Meanwhile, a novel azobenzene-based ionic liquid [Azo-1][NTf_2] was also used as a candidate for photoresponsive group to study how ionic liquid mixture influence the photo-switchable LCST behaviors. **Figure 14** shows phase transition behavior of PPhEtMA in IL mixture with [Azo-1][NTf_2] and [C_1mim][NTf_2]. We still observed a decreasing T_{cp} in *trans*-ILs with a similar ΔT_{cp}. The photoinduced LCST behaviors remained unchanged where PPhEtMA shows a lower T_{cp} in *cis*-ILs. It seems that the ΔT_{cp} is mainly influenced by azobenzene polarity changes, rather than the imidazolium part. It shows T_{cp} is around 37ºC, which is closed to room temperature, offering its widely potential application.

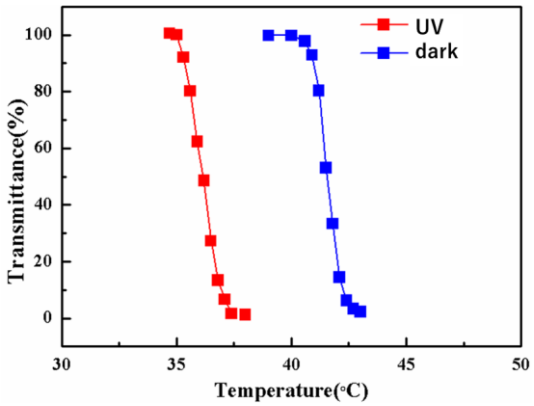

Figure 14. Turbidity measurements of 7 wt% PPhEtMA in the ionic liquid mixture and the weight ratio of [Azo-1][NTf_2]/[C_1mim][NTf_2] is 10/90 under UV light (red) or in the dark (blue).

The similar photoresponsive LCST behaviors for PBnMA polymer solutions were obtained that *trans*-T_{cp} was lower than *cis*-T_{cp} in newly [Azo-1][NTf_2] and [C_1mim][NTf_2] mixing system as shown in **Figure 15**. Obviously, ΔT between in the dark and under UV is quite larger than in [Azo][NTf_2] and [C_1mim][NTf_2] mixing system.

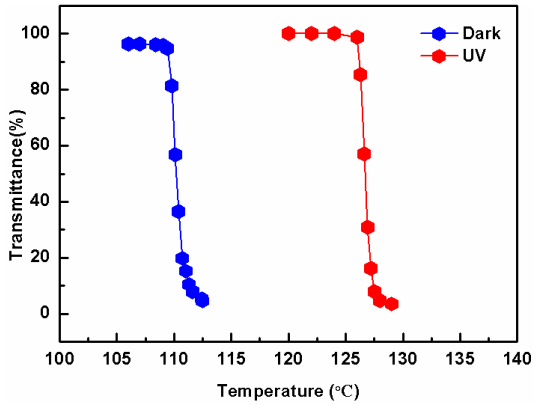

Figure 15. Turbidity measurements of 7 wt% PBnMA in the ionic liquid mixture under UV light (red) or in the dark(blue). The weight ratio of [Azo-1][NTf_2]/[C_1mim][NTf_2] is 10/90.

Besides, a smaller molecule weight of the PBnMA polymer similar to PPhEtMA (30,000) has also been conducted for the transmittance experiment as shown in **Figure 16**. The resultant system in the ILs blended with 10 wt% [Azo][NTf_2] exhibit *trans*-T_c and *cis*-T_c of 155 °C and 159 °C, respectively. The polymer shows a higher *cis*-T_{cp} than it in the dark, whose result is similar to the PBnMA with a higher molecule amount.

In this small chapter, by changing ionic liquid compounds, there is no photoresponsive behavior change towards UV source. It suggested that

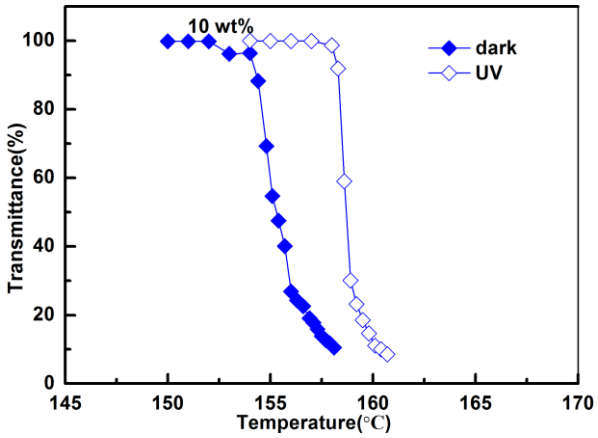

Figure 16. Temperature dependence of transmittance at 612 nm for 7 wt% PBnMA in 10 wt% [Azo][NTf_2]/[C_1mim][NTf_2] mixtures measured at a heating rate of 0.3 °C/3min in the absence of light (filled) or under UV light irradiation (hollow). The weight fraction of [Azo][NTf_2] in the ILs is indicated. "10 wt%" means the weight ratio of [Azo][NTf_2]/[C_1mim][NTf_2] is 10/ 90.

photoresponsive properties are much more involved to polymer structure, irrespective of ionic liquid mixture combinations.

3.3.3. Mechanism of photoresponsive LCST behaviors

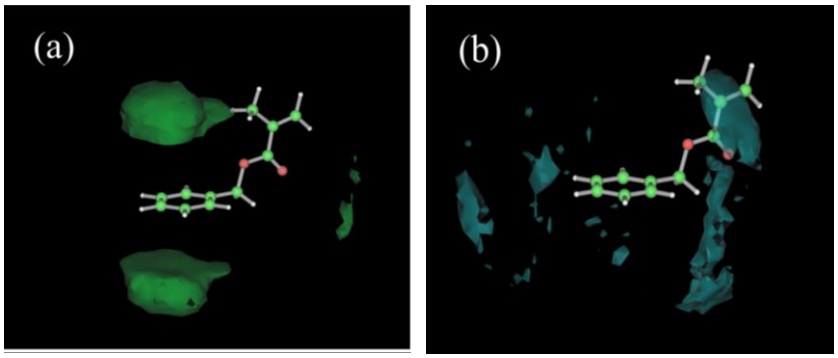

Figure 17. Space distribution functions, SDFs for center of mass of (a) $[C_2mim]^+$ and (b) $[TFSA]^-$ around BnMA. [22]

^{1}H-NMR is usually used to analysis the intermolecular interactions. In terms of smaller value of ΔH and ΔS for LCST behaviors, perhaps this tiny structural difference can influence the interaction between polymer and ILs depending on photoisomerization of azobenzene compounds. Herein, due to higher viscosity of polymer solutions, we replace polymers by molecular models. Small molecule models, benzyl isobutyrate (Bn) and phenethyl isobutyrate (Ph) worked as the models of PBnMA and PPhEtMA, respectively. The weight ratio of Bn or

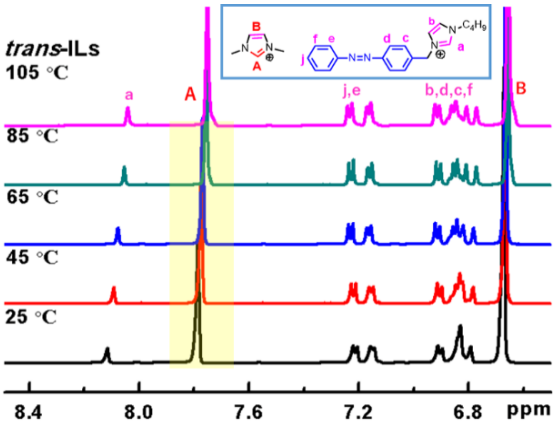

Figure 18. Temperature-dependent ^{1}H-NMR of *trans*-ILs without model molecule. The weight ratio of $[Azo][NTf_2]$ /$[C_1mim][NTf_2]$ = 20/80.

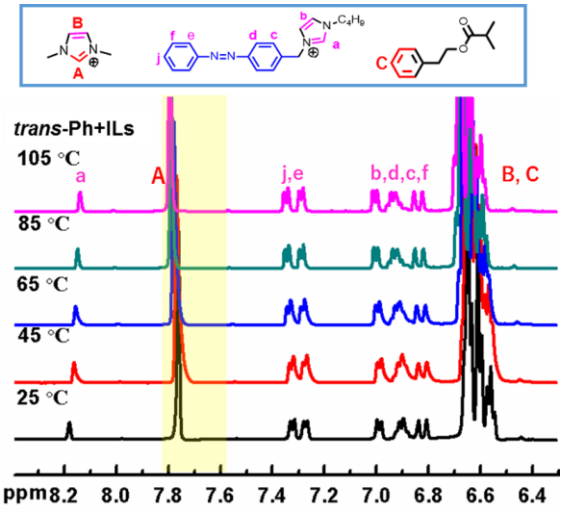

Figure 19. Temperature-dependent ^{1}H-NMR of *trans*-ILs without model molecule. The weight ratio of [Azo][NTf_2] /[C_1mim][NTf_2] is 20/80.

Ph/[Azo][NTf_2]/[C_1mim][NTf_2] is 20/16/64. we have employed ^{1}H-NMR experiments at different temperatures from 25 °C to 105 °C. Actully, the similar method for using molecular models has also been reported to explain the π-cation interaction for negative Δ*S* in LCST behaviors, as shown in **Figure 17** [22-28]. As is indicated, cations (green color) are located above the benzyl rings while the anions are surrounding around the polymer chains, particulary around the IL-phobic area.

Temperature-dependent chemical shifts of the solutions are discussed first in *trans*-ILs in **Figure 18**. The A proton shifted to highfield due to enhancing molecular interaction with increasing temperature. Ph-added ILs (Ph + ILs) was taken as an example to understand the photoresponsive LCST behavior in details. In *trans*-Ph+ILs, to our surprise, an increasing temperature induced a downfield shift of the **A** proton of [C_1mim] cation in **Figure 19**, while an upfield shift was observed in *trans*-ILs without the molecular models in **Figure 18**. The presence of solvation interaction between aromatics and imidazolium cations called as π-cation interaction is reported to induce LCST phase transition behaviors [22]. The opposite shifts of the **A** proton are related to LCST behavior as a cooperative proof. Thus, by increasing temperature, decreasing electron density of [C_1mim] cation (downfield shift of the **A** proton) suggests a decreasing interaction between the molecular model and ILs, corresponding to a LCST type phase transition behavior. Namely, by increasing temperature, decreasing interaction makes polymer insoluble in the solvent. Similar temperature-dependent downfield chemical shifts of the **A** proton were also observed in *trans*-Ph + ILs in **Figure 20**. Another cooperative proof for the A proton related to LCST behavior was shown in **Figure 21**. By addinng Bn molecular models,

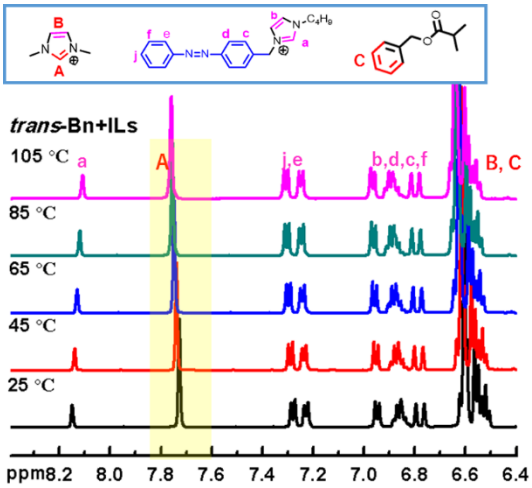

Figure 20. Temperature-dependent ^{1}H-NMR of *trans*-Bn+ILs (model molecule of PBnMA (benzyl isobutyrate; Bn) in the mixed ILs with *trans*-form azobenzene). The weight ratio of Bn/[Azo][NTf_2]/[C_1mim][NTf_2] = 20/16/64.

the chemical shift of A proton moved to upfield rather than downfield due to diluted effect. It suggested that there is intereaction existed between Bn and A proton for increaing electrodensity of A proton.To conclude, the A proton can serve as an indicator for LCST behavior.

By comparing with chemical shifts of **A** proton in the dark, a UV responsive chemical shifts of **A** proton were obtained, resembling the UV responsive solvation interaction. Herein we summarized the chemical shift differences ($\Delta\delta = trans\delta - cis\delta$)

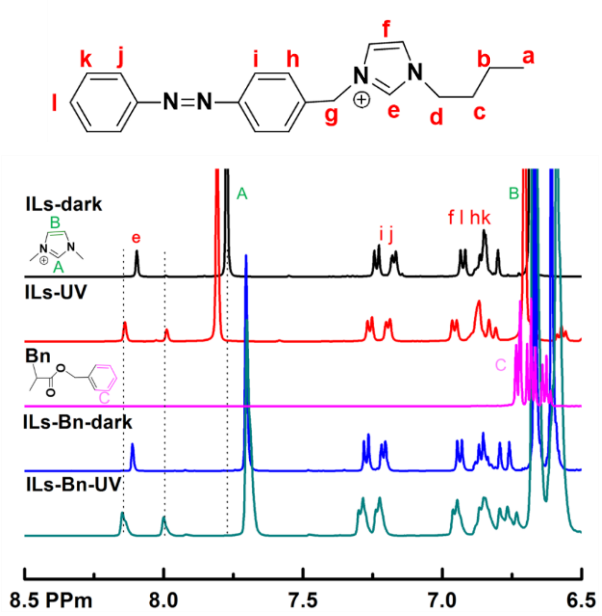

Figure 21. ^{1}H-NMR of mixed solutions at 30 ℃.

of the **A** proton at different temperatures between under UV and in the dark, as shown in **Figure 22**. In the case of PPhEtMA model solutions, $\Delta\delta$ value of **A** proton was negative, ascribed to a downfield shift in *cis*-Ph + ILs under UV irradiation. The decreasing electron density indicates the weakening solvation interaction between the polymer and ILs under UV irradiation. It means that the solubility of the polymer in *cis*-ILs is decreased, consequently showing a lower micellization temperature in *cis*-ILs. However, it is noticeable that for PBnMA model compound, $\Delta\delta$ values of the A proton were positive, and small upfield chemical-shifts were observed towards UV irradiation, indicating the slightly enhanced interaction between polymer and ILs, resulted in a higher micellization temperature. The different UV responsive chemical shifts between ILs and molecular models just would explain the different UV responsive micellization behaviors. Namely, the interaction between PPhEtMA/PBnMA and [C_1mim][NTf_2] could be affected by photoisomerization of [Azo][NTf_2].

We consider again solubility of PPhEtMA and PBnMA (3 wt%) in different ILs. In [C_1mim][NTf_2], PPhEtMA is insoluble, while PBnMA exhibits T_{cp} of 100 °C. When one of *N*-substituents in the [C_1mim] is changed from methyl to ethyl, i.e., [C_2mim][NTf_2] is used as the solvent, T_{cp}s of PPhEtMA and PBnMA become 110 °C and 42 °C, respectively, which is consistent with our previous report.[19] In *trans*-[Azo][NTf_2], both PPhEtMA and PBnMA are completely soluble (*vide supra*). Based on a concept; *"like dissolves like"*, these results suggest that PPhEtMA and PBnMA are soluble in the most hydrophobic ILs (*trans*-[Azo][NTf_2]) and that PPhEtMA is more hydrophobic than PBnMA. We have reported that solubility of PMMA in different ILs and found that solubility of PMMA is rather affected by anionic structures, less affected by cationic structures, and most rationally explained in terms of hydrophobicity matching between PMMA and ILs [25, 29]. When *trans*-

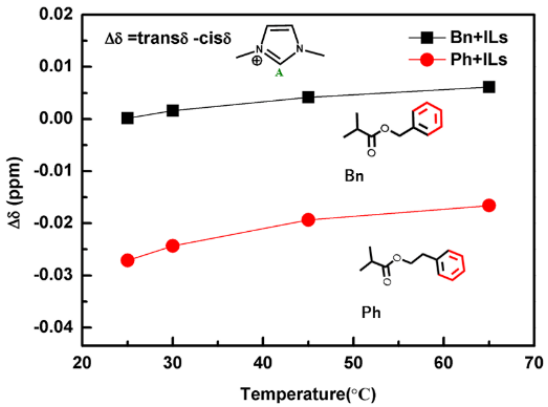

Figure 22. A proton chemical shift difference of [C_1mim] cation in PPhEtMA and PBnMA model solutions at 25, 30, 45, and 65 °C between under UV irradiation and in the dark.

[Azo][NTf_2] is added to [C_1mim][NTf_2] (5/95 in weight ratio) hydrophobicity of the mixture increases compared to [C_1mim][NTf_2] itself, which reflects the change in T_{cp}s; T_{cp} of PBnMA becomes 120 °C and T_{cp} of PPhEtMA appears at 49 °C. By the photoisomerization of *trans*-[Azo][NTf_2] to *cis*-[Azo][NTf_2], the T_{cp}s are altered to 123 °C (increase) and 45 °C (decrease), respectively. The effect of the photoisomerization on the T_{cp} change is different. It would be plausible to consider that hydrophobicity of PBnMA becomes closer to that of *cis*-[Azo][NTf_2]/[C_1mim][NTf_2] by the photoisomerization. On the contrary, hydrophobicity of PPhEtMA becomes a little apart from that of *cis*-[Azo][NTf_2]/[C_1mim][NTf_2]. Such subtle compatibility change would be reflected in the chemical shift of **A** proton in [C_1mim] (*vide supra*).

3.4 Conclusions

Instead of the conventional reoprted photoinduced thermoresponsive behavior in ionic liquids, water or other organic solvents achieved by photofunctional polymers [30-34], here, we reported a facile photoinduced LCST phase behavior of nonfunctionalized polymers (poly(benzyl methacrylate) (PBnMA) and its derivatives in mixed ILs (1,3-dimethylimidazolium bis(trifluoromethanesulfonyl)amide; [C_1mim][NTf_2] and a newly designed functionalized IL containing an azobenzene moiety (1-butyl-3-(4-phenylazobenzyl)imidazolium bis(trifluoromethanesulfonyl)amide; [Azo][NTf_2])) as a small-molecular photo trigger. Interestingly, the length of the alkyl spacer between the ester and aromactic group, which is the only structural difference between the two polymers, has a great influence on the LCST phase behavior. The phase transition temperature (T_{cp}) of PBnMA in the IL mixtures ([C_1mim][NTf_2]/[Azo][NTf_2]) rich in *cis*-[Azo][NTf_2] under UV light irradiation was higher than in IL mixtures rich in *trans*-[Azo][NTf_2] obtained in the absence of light. The T_{cp} of PPhEtMA, however, exhibited an opposite trend, where the polymer in the IL mixtures rich in *cis*-[Azo][NTf_2] had a lower T_{cp} than in IL mixtures rich in *trans*-[Azo][NTf_2].

By changing polymer strcutures and ionic liquid structures, we found that photoresponsive LCST behaviors of PPhEtMA and PBnMA were remianed unchanged. It seems that isomerization of azobenzene molecule affects the interaction between polymer and ILs and this circumstance is very sensitive to a tiny change from polymer, which is in consistent with small values of entropy and

enthapy of LCST behaviors. On the basis of spectroscopic studies, the different phase transition temperature (T_{cp}) of PBnMA and PPhEtMA may attribute to the different cooperative interactions between polymer with $[C_1mim][NTf_2]$. Through temperature dependent ^1H NMR measurements, it seems that the different photoresponsive solvation interactions of the polymers with $[C_1mim][NTf_2]$ could cause the interesting photoresponsive phase transition behaviors. This study gave an insight into molecular interactions that could lead to the development of novel photo/ thermoresponsive materials in ILs via a photoresponsive IL rather than photoresponsive polymers.

3.5 References

[1] K. Kodama, H. Nanashima, T, Ueki, H. Kokubo, M. Watanabe, *Langmuir* **2009**, *25*, 3820.

[2] T. Ueki, A. Yamaguchi, N. Ito, K. Kodama, J. Sakamoto, K. Ueno, H. Kokubo, M. Watanabe, *Langmuir* **2009**, *25*, 8845.

[3] Feng Z, Lin L, Yan Z, et al. *Macromol. Rapid Commun.* **2010**, 31, 640.

[4] Ishii N, Mamiya J, Ikeda T, et al. *Chem. Commun.* 2011, 47, 1267.

[5] Akiyama H, Tamaoki N. *Macromolecules* 2007, 40, 5129.

[6] He J, Tremblay L, Lacelle S, Zhao Y. Polymer Chemistry, **2014**, 5, 5403.

[7] Feng Z, Lin L, Yan Z. *Macromol. Rapid Commun.* **2010**, 31, 640.

[8] Boissiere O, Han D, Tremblay L, Zhao Y. *Soft Matter*. **2011**, 7, 9410.

[9] Jochum F D, Theato P. *Chem. Commun*. **2010**, 46, 6717.

[10] He J, Tremblay L, Lacelle S, et al. *Poly. Chem.* **2014**, 5, 5403.

[11] Ueki T, Nakamura Y, Yamaguchi A, Niitsuma K, Lodge T P, Watanabe M. *Macromolecules* **2011**, *44*, 6908.

[12] Viswanathan N K, Kim D Y, Tripathy S K. *J. Mater. Chem.* **1999**, 9, 1941.

[13] Zhao Y, Qi B, Tong X, Zhao Y. **Macromolecules 2008**, 41,3823.

[14] Fukuda T, Matsuda H, Shiraga T, et al. *Macromolecules* **2000**, 33, 4220.

[15] Zhu J, Zhu X, Cheng Z, Liu F, Lu J, *Polymer* **2002**, 43, 7037.

[16] Kitazawa Y, Ueki T, Imaizumi S, Lodge T P, Watanabe M, *Chem. Lett.* **2014**, 43, 204.

[17] Willcock H, O'Reilly R K. *Polym. Chem.* **2010**, 1, 149.

[18] Matyjaszewski K, Miller P J, Shukla N, Immaraporn B, et al. *Macromolecules* **1999**, 32, 8716.

[19] Matyjaszewski K. *Macromolecules* **2012**, 45, 4015.

[20] Xue L, Agarwal U S, Lemstra P J. *Macromolecules* **2002**, 35, 8650.

[21] T. Ueki, M. Watanabe, *Bull. Chem. Soc. Jpn*. **2012**, 85, 33.
[22] Fujii K, Soejima Y, Kyoshoin Y, et al. *J. Phys. Chem. B* **2008**, 112, 4329.
[23] Dougherty D A. *Science* **1996**, 271, 163.
[24] Gallivan J P, Dougherty D A. *Proceedings of the National Academy of Sciences* **1999**, 96, 9459.
[25] Mecozzi S, West A P, Dougherty D A. *J. Am. Chem. Soc.* **1996**, 118, 2307.
[26] Ma J C, Dougherty D A. *Chem. Rev.* **1997**, 97, 1303.
[27] Fukushima T, Asaka K, Kosaka A, et al. *Angew. Chem. Int. Ed.* **2005**, 44, 2410.
[28] Fukushima T, Aida T. *Chem. Eur. J.* **2007**, 13, 5048.
[29] Ueno K, Fukai T, Nagatsuka T,Yasuda T, Watanabe M. *Langmuir* **2014**, 30, 3228.
[30] Jochum F D, Zur Borg L, Roth P J, et al. *Macromolecules* **2009**, 42, 7854.
[31] Jochum F D, Theato P. *Polymer* **2009**, 50, 3079.
[32] Yuan W, Jiang G, Wang J, et al. *Macromolecules* **2006**, 39, 1300.
[33] Schattling P, Jochum F D, Theato P. *Chem. Commun.* **2011**, 47, 8859.
[34] Akiyama H, Tamaoki N. *J. Polym. Sci., Part A: Polym. Chem.* **2004**, 42, 5200.

Chapter Four

Photo/thermoresponsive micellizations and gelations of the PMP solution

The recent development of polymeric materials in ILs has generated significant excitement, and we are particularly interested in stimuli responsive self-assembling of block copolymers in ILs. For example, poly(*N*-isopropylacrylamide) (PNIPAm) exhibits an upper critical solution temperature (UCST) behavior in imidazolium-based ILs [1-3] and polyethers such as poly(ethylene oxide) (PEO) and its derivatives are found to show a lower critical solution temperature (LCST) behavior in ILs [4-5]. By copolymerization of the LCST and UCST as AB diblock copolymer, Prof. Lodge and coworkers have reported micelles with thermo-responsive, switchable cores and coronas; in this system, PEO-PNIPAm block copolymer self-assembles into PNIPAm-core and PEO-core micelles at low and high temperatures, respectively [3]. This tunable thermoresponsive micellization behavior can be applied in micellar shuttle systems that are relevant to molecular storage, transport, and separation [6-10]. Most recently, we have extended thermoresponsive polymers in ILs to dual responsive (photo/thermo) polymers via the copolymerization of an azobenzene-containing monomer with NIPAm as the main monomer [11]. A random copolymer consisting of 4-phenylazophenyl methacrylate (AzoMA) and NIPAm (poly(AzoMA-*r*-NIPAm)) showed photoresponsive UCST behavior, where a cloudy poly(*trans*-AzoMA-*r*-NIPAm) solution became transparent solution under UV irradiation. The increasing polarity of poly(*cis*-AzoMA-*r*-NIPAm) increases the polymer solubility in the IL. Based on the photoresponsive UCST behaviors, a diblock copolymer, PEO-P(AzoMA-*r*-NIPAm), underwent a light-controlled micellization/demicellization transition behavior in ILs.[12] ABA triblock copolymer based on similar A endblocks have also been reported for photo/thermoresponsive sol-gel transitions. In those study, it was necessary to carefully control the azobenzene content because azobenzene affects the phase transition temperature. However, to obtain desirable functional block copolymers, the optimal azobenzene content must be determined, which is a tedious process [13]. In addition, when azobenzene is in the side chains, the thermal *cis*-to-*trans* return rates increase, resulting a short *cis*-azobenzene lifetime.[14] In contrast, the introduction of azobenzene groups to the IL structure may simplify or solve these issues to some extent. The thermal isomerization of azobenzene may also be suppressed in ILs.[15] In addition to some azobenzene-based polymer systems in water or other organic solvents [16-17], this is the first study concerning the photoresponsive self-assembling of ABA triblock copolymers. Combined with a better understanding of photoresponsive behaviors of LCST homopolymers, a well-designed ABA triblock copolymer has been utilized to inducing a percolating network in ILs above LCST. Poly(2-phenylethyl methacrylate)-b-poly(methyl methacrylate)-b-poly(2-phenylethyl methacrylate) (PMP) was designed and synthesized via well-established

ATRP using poly(methyl methacrylate) (PMMA) as a macroinitiator, where the A blocks are LCST segment, PPhEtMA, while B midblock is PMMA, totally compatible with ILs. We herein have investigated photoresponsive unimer to micelle and sol-gel transitions of PMP triblock copolymers based on a photoswitchable ionic liquid.

4.1 Synthesis of PMP polymer

4.1.1 Materials

Copper (I) bromide (CuBr) and copper (II) bromide ($CuBr_2$) were purchase from Wako Chemicals and dried in a vacuum oven at 60 °C overnight. Methyl methacrylate (MMA) were purchased from Wako Chemicals. 2-Phenylethyl methacrylate (PhEtMA) monomer was prepared according to a previous report [18]. Prior to use, these monomers had been purified by the distillation under reduced pressure over CaH_2. *N*,*N*,*N*',*N*'',*N*''-Pentamethyldiethylenetriamine (PMDETA) was purchased from TCI and distilled before use. A bifunctional initiator of ATRP, ethylene glycol bis(2-bromoisobutyrate), was synthesised according to the reported[19-20].1-Butylimidazole and 1-methylimidazole were purchased from TCI and distilled before use. Ionic liquid containing azobenzene molecule was prepared as previously reported. All other chemical reagents were used as received, unless otherwise noted.

4.1.2 Polymerization of PMP

Synthesis of PMMA macroinitiator

A PMMA macroinitiator was synthesized via ATRP with a bifunctional initiator. Pre-dried mixture of CuBr (16 mg, 0.11 mmol), $CuBr_2$ (1.0 mg, 4.5 μmol), and PMDETA (39 μL, 0.19 mmol) were dissolved in anisole (40 mL) at room temperature to obtain a transparent solution. The solution of MMA (20 mL, 0.19 mol) and bifunctional initiator (37.6 mg, 0.34 mmol) was added at room temperature. After being degassed three times by the method of freeze-pump-thaw cycles, the polymerization began at 60 °C for 6 h and was terminated by quenching the solution with dry ice/methanol. PMP was characterized using ^{1}H-NMR spectroscopy and size

exclusion chromatography (SEC). The number-average molecular weight (M_n) was calculated by ^{1}H-NMR, and the dispersity (M_w/M_n, where M_w is the weight-average molecular weight) was determined by SEC calibrated with PMMA standards using THF as the eluent. **Table 1** shows the related results.

Table 1. Molecular weight of polymers synthesized in this study.

	M_n (kDa)[a]	PDI (M_w/M_n)[b]
PMMA [c]	42	1.13
PMP	30-42-30	1.16

[a] M_n of PMMA was estimated by using ^{1}H-NMR. The M_n of PMP and BMB was calculated from the results of the ^{1}H-NMR based on precursor. [b] Determined by SEC analysis in THF. [c] Macroinitiator of PMP and BMB via ATRP method.

Synthesis of triblock copolymer PMP

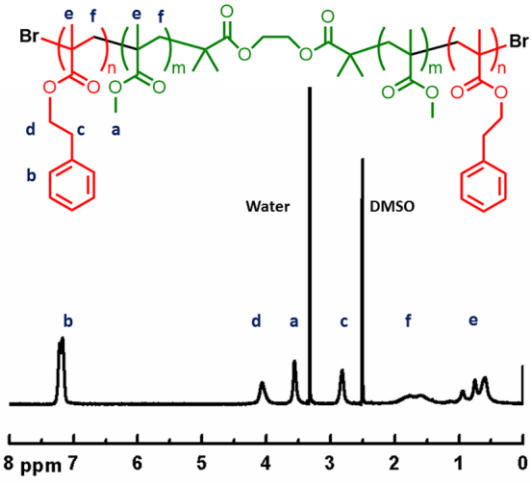

Figure 1. ^{1}H NMR spectra of PMP triblock copolymers in $CDCl_3$.

PMP was synthesized using ATRP polymerization using PMMA as a macroinitiator, similar to the reported procedure [20]. The polymerization was performed under argon atmosphere. Pre-dried mixture of CuBr (32 mg, 0.23 mmol) and $CuBr_2$ (1.0 mg, 4.5 μmol), PMMA macro initiator (9.5 g, 0.23 mmol), PhEtMA (5.0 g, 26 mmol), PMDETA (57 μL, 0.27 mmol) were mixed in anisole (90 mL) at room temperature. Then the homogeneous solution was degassed three times in use of freeze-pump-thaw cycles, and polymerization was carried out at 80 °C and terminated by quenching the solution with dry ice/methanol. The produce was purified by reprecipitation twice using ethyl acetate as a good solvent and methanol

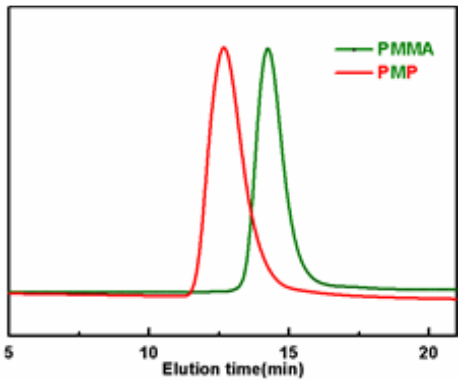

Figure 2. Size exclusion chromatography (SEC) elution curves of PMP and PMMA macroinitiator using THF as an eluent.

as a poor solvent. PMP was dried for 14 h at 60 °C under vacuum and characterized using ^{1}H-NMR analysis (M_n) as shown in **Figure 1** by comparing the proton e and proton c. And SEC (M_w/M_n) was determined by SEC calibrated with polystyrene standards using THF as the eluent as listed in **Table 1** and shown in **Figure 2**.

4.2 Photo/thermoresponsive micellization behaviors

4.2.1 Experiments

All polymer solutions used in the study were dissolved in ILs assisted by the co-solvent evaporation method. PMP (weight ratio of polymer/ILs = 0.1/99.9) in mixed ionic liquids of $[C_1mim][NTf_2]$ and $[Azo][NTf_2]$ (the weight ratio of $[Azo][NTf_2]/[C_1mim][NTf_2]$ = 5/95) were prepared as follows: triblock copolymers were first dissolved in THF (co-solvent), then an appropriate amount of ILs mixture was added into the solution and stirred for 12 h to obtain a transparent solution at 40 °C. Sample solutions were passed through 0.20 μm filters to eliminate dust prior to use. Excess THF in the polymer solution was removed under reduced pressure while heating at 40 °C for 48 h.

Dynamic light scattering (DLS) experiments. DLS measurements were performed on an Otsuka Electronic DLS-6500 equipped with an ALV correlator and an argon laser (632 nm). Experiments were carried out by increasing temperature from 25°C to 140 °C within an accuracy of ±0.1 °C by 10 °C/h. Meanwhile, the correlation functions $g_2(q, t)$ were recorded at scattering angles 90° at each temperature.

For solutions containing monodisperse particles, the electric field correlation function $g_1(q, t)$ can be analyzed by utilizing the method of cumulants [21-25]:

$$g_1(q,t) = \mathrm{A}\exp(-\Gamma t) = \exp(-D_0 q^2 t) \qquad (1)$$

where q is the scattering vector ($q = (4\pi n/\lambda \sin(\theta/2))$), in which n is the refractive index of the solution, λ is the wavelength of the light in vacuum, and θ is the scattering angle. Meanwhile, Γ is the decay rate, and D_0 is the mutual diffusion coefficient at the infinitely dilute limit. The record intensity correlation function $g_2(q, t)$ was converted to $g_1(q, t)$ through the Siegert relation. The hydrodynamic radius, R_h can be estimated with the knowledge of the solvent viscosity (η) according to the Stokes-Einstein equation [26-31].

$$R_h = (k_b T)/6\pi\eta D_0 \qquad (2)$$

For solutions with poly-dispersed particles,

$$g_1(q,t) = \mathrm{A}\exp(-\Gamma t)\,(1 + (1/2!)\mu_2 t^2 + (1/3!)\mu_2 t^3) \qquad (3)$$

Where Γ is the decay rate and μ_2/Γ^2 means the width of the distribution. In this work, the apparent hydrodynamic radius, R_h was calculated by equations (2) by replacing $D = \Gamma/q^2$ in 0.1 wt% solutions for D_0. The distribution of R_h was estimated by applying the inverse Laplace transformation to $g_1(q, t)$ with the well-established CONTIN program and by a sum of two exponentials. To estimate R_h, the temperature dependence of the viscosity of mixed ILs, where the weight ratio of $[C_1mim][NTf_2]$: $[Azo][NTf_2]$ was 5:95, was calculated from the appreciate Vogel-Tammann-Fulcher (VTF) equations. Moreover, the refractive index of mixed ILs was measured using

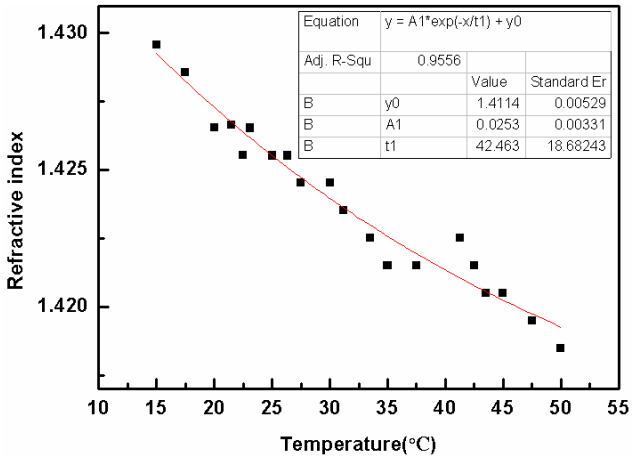

Figure 3. Refractive indices in various temperatures.

an Abbe refractometer NAR-1T attached with a thermostatic bath with a temperature range between 10 and 50 °C. To obtain the refractive indices above 50 °C, the analytical curve was estimated by using the refractive indices in the temperature range 10−50 °C, and those above 50 °C were calculated by extrapolation of the curve as indicated in **Figure 3** [32-36].

Cryo-transmission electron microscope (TEM). The solutions were diluted with THF, dropped onto a TEM copper grid covered with a perforated carbon film (Pelco International, USA), and blotted with filter paper to form a thin liquid film of the sample (100–200-nm thickness). The thin sample was plunged into liquid ethane at its freezing temperature (−183 °C) to form a vitrified specimen and then transferred to liquid nitrogen (−196 °C) for storage. The vitrified specimens were examined with a JEM-2100F transmission electron microscope (JEOL, Japan) operating at an accelerating voltage of 120 kV. UV irradiation was not possible during the TEM measurements. Consequently, the PMP solutions were measured in the dark.

4.2.2 Thermoresponsive micellization behaviors

Both triblock copolymers are totally soluble in [Azo][NTf_2] in a measuring temperature range between 30 and 200 °C. Also, highly concentrated [Azo][NTf_2] absorbs most of light source and prevent the light getting through the polymer solutions. Therefore, only a small amount of [Azo][NTf_2] was mixed with [C_1mim][NTf_2] to use as photoresponsive solvents for the study of photoresponsive self-assembling/disassembling of the LCST triblock copolymers. The lower critical micellization temperature (LCMT) of the PMP (0.1 wt%) in the IL mixture (weight ratio of [Azo][NTf_2] and [C_1mim][NTf_2] = 5/95) was measured by the means of DLS. The normalized scattered intensity was defined as the intensity at each temperature divided by that measured at 25 °C. For PMP triblock copolymer solutions in the dark, the normalized scattered intensity suddenly enhanced by heating the sample at 65 °C (**Figure 4a**). A similar increase in the aggregation temperature was also observed in other thermoresponsive block copolymer systems; this was attributed to the presence of the covalently bonded solvatophilic in the IL[20]. Such a discontinuous increase in the scattering intensity implies that the triblock copolymer PMP self-assembles into micelle sufficiently and the size is larger enough to scatter incident light.[19] Above 75 °C, the increasing scattering intensity suggests the incensement of particle numbers. The mean hydrodynamic radius (R_h) was evaluated by the temperature cumulant analysis (**Figure 4b**). At lower temperatures below LCMT, the R_h value is

below 10 nm, unimer state, in consistent with individual PMP polymer chains with a total molecular weight around 10 kDa. The radius R_h increased significantly in *trans*-ILs at 65 °C, suggesting that the PMP triblock copolymer self-assembled into micelles with PPhEtMA cores surrounded by well-solvated solvatophilic PMMA shells. Under UV irradiation, there was an abrupt increase of the scattering intensity at 55 °C as shown in **Figure 4a**. The values (**Figure 4b**) above 85 °C in *cis*-ILs are slightly larger than these in *trans*-ILs. Increased polarity by *trans*-to-*cis* azobenzene isomerization can change the interface energy between ILs and polymer chains,

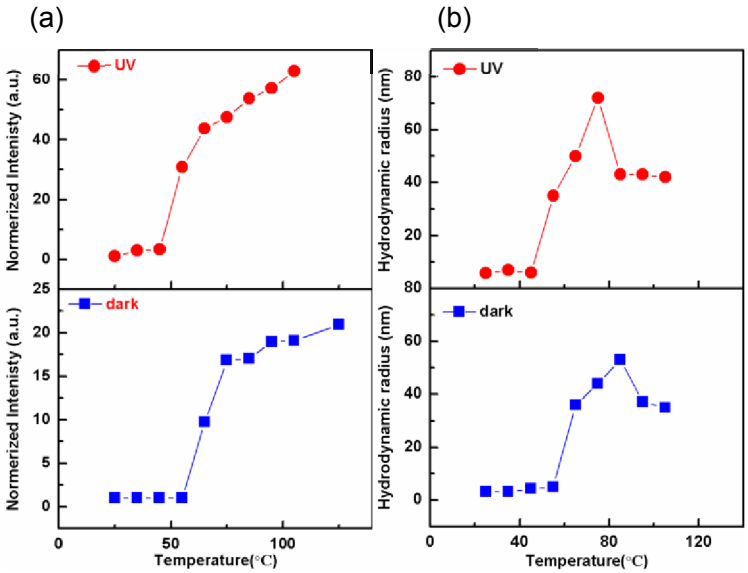

Figure 4. (a) Temperature dependence of the normalized scattering intensity and (b) hydrodynamic radius (R_h) for 0.1wt% PMP in ILs in the dark (blue) and UV irradiation (red) at a scattering angle of 90° and the weight ratio of [Azo][NTf_2]/[C_1mim][NTf_2] is 5/95. The normalized scattering intensity is defined as the intensity at each temperature divided by that measured at 25 °C.

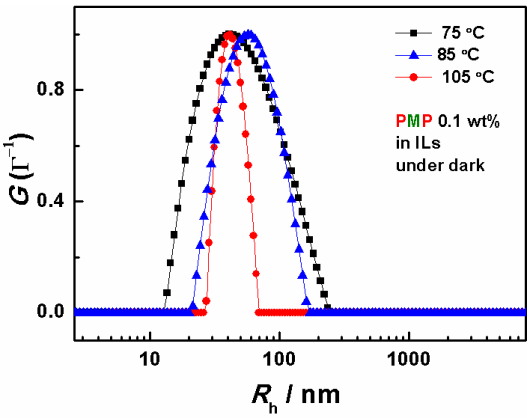

Figure 5. Hydrodynamic radius distribution for 0.1 wt% (a) PMP solution above the LCST temperatures in the dark. The weight ratio of [Azo][NTf_2]/[C_1mim][NTf_2] = 5/95. $G(\Gamma^{-1})$ corresponds to the characteristic decay time distribution functions.

inducing a change of particle size and number. Therefore, a higher normalized scattering intensity obtained in *cis*-ILs is reasonable, since scattering intensity is proportional to the number and size of particles [24-25, 37-41]. In short, micellization temperatures for PMP solutions are dependent on photoisomerization of azobenzene molecules, and micellization temperature in *cis*-ILs is around 10 °C lower than that in *trans*-ILs, because PPhEtMA shows a lower T_{cp} (45 °C) in *cis*-ILs compared with that in *trans*-ILs.

Here, note that micelles with larger R_h values around 200 nm in *trans*-ILs were emerged below 85 °C in the dark as shown in **Figure 5**, however, the fraction of those larger particles is low. In this regime, an association in polydisperse and loose aggregations of triblock copolymers is perhaps ascribed to induce the large radius. Particularly, [Azo][NTf_2] as a good solvent will lower the solvent selectivity for aggregate structure, thus, resulting in a large radius as well [42-45]. Also, the increasing size of micelle above LCMT may be originated from the swelling of the micelles by ILs. At 105 °C, the R_h peak related to the large particles completely disappeared and R_h distribution is basically kept narrow and constant. That is to say, the polymer solution exhibits an aggregate compaction as the temperature increased above the LCST. In addition, the viscosity of the solution decreased with increasing temperature as expected (**Figure 6**), suggesting that there is only micelle existed, without morphology transition from micelle to vesicles above LCST [46-50].

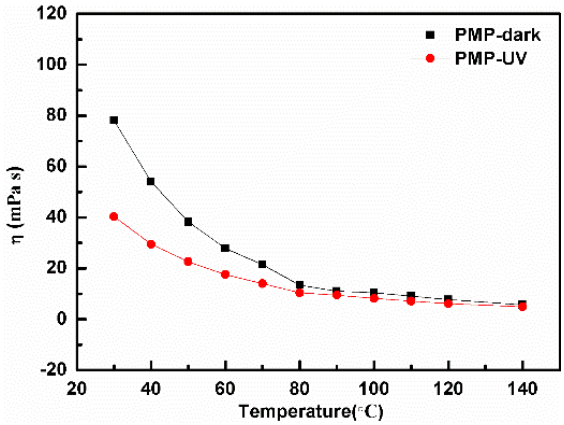

Figure 6. Temperature dependence of viscosity in 0.1 wt% PMP solutions in IL mixture in the dark (black) and under UV irradiation (red). The weight ratio of [Azo][NTf_2]/[C_1mim][NTf_2] = 5/95.

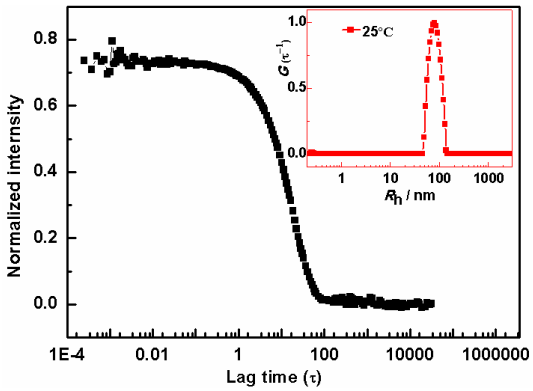

Figure 7. Hydrodynamic radius distribution for 1 wt% PMP solutions at 25 °C in the dark. The weight ratio of [Azo][NTf_2] /[C_1mim][NTf_2] is 5/95.

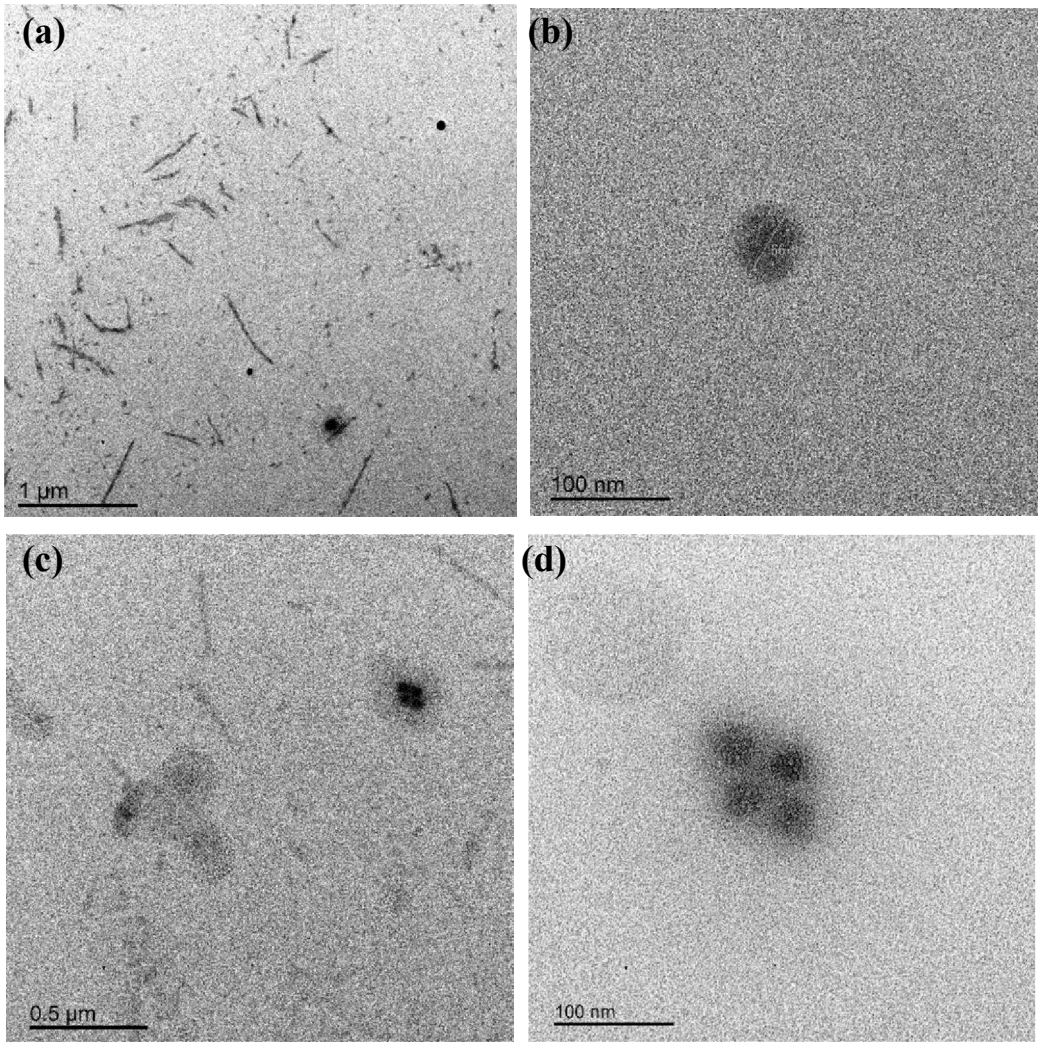

Figure 8. The cryo-TEM image of 1 wt% PMP polymer in *trans*-ILs quenched by liquid nitrogen. The weight ratio of [Azo][NTf_2]/[C_1mim][NTf_2] was 5/95.

A 1 wt% PMP solution showed LCMT behavior at 25 °C in **Figure 7** and micelle were formed at room temperature, which was advantageous for preparing thin film by diluting method under TEM observation. However, micellization temperature of 0.1 wt% PMP solution was above 65 °C, and the temperature was too high to process thin layer by quenching. Further, processing the UV source upon the measurements was also infeasible. Therefore, the micellar morphology of 1 wt% PMP solution and single micelle were observed by cryo-TEM as shown in **Figure 8**, respectively. Only micelles formed at room temperature in *trans*-ILs were observed. And morphology coexisted in the systems as reported in similar systems, which is in good agreement with the existence of loose aggregations at lower temperature suggested by DLS results. There were some wormlike micelles and sphere as shown **Figure 8a and Figure 8c**. **Figure 8d** shows a small aggregation micelle. The size of single micelle agrees well with the value observed in DLS, around 66 nm.

4.2.3 Photoinduced micellization behaviors

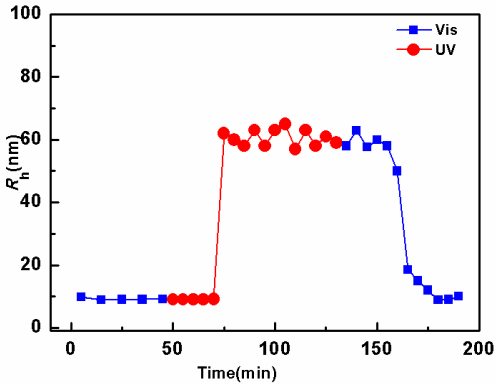

Figure 9. Photoinduced self-assembly of PMP at 55 ºC by illumination of vis-UV-vis by illumination of UV-vis-UV. Hydrodynamic radius (R_h) for 0.1 wt% solution under vis (blue) and UV irradiation (red) at a scattering angle of 90° was plotted and the weight ratio of [Azo][NTf_2]/[C_1mim][NTf_2] was 5/95.

Taken an advantage of the micellization temperature differences between in *cis*-ILs and *trans*-ILs and the distinct difference in the photoresponse between PMP and BMB solutions, we next demonstrate photoinduced "*unimer-to-micelle*" and "*micelle-to-unimer*" transitions at constant temperatures. Reversibly photoinduced self-assembly change between unimer and micelle for a PMP solution was successfully achieved, as shown in **Figure 9**. After keeping PMP polymer solutions at 55 °C under visible light irradiation overnight, that single polymer chains self-assemble into micelles in *cis*-ILs. Early in the aggregation process, there are unimers and relatively large aggregates (micelles) coexisted as shown in **Figure 10a**. After

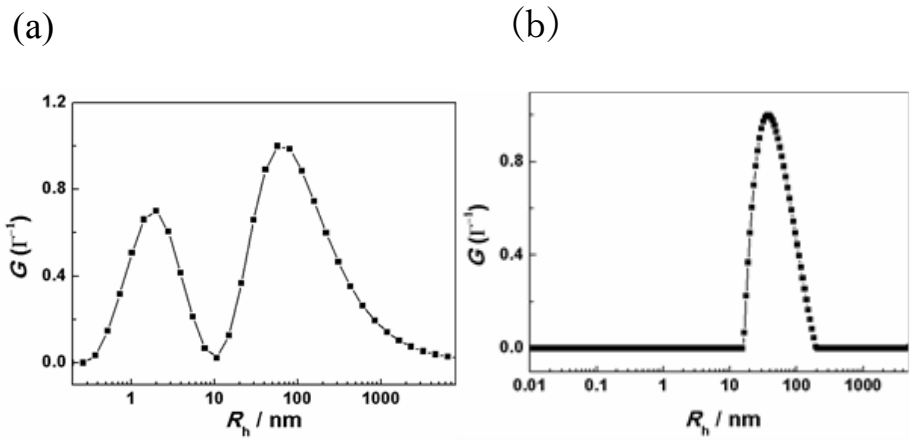

Figure 10. Photoinduced self-assembling process of PMP triblock copolymer at 55 ºC upon UV light irradiation for 45 min (a) and 80 min (b).

80 minutes later, complete micellization was observed in **Figure 10b**. Under visible light irradiation again, the demicellization process occurred since *trans*-ILs is compatible with PPhEtMA segments at current temperature. Decreasing R_h indicates the photoresponsive micelle to unimer transition under visible light illumination. The rapid demicellization (50 min) was observed as less polymer diffusion is required.

4.3 Photo/thermoresponsive sol-gel transitions

4.3.1 Experiments

Rheological measurement was taken on an Anton Paar Physica MCR 301 Rheometrics using a 25 mm diameter cylindrical rotor on a glass plate to let light get through. A gap spacing of approximately 0.2 mm was used for the all experiments. Temperature dependence of the elastic moduli in the range of was conducted with a strain (γ) of 2% from 30 to 140 °C at 0.3 ºC/min. The intersection of G′ and G" curves was taken as the critical gelation temperature of the ion gels. The dynamic frequency measurements were taken at various temperatures to study the relaxation time of polymer in *trans*-ILs and *cis*-ILs and the measurements was performed after waiting 60 min to achieve equilibrium. Dynamic strain sweep was performed at 0.1 rad/s to determine the linear viscoelastic regime of the ion gels above the gelation temperature. The upper limit of the linear viscoelastic regime is defined as the critical strain, γ_c, below which the dynamic modulus remains invariant.

4.3.2 Thermoresponsive sol-gel transitions

We previously discussed the photo/thermo-responsive LCST behaviors of PPhEtMA homopolymers in ionic liquid mixtures. PPhEtMA shows a higher cloud temperature in *trans*-ILs compared with that in *cis*-ILs. The difference in cloud temperatures under UV and in the dark is defined as bistable temperature. Thus, cloudy PPhEtMA solution become clear under visible light irradiation and again become turbid under UV illumination within bistable temperature window. A photoswitchable aggregation behavior of PPhEtMA was achieved.

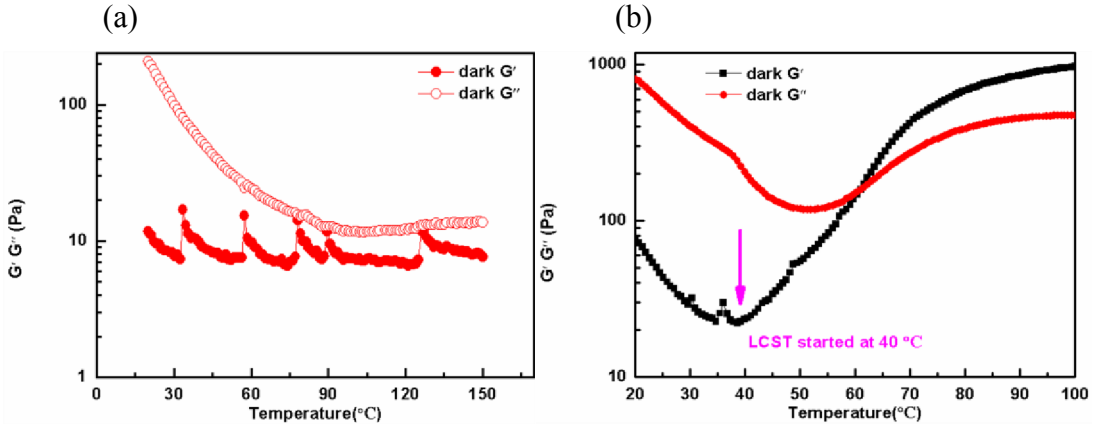

Figure 11. Dynamic temperature sweeps of 10 wt% PMP (a) and 20wt% PMP (b) in ionic liquid mixtures at a heating rate of 0.3°C/min. The weight ratio of [Azo][NTf_2] /[C_1mim][NTf_2] is 5/95.

The thermoresponsive gelation of PMP gives rise to the different soluble behaviors of three blocks. At lower temperatures, all segments are totally compatible with ionic liquid mixtures, while at a higher temperature, endblocks occurred LCST behaviors, leading to self-assembly of triblock copolymers. Thus, micelle was formed with PPhEtMA cores and PMMA corna. In polymer solutions (< 10 wt%), micelles do not exhibit the long-range order or form gels and thus behave as viscoelastic fluids as shown in **Figure 11(a)**. By increasing the polymer concentration to 20 wt%, we observed the gelation of PMP in ionic liquid mixtures and then characterized the network formed at higher temperatures in the dark as shown in **Figure 11(b)**.

By increasing [Azo][NTf_2] content as the weight ratio of [Azo][NTf_2] /[C_1mim][NTf_2] is 10/90, there is no gelation behavior observed in 20 wt% polymer solutions as shown in **Figure 12(a)** in the dark. It seems that [Azo][NTf_2] as a good solvent can greatly swollen the cores and shells, resulting an inefficient and loosely aggregated polymeric network. Even in such a higher concentrated polymer

(a) (b)

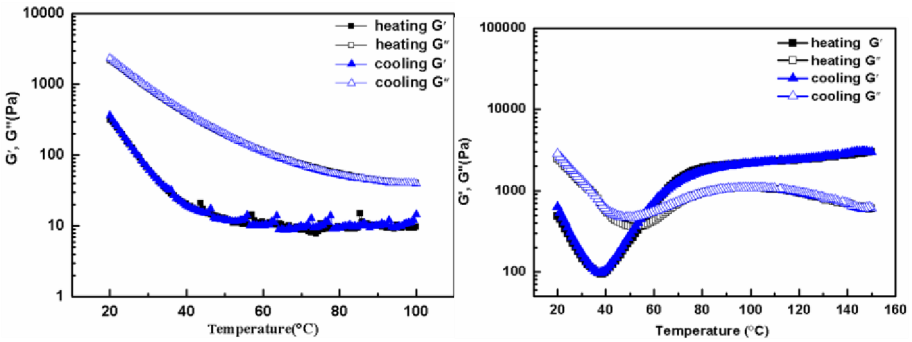

Figure 12. Dynamic temperature sweep of 20 wt% (a) and 30 wt% PMP (b) in the ionic liquid mixture in the dark upon heating (black colour) and cooling process (blue colour) at a rate of 0.3ºC/min. The weight ratio of [Azo][NTf_2] /[C_1mim][NTf_2] is 10/90.

solutions, no gel was formed, showing a liquid-like behavior when LCST behavior did occur.

Dynamic temperature sweeps of 30wt% PMP samples in ionic liquid mixture with the weight ratio of [Azo][NTf_2]/[C_1mim][NTf_2] 10/90 was shown in **Figure 12 (b)**, demonstrated the thermoreversible gelation of PMP arising from the assembling of PPhEtMA micelle cores under dark. G′ and G" were measured from 20 to 140 ºC with a temperature ramp of 0.3 ºC/min. Polymer solutions show similar rheological response as reported in other thermoresponsive ion gel systems. At a lower temperature, the systems display as a viscoelastic fluid. Upon heating, G′ and G" increased sharply, ascribed to a solid-like state where G′ is greater than G". The temperature when there is an intersection between G′ and G" is called as sol-gel transition temperature (T_{gel}). For 30 wt% PMP polymer solutions, G′ and G" values intersected at 54.3ºC. Cooling the sample produced the similar curves, with a slightly higher gelation temperature at 55.6 ºC. This modest hysteresis (~2 ºC) agrees well with previous studies of PPhEtMA cores in common ionic liquid for a bigger difference between gelation temperature and glass temperature of PPhEtMA cores. Upon the cooling, the network disappears via the disrupting the physically associated cross-linker points of PPhEtMA blocks.

There is a notable decreasing of G" and an increasing of G′ above 110 ºC (**Figure 12(b)**). We hypothesize that this feature results from excluding remaining [C_1mim][NTf_2] in PPhEtMA micelle cores, since [Azo][NTf_2] is a good solvent for PPhEtMA while PPhEtMA is insoluble in [C_1mim][NTf_2]. Without addition of [Azo][NTf_2], in 100 wt% [C_1mim][NTf_2], an opposite trend is observed as

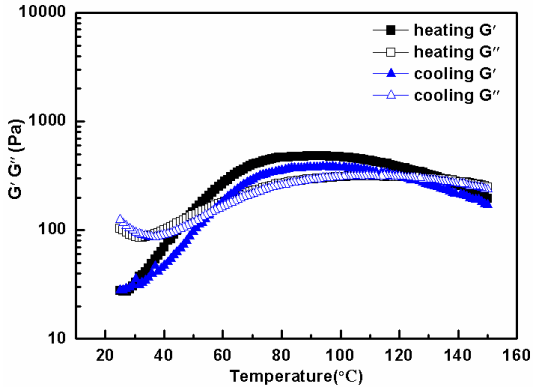

Figure 13. Dynamic temperature sweep of 20 wt% PMP in neat [C_1mim][NTf_2] upon heating (black color) and cooling process (blue color) at a rate of 0.3ºC/min.

demonstrated in **Figure 13**. G′ is decreasing while G" is increased above 110 ºC because of melting polymers with a lower T_g (35 ºC). At a higher temperature, far away from T_g of PPhEtMA segment, the polymer will melt and result a rubbery cross-linker points, with decreasing G′ value and increasing G". Obviously, adding [Azo][NTf_2] contributes to an opposite rheology behavior. Above the gelation temperature, the ionic liquid mixture contained in the PPhEtMA cores will be excluded out. [C_1mim][NTf_2] is believed to be expelled first since PPhEtMA is insoluble in [C_1mim][NTf_2] and small size of [C_1mim][NTf_2] favors its moving in networks. [Azo][NTf_2] with a bigger cation is totally compatible with PPhEtMA, giving favor to stay in cores even at a higher temperature. Thus, increasing polymer concentration in the cores by increasing temperature are assumed to contribute the increasing G′ value and decreasing G". This behavior is consistent with SAXS experiment, which we will discuss later.

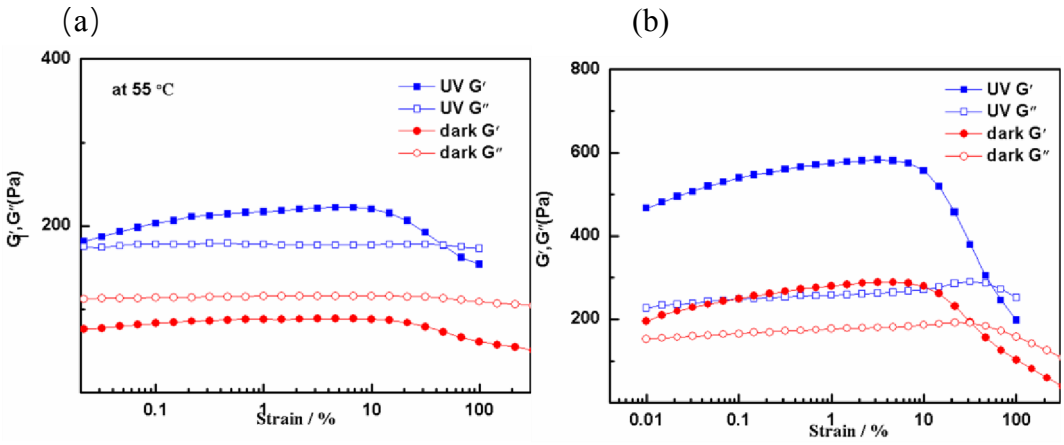

Figure 14. Strain dependence of the G' and G" for 20 wt% PMP polymers in mixed solution of [Azo][NTf_2] and [C_1mim][NTf_2] at 55 and 80 ºC. The weight ratio of [Azo][NTf_2]/ [C_1mim][NTf_2] is 5/95 (f=1 Hz, ω = 6.28 rad/s).

Strain-dependent measurements of the ABA triblock copolymer solution showed that G′ and G" values were strain independent in the range γ = 0.01–50% as demonstrated in **Figure 14**. At 55 ºC, under UV irradiation there was gel formed at strain of 45%, and it acted like a viscoelastic fluid in the dark. At 80 ºC, a stronger gel was formed compared with the gel in the dark. Those phenomena were in consistent with temperature dynamic sweep behaviors. G′ value is higher under UV than that in the dark, due to a compact cross-linker points, owing to the fact that *cis*-ILs has a lower affinity to the polymers PPhEtMA than *trans*-ILs.

The rheology measurement was also conducted under UV irradiation, a much more lower gelation temperature was observed at 50.7 ºC as shown in **Figure 15**. Clearly, the temperature for starting aggregation in *cis*-ILs (34.2 ºC) as 10 ºC lower than that in *trans*-ILs (44.4 ºC) due to a lower affinity of *cis*-ILs (*cis*-IL: [Azo][NTf_2] exists mainly in the *cis*-[Azo][NTf_2] form) to PPhEtMA. At a higher temperature above 100 ºC, the values of G′ in *trans*- and *cis*-ILs are similar because *cis*-azobenzene cannot survive.

Dynamic frequency sweeps were performed across a temperature range, with those three representative temperatures of 40, 65 and 90ºC in *trans*-ILs as shown in **Figure 16**. At 40 ºC, G′ < G", consistent with liquid-like behavior, G′~ ω^1, G"~ω^2. The power law fits the display terminal rheological behavior for a viscoelastic fluid. The deviation of G′ at a lower frequency from predicted dependence is likely attributed by an addition frequency relaxation. At 65 ºC, G′ and G" overlap and follow the same power dependence: G′≈ G"~ $\omega^{0.5}$. This dependence resembles the sol-gel transitions behavior between liquid-like and solid-like (T_{gel}). At a temperature of 90

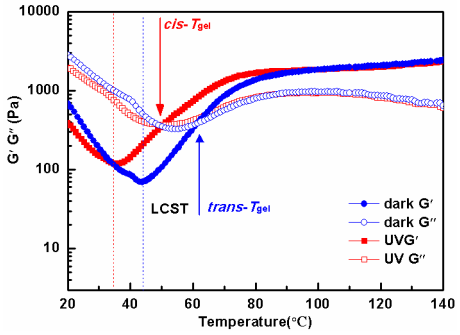

Figure 15. Dynamic temperature sweep of 30 wt% PMP in ionic liquid mixtures under UV upon heating (black colour) and cooling process (blue colour) at a rate of 0.3ºC/min. The weight ratio of [Azo][NTf_2] /[C_1mim][NTf_2] is 10/90.

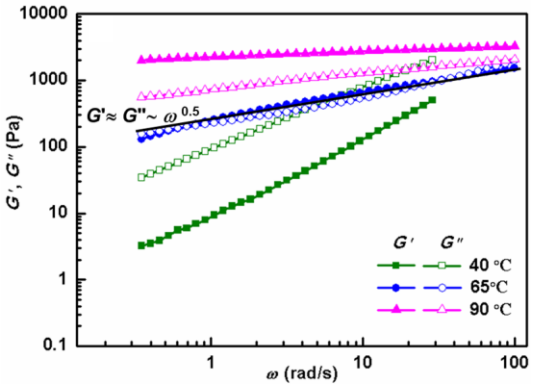

Figure 16. Dynamic frequency sweep of 30 wt % PMP in the IL mixture at 40 ºC (green), 65 ºC (blue) and 90 ºC (pink) with a strain amplitude of 3%. The weight ratio of [Azo][NTf_2]/[C_1mim][NTf_2] is 10/90.

ºC, *G′* values were greater than *G″* values at the whole frequency range, and were almost independent of frequency, suggesting a solid-like state.

4.3.3 Photoinduced sol-gel transitions

A reversible sol-gel-sol transition cycle showed changes in the macroscopic state of the composite induced by a small molecular trigger as shown in **Figure 17**. The ion gel was kept at a bistable temperature of 57 ºC upon visible light illumination overnight to generate *trans*-ILs. Followed by switching to UV source at time, 20min, the G′ value started to increase immediately and reached at 700 Pa while G″ was slightly increased. The illumination then switched back to visible light to reform the *trans*-ILs, the G′ dropped to the initial level and lower than G″, back to initial sol

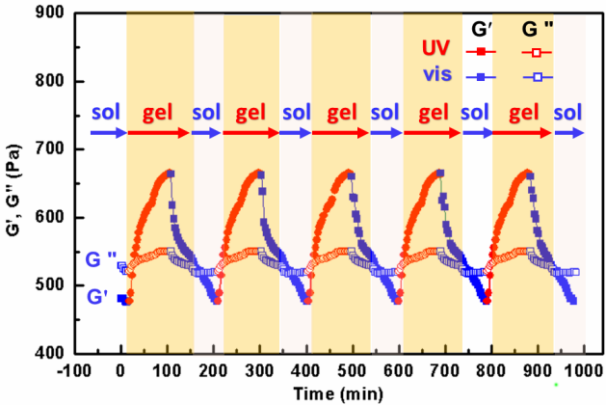

Figure 17. Photo responsive dynamic shear moduli G′ (solid) and G″ (open) for 30 wt% PMP polymers in mixed solution of [Azo][NTf_2] and [C_1mim][NTf_2] (w = 1 rad/s, g = 1%). The weight ratio of [Azo][NTf_2] / [C_1mim][NTf_2] is 10/90

state, which takes a longer time, around 90 min. The result suggested that the polymer network in the azobenzene containing can achieve the sol-gel transitions

$$G' = vkT = fnkT$$

based on the photoswitching assemble/ disassemble of PPhEtMA segments. The photoresponsive sol-gel transition temperature was controlled by the photochromic state of azobenzene in ionic liquid that can dramatically change the solubility behavior of PPhEtMA. Elasticity theory [54-57] predicts that the network modulus G′

where v is the number density of elastic effective chains, k is Boltzmann constant, T is absolute temperature, f is the faction of elastically effective chains, and n is the number density. From this relation, n after several cycles, barely no change, was estimated to be around 1.56×10^{23} m^{-3}.

4.4 Small-angle X-ray scattering experiments

4.4.1 Experiments

Small-angle X-ray scattering experiments were performed on the 20 wt% sample using Anton Parr SAXSess mc^2 instrument. The capillary was purchased from TOHO and the diameter is 1.5mm. The sample was flam-sealed before conducting measurements under vacuum on a TCS120 sample holder with a precise temperature control from -30 to 120 ºC.

4.4.2 Results of SAXS measurements

We conducted small-angle X-ray scattering (SAXS) experiments for the ion gel containing 20 wt% PMP in ionic liquid mixture. **Figure 18** shows SAXS data of 20 wt% PMP/ILs composites at 60ºC. The 20 wt% PMP solution showed a distinct first form factor minimum at q = 0.24 nm^{-1}. Given that the electron density difference between PPhEtMA and ILs is much larger than that between PMMA and ILs, we consider the scattering intensity mainly comes from the PPhEtMA core and therefore, the PPhEtMA core radius (R_c) can be calculated as 18.7 nm from the relationship of qR_c = 4.49 for hard spheres [58-60]. The aggregation number (N_{agg}) of 586 was

estimated from the R_c and the density of PPhEtMA, ρ = 1.129 g/cm^3. But this value suggests the cores are swollen by ionic liquid. From **Figure 18** at 60 ºC above the LCST temperature, we observed Bragg reflections at $\sqrt{3}\ q^*$: $\sqrt{4}q*$:$\sqrt{8}\ q^*$:$\sqrt{11q*}$:$\sqrt{16}q*$: $\sqrt{20}$ (q^* = 0.064 nm^{-1}) as indicated filled triangles, and the peaks suggest the PPhEtMA sphere aggregations were packed as face-centered cubic structure [61-65]. We can also estimate the average distance between two neighboring PPhEtMA domains is 28.9 nm by assuming the formation of simple cubic lattice ($d = 2\pi/q^*$) from the first Bragg peak maximum. The value is reasonable judging from R_h and R_c of PMP micelle (60 nm from dynamic light scattering measurements).

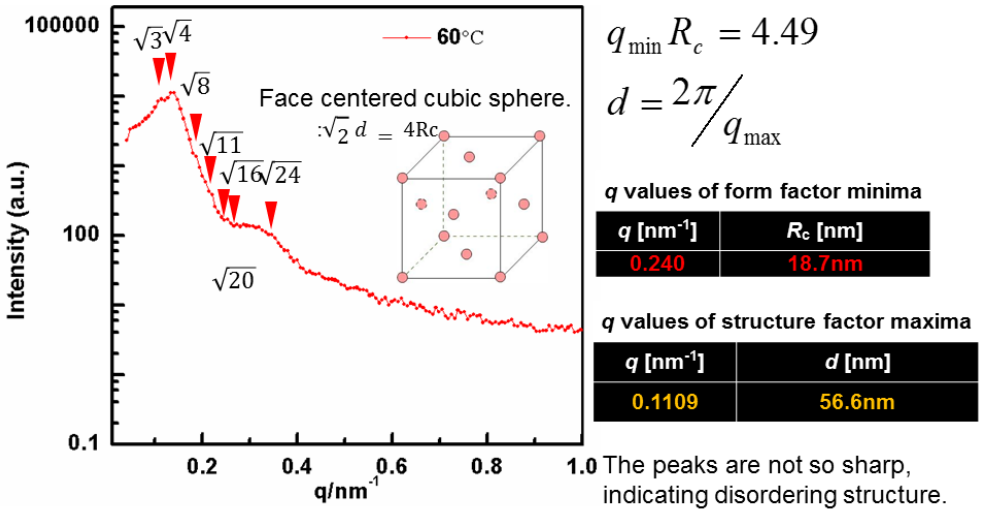

Figure 18. SAXS data of 20 wt% PMP in the IL mixture at 60 ºC. and the weight ratio of [Azo][NTf$_2$] / [C$_1$mim][NTf$_2$] is 5/95.

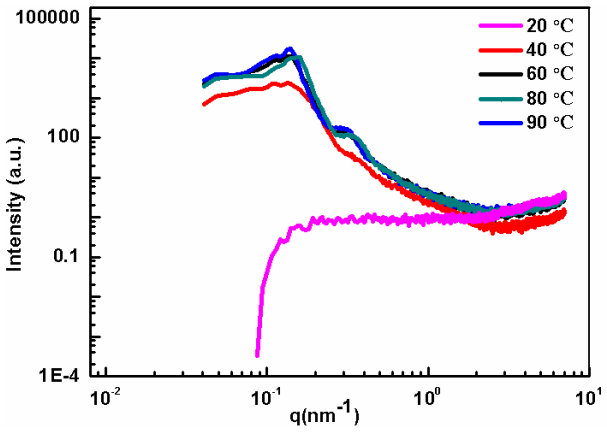

Figure 19. SAXS independent on increasing temperature for 20 wt% PMP triblock copolymers in mixed ILs. The weight ratio of [Azo][NTf$_2$] / [C$_1$mim][NTf$_2$] is 5/95.

Additionally, temperature dependence of the morphology in the ion gel was also investigated.

We conducted SAXS measurement with heating from 25 to 90 °C. LCST behavior are assumed to occur around 40℃ when some weak peak appeared (see **Figure 19**). By increasing temperature, the peak shape become clear because harder cores are formed with expelling ionic liquid out the cores, eventually yielding the close-packing of the micelles (gelation) by PMP molecules, similar phenomena have been reported in NIPAm in water phase. Notably, there is a tiny shift at 80 °C. Perhaps at 80 °C, most of ionic liquids was expelled out, the structure become compact. However, at 90 °C azobenzene ionic liquid can continue to swollen the core and shell because azobenzene ionic liquid shows temperature-independent positive affinity to PPhEtMA cores (PPhEtMA is totally soluble in Azo ionic liquid). In another hand, from the temperature dependence result of the elastic moduli, it was also indicated that the above 40°C, G′ value, resembling solid property, abruptly increased in **Figure 20**, indicating the beginning of aggregation of PPhEtMA, in consistent with SAXS result. Also, both indicated polymeric network is dominated by excluding ionic liquid out to form the PPhEtMA cores. Increasing temperature attributed to increasing polymer concentration in the cores, resulting an ion gel induced by LCST behaviors.

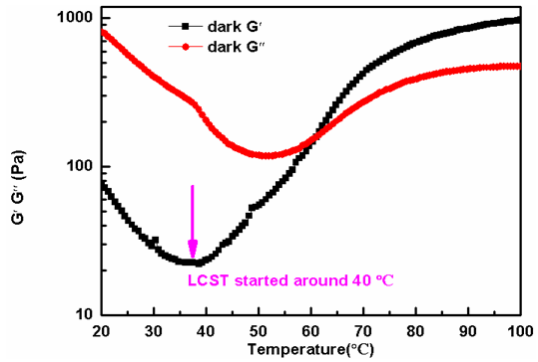

Figure 20. Temperature dependence of the dynamic shear moduli (G' and G'') for 20 wt% polymers in mixed solution of [Azo][NTf_2] and [C_1mim][NTf_2] (w = 1 rad/s, g = 1%).The weight ratio of [Azo][NTf_2] / [C_1mim][NTf_2] is 5/95.

4.5 Conclusions

After a better understanding of photoresponsive LCST behaviors, a well-designed ABA triblock copolymer has been utilized to inducing a percolating network in ILs.

Poly(2-phenylethyl methacrylate)-b-poly(methyl methacrylate)-b-poly(2-phenylethyl methacrylate) (PMP) was designed and synthesized via well-established ATRP using poly(methyl methacrylate) (PMMA) as a macroinitiator, where the A blocks are LCST segment, PPhEtMA, while B midblock is PMMA, totally compatible with ILs. In a diluted polymer solution, the hydrodynamic radius R_h value is below 10 nm, unimer state, in consistent with individual PMP polymer chains with a total molecular weight around 10 kDa at lower temperatures. But R_h increases significantly in *trans*-ILs at 65 ºC, suggesting that the PMP triblock copolymer self-assembles into micelles with PPhEtMA cores surrounded. Similar behavior has been observed in *cis*-ILs and micellization temperature (55 ºC) is lower than 65 ºC in *trans*-ILs. Between these temperature range, photoinduced micellization occurred owing that aggregating behaviors of the A blocks dependent on photoisomerization of azobenzene IL. At a modest concentration of polymer solutions, the A blocks associate into micellar cross-linkers, and the B blocks provide bridging connections between micelles, forming a polymeric network. Meanwhile, two different gelation temperatures based on isomerization of azobenzene ILs was obtained and in this temperature range, so was the photoinduced sol-gel transitions.

It is well-known that to process molecule materials to be a product, light as an external stimulus to process material is attractive and promising for its environment friendly, low toxic and precise control without contacting. Our research here provides a facile and novel way to process polymer materials based on solubility change switched by an azobenzene molecular trigger, different from reported light processable materials based on azobenzene functionalized polymers.

4.6 References

[1] Nayak P K, Hathorne A P, Bermudez H. *Phys. Chem. Chem. Phys*. **2013**, 15, 1806.
[2] Ueki T, Watanabe M. *Chem. Lett*. **2006**, 35, 964.
[3] Lee H N, Bai Z, Newell N, Lodge T P. *Macromolecules* **2010**, 43, 9522.
[4] Lee H N, Newell N, Bai Z, Lodge T P. *Macromolecules* **2012**, 45, 3627.
[5] Kodama K, Tsuda R, Niitsuma K, Tamura T, Ueki T, Kokubo H, Watanabe M. *Polym. J.* **2011**, 43, 242.
[6] He Y, Lodge T P. *J. Am. Chem. Soc*. **2006**, 128, 12666.
[7] Vijayakrishna K, Mecerreyes D, Gnanou Y, et al. *Macromolecules* **2009**, 42, 5167.

[8] Soto Figueroa C, del Rosario Rodriguez-Hidalgo M, Vicente L. *Soft Matter*, **2012**, 8,1871.
[9] Guerrero Sanchez C, Wouters D, Hoeppener S, et al. *Soft Matter.* **2011**, 7, 3827.
[10] Ueki T, Sawamura S, Nakamura Y, et al. *Langmuir* **2013**, 29, 13661.
[11] Ueki T, Nakamura Y, Yamaguchi A, Niitsuma K, Lodge T P, Watanabe M. *Macromolecules* **2011**, 44, 6908.
[12] Ueki T, Nakamura Y, Lodge T P, Watanabe M. *Macromolecules* **2012**, 45, 7566.
[13] Killian C M, Tempel D J, Johnson L K, Brookhart M. *J. Am. Chem. Soc.* **1996**, 118, 11664.
[14] Kumar G S, Neckers D C. *Chem. Rev*. **1989**, 89, 1915.
[15] Baba K, Ono H, Itoh E, Itoh S, Noda K, Usui T, Ishihara K, Inamo M, Takagi H D, Asano T. *Chem. Eur. J.* **2006**, 12, 5328.
[16] Zhao Y. *J. Mater. Chem*. **2009**, 19, 4887.
[17] Jochum F D, Theato P. *Chem. Commun.* **2010**. 46, 6717.
[18] Kitazawa Y, Ueki T, Imaizumi S, Lodge T P, Watanabe M. *Chem. Lett.* **2013**, 43, 204.
[19] Matyjaszewski K, Miller P J, Shukla N, Immaraporn B, Gelman A, Luokala B, Siclovan T M, Kickelbick G, Vallant T, Hoffmann H, Pakula T. *Macromolecules* **1999,** 32, 8716.
[20] Kitazawa Y, Ueki T, Niitsuma K, Imaizumi S, Lodge T P, Watanabe M. *Soft Matter*. **2012**, 8, 8067.
[21] Kakizawa Y, Harada A, Kataoka K. *J. Am. Chem. Soc.* **1999**, 121, 11247.
[22] Hassan P A, Kulshreshtha S K. J. *Colloid Interface Sci.* **2006**, 300, 744.
[23] Poppe A, Willner L, Allgaier J, et al. *Macromolecules* **1997**, 30, 7462.
[24] Tokuda H, Hayamizu K, Ishii K, Susan M A B H, Watanabe M. *J. Phys. Chem. B*. **2004**, 108, 16593.
[25] Tokuda H, Tsuzuki S, Susan M A B H, Hayamizu K, Watanabe M. *J. Phys. Chem. B*. **2006,** 110, 19593.
[26] Edward J T. *J. chem. Educ*, **1970**, 47, 261.
[27] Wilke C R, Chang P. *AIChE Journal* **1955**, 1, 264.
[28] Kholodenko A L, Douglas J F. *Physical Review E* **1995**, 51, 1081.
[29] Huang X J, Rogers E I, Hardacre C, et al. *J. Phys. Chem. B.* **2009**, 113, 8953.
[30] Harris K R. *J. Phys. Chem. B*. **2010**, 114, 9572.
[31] Morgan D, Ferguson L, Scovazzo P. *Ind. Eng. Chem. Res.* **2005**, 44, 4815.
[32] Tariq M, Forte P A S, Gomes M F C, et al. *J. Chem. Thermodyn.* **2009**, 41, 790.

[33] Huddleston J G, Visser A E, Reichert W M, et al. *Green chem.* **2001**, 3, 156.
[34] Zafarani Moattar M T, Majdan Cegincara R. *J. Chem. Eng. Data.* **2007**, 52, 2359.
[35] Deetlefs M, Seddon K R, Shara M. *Phys. Chem. Chem. Phys.* **2006**, 8, 642.
[36] Mokhtarani B, Mojtahedi M, Mortaheb H R, et al. *J. Chem. Eng. Data.* **2008**, 53, 677.
[37] LaRue I, Adam M, Pitsikalis M, Hadjichristidis N, Rubinstein M, Sheiko S. *Macromolecules* **2006**, 39, 309.
[38] Okabe S, Sugihara S, Aoshima S, Shibayama M. *Macromolecules* **2003**, 36, 4099.
[39] Wang G, Tong X, Zhao Y. *Macromolecules* **2004**, 37, 8911.
[40] Feng Z, Lin L, Yan Z, Yu Y. *Macromol. Rapid Commun*. **2010**. 31, 640.
[41] Tamura S, Ueki T, Ueno K, Kodama K, Watanabe M. *Macromolecules* **2009**, 42, 6239.
[42] Alexandridis P, Yang L. *Macromolecules* **2000**, 33, 5574.
[43] Nagarajan R, Wang C. *Langmuir* **2000**, 16, 5242.
[44] Yang L, Alexandridis P. *Langmuir* **2000**, 16, 4819.
[45] Koňák Č, Ganchev B, Teodorescu M, et al. *Polymer* **2002**, 43, 3735.
[46] Day R A, Robinson B H, Clarke J H R, et al. Journal of the Chemical Society, Faraday Transactions 1: Physical Chemistry in Condensed Phases, **1979**, 75, 132.
[47] Menger F M. *Acc. Chem. Res.* **1979**, 12, 11.
[48] Lin Z, Cai J, Scriven L E, et al. *J. Phys. Chem.* **1994**, 98, 5984.
[49] Kalur G C, Frounfelker B D, Cipriano B H, et al. *Langmuir* **2005**, 21, 10998.
[50] Maeda H, Tanaka S, Ono Y, et al. *J. Phys. Chem. B.* **2006**, 110, 12451.
[51] De Gennes P G. *Journal de Physique Letters*, **1976**, 37, 1.
[52] Shih W H, Shih W Y, Kim S I, et al. *Physical review A* **1990**, 42, 4772.
[53] Aggeli A, Bell M, Boden N, et al. *Nature* **1997**, 386, 259.
[54] Mitchell J R. *J. Texture Studies*. **1980**, 11, 315.
[55] Hong W, Zhao X, Zhou J, et al. *J. Mech. Phys. Solids* **2008**, 56, 1779.
[56] Rubinstein M, Colby R H. Polymer Physics, Oxford University Press, New York, **2003**.
[57] Zhang S, Lee K H, Sun J H, Frisbie C D, LodgeT P. *Macromolecules* **2011**, 44, 8981.
[58] Liu Y, Nie H, Bansil R, et al. *Physical Review E* **2006**, 73, 061803.
[59] Laurati M, Stellbrink J, Lund R, et al. *Physical Review E*, **2007**, 76, 041503.
[60] Boon N, Schurtenberger P. *Phys. Chem. Chem. Phys.* **2017**. DOI: 10.1039/C7CP02434G.

[61] Daniel C, Hamley I W, Mingvanish W, et al. *Macromolecules* **2000**, 33, 2163.
[62] Hamley I W, Pople J A, Diat O. *Colloid Polym. Sci.* **1998**, 276, 446.
[63] Hamley I W, Pople J A, Fairclough J P A, et al. *J. Chem. Phys.* **1998**, 108, 6929.
[64] Hamley I W, Mortensen K, Yu G E, et al. *Macromolecules* **1998**, 31, 6958.
[65] Huang Y Y, Chen H L, Hashimoto T. *Macromolecules* **2003**, 36, 764.

Chapter Five

Photo/thermoresponsive micellizations and gelations of the BMB solution

5.1 Synthesis of BMB triblock copolymers

Synthesis of PMMA macroinitiator

A PMMA macroinitiator was synthesized via ATRP with a bifunctional initiator. Pre-dried mixture of CuBr (16 mg, 0.11 mmol), $CuBr_2$ (1.0 mg, 4.5 μmol), and PMDETA (39 μL, 0.19 mmol) were dissolved in anisole (40 mL) at room temperature to obtain a transparent solution. The solution of MMA (20 mL, 0.19 mol) and bifunctional initiator (37.6 mg, 0.34 mmol) was added at room temperature. After being degassed three times by the method of freeze-pump-thaw cycles, the polymerization began at 60 °C for 6 h and was terminated by quenching the solution with dry ice/methanol. PMP was characterized using ^{1}H-NMR spectroscopy and size exclusion chromatography (SEC). The number-average molecular weight (M_n) was calculated by ^{1}H-NMR, and the dispersity (M_w/M_n, where M_w is the weight-average molecular weight) was determined by SEC calibrated with PMMA standards using THF as the eluent (**Figure S1**). **Table 1** shows the related results.

Table 1. Molecular weight of polymers synthesized in this study.

	M_n (kDa)[a]	PDI (M_w/M_n)[b]
PMMA [c]	42	1.13
BMB	32-42-32	1.10

a M_n of PMMA was estimated by using ^{1}H-NMR. The M_n of BMB was calculated from the results of the ^{1}H-NMR based on precursor. b Determined by SEC analysis in THF. c Macroinitiator of BMB via ATRP method.

Synthesis of triblock copolymer BMB

BMB was prepared by the similar way of PMP block copolymer as follows. Pre-dried mixture of CuBr (32 mg, 0.23 mmol) and $CuBr_2$ (1.0 mg, 4.5 μmol), PMMA macro initiator (9.5 g, 0.23 mmol), BnMA (15 g, 85 mmol), PMDETA (57 μL, 0.27 mmol) were mixed in anisole (90 mL) at room temperature. Then the homogeneous solution was degassed three times in use of freeze-pump-thaw cycles, and polymerization was carried out at 80 °C and terminated by quenching the solution with dry ice/methanol. The product was purified by reprecipitation twice using ethyl acetate as a good solvent and methanol as a poor solvent. BMB was dried for 8 h at

65 °C under vacuum and characterized by the similar manner of PMP (**Figure 1**) as listed in **Table 1**.

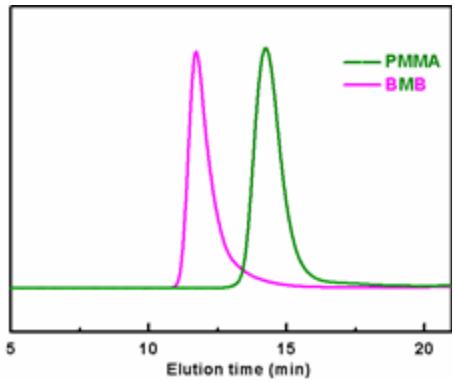

Figure 1. Size exclusion chromatography (SEC) elution curves of BMB and PMMA macroinitiator using THF as an eluent.

5.2 Photo/thermoresponsive micellization behaviors

5.2.1 Thermoresponsive micellization behaviors

As for BMB triblock copolymer solutions, corresponded DLS measurements also have been conducted in the dark and under UV irradiation, respectively. In the dark at lower than 100 °C, R_h was lower than 10 nm, ascribed to the single polymer chains (**Figure 2**). A discontinuously increasing scattering intensity and R_h were observed at 110 °C when LCMT occurred. There is one aggregation peak appeared at 110 °C when LCST occurred, ascribed to the micelle formed, 63 nm (**Figure 2**). By further increasing temperature, a narrower distribution of micelle size was obtained in **Figure 3.** Again, under UV irradiation, the LCMT phenomenon occurred at 120 °C, higher than that in *trans*-ILs, whose results coincide with PBnMA homopolymer systems that T_{cp} in *cis*-ILs is higher than *trans*-ILs. The normalized scattering intensity in *cis*-ILs was also much higher than that in *trans*-ILs above LCMT (**Figure 2a**), similar to the behavior of PBnMA homopolymer solutions. The polarity change of the solvents perhaps is mainly responsible for such behavior with increasing number and micellar size [1-5]. In short, micellization temperature dependences on photo-isomerization of [Azo][NTf_2] are still retained that the micellization

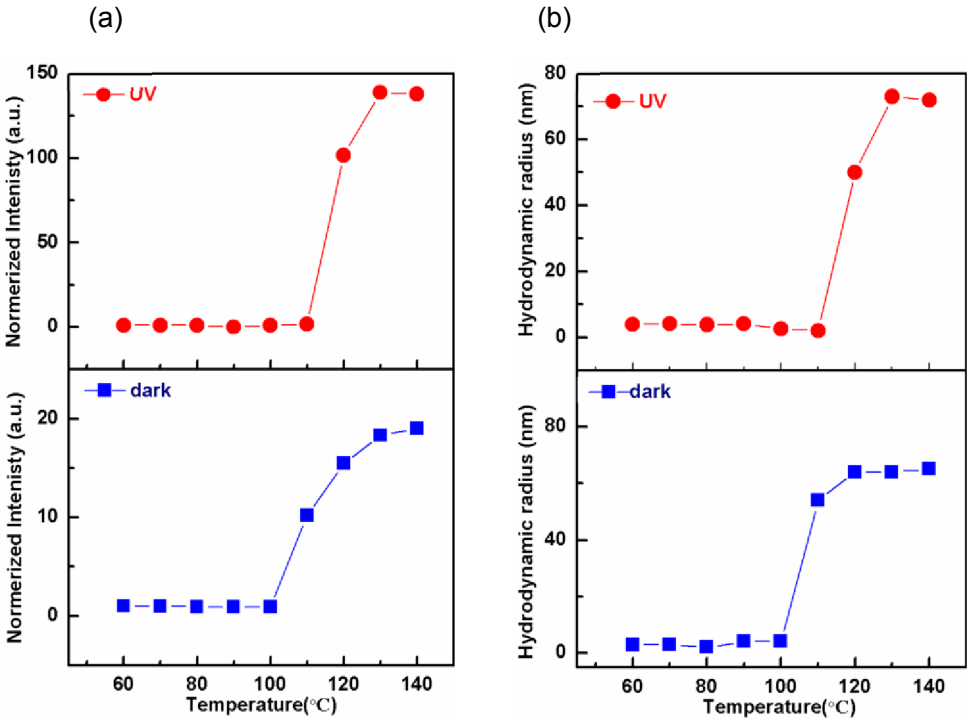

Figure 2. Temperature dependence of (a) normalized scattering intensity and (b) hydrodynamic radius (R_h) for 0.1 wt% BMB in ILs in the dark (blue) and UV irradiation (red) at a scattering angle of 90° and the weight ratio of [Azo][NTf_2]/[C_1mim][NTf_2] was 5/95. The normalized scattering intensity is defined as the intensity at each temperature divided by that measured at 25 °C.

temperature in *cis*-ILs is higher than that in *trans*-ILs. Note that the photoresponse is just against with that in PMP solutions.

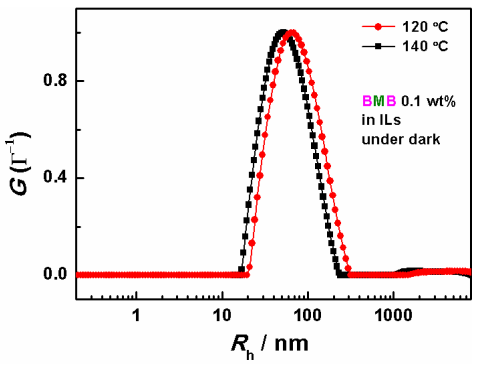

Figure 3. Hydrodynamic radius distribution for 0.1 wt% BMB solutions above the LCST temperatures in the dark. The weight ratio of [Azo][NTf_2]/[C_1mim][NTf_2] = 5/95. $G(\Gamma^{-1})$ corresponds to the characteristic decay time distribution functions.

5.2.2 Photoresponsive micellization behaviors

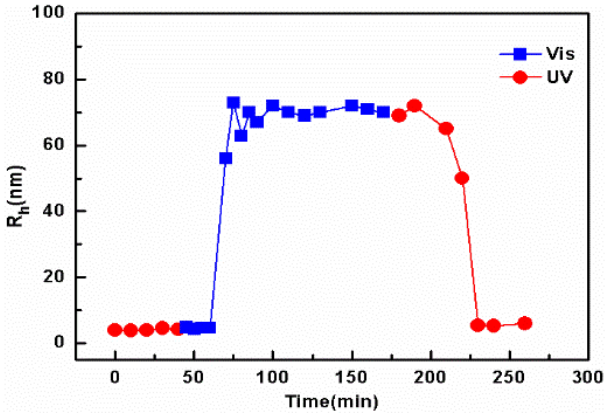

Figure 4. Photoinduced self-assembly of BMB at 110 ºC by illumination of UV-vis-UV. Hydrodynamic radius (R_h) for 0.1 wt% solution under vis (blue) and UV irradiation (red) at a scattering angle of 90° was plotted and the weight ratio of [Azo][NTf_2]/[C_1mim][NTf_2] was 5/95.

The photoresponsive micellization/demicellization of the BMB solution was also performed with tuning the light sources, visible or UV illumination (**Figure 4b**). Before moving to visible illumination, the BMB solution was irradiated by UV light overnight at 110 °C to gain *cis*-ILs. The unimer takes 25 min to start the aggregation under visible light irradiation, following with unimer to micelle transitions and demicellizations from micelle to unimer cost a shorter time, 40 mins owing to the absence of polymer diffusion step.

5.3 Thermoresponsive gelation of BMB polymer

5.3.1 Experiments

Rheological measurement was taken on an Anton Paar Physica MCR 301 Rheometrics using a 25-mm diameter cylindrical rotor on a glass plate to let light get through. A gap spacing of approximately 0.2 mm was used for the all experiments. The elastic moduli (G′ and G") was examined in the linear viscoelastic regime. The intersection of G′ and G" curves was taken as the critical gelation temperature of the ion gels.

5.3.2 Thermoresponsive sol-gel transitions

We previously discussed the photo/thermos-responsive LCST behaviors of PBnMA homopolymers in ionic liquid mixtures in **Chapter 3**. PBnMA shows a lower cloud temperature in *trans*-ILs compared with that in *cis*-ILs. The different cloud temperatures under UV and in the dark is defined as bistable temperature window. In the bistable temperature range, PBnMA polymer solution became cloudy under visible light irradiation yet again turned to be transparent upon UV illumination. The thermoresponsive gelation of BMB gives rise to the different compatibilities of three blocks. At lower temperature, all segments are totally compatible with ionic liquid mixtures, while at a higher temperature, endblocks occurred LCST behaviors, leading to self-assembly of triblock copolymers.

Dynamic temperature sweeps of 20 wt% BMB samples in ionic liquid mixture with the weight ratio of [Azo][NTf_2]/[C_1mim][NTf_2] 5/95 shown in **Figure 5**, demonstrate the thermoreversible gelation of BMB arising from the assembling of PBnMA micelle cores under UV. G′ and G" were measured from 20 to 140 ºC with a temperature ramp of 0.3 ºC/min. Polymer solutions show similar rheological response as reported in thermoresponsive ion gel systems [6-13]. At a lower temperature, the systems displayed as a viscoelastic fluid. Upon heating above 110 ºC, G′ increased sharply, ascribed to LCST behavior. G′ and G" values intersected at 129.2ºC, which is in agreement with the T_{gel} decided by frequency sweep measurements. Cooling the sample produced the similar curves, with a slightly higher gelation temperature at 130.9ºC. This modest hysteresis (~2 ºC) is reasonable

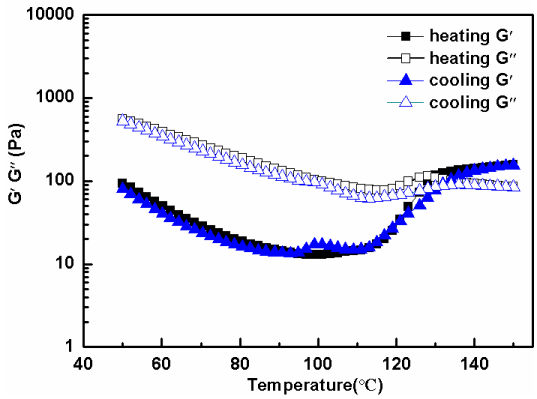

Figure 5. Dynamic temperature sweep of 20 wt% BMB in the ionic liquid mixture under UV upon heating (black colour) and cooling process (blue colour) at a rate of 0.3ºC/min. The weight ratio of [Azo][NTf_2] /[C_1mim][NTf_2] is 5/95.

owing to a larger difference between gelation temperature and glass temperature of PBnMA cores. Upon the cooling, the network disappears via the disrupting the physically associated cross-linker points of PBnMA blocks.

5.3.3 Photoresponsive gelation behaviors

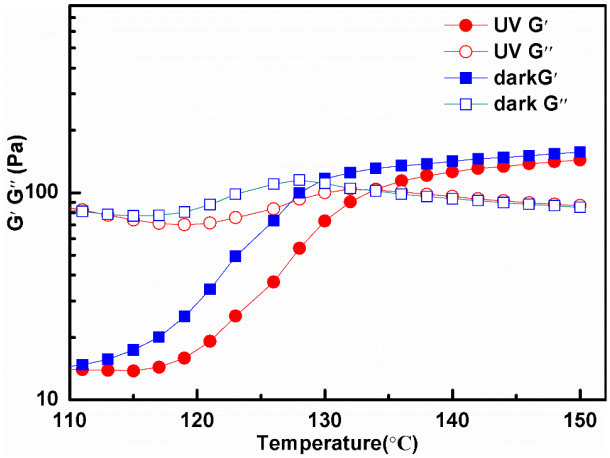

Figure 6. Temperature dependence of the dynamic shear moduli (G' and G'') and SAXS for 20 wt% BMB triblock copolymers in the mixed IL (w = 1 rad/s, g = 1%). The weight ratio of [Azo][NTf_2] / [C_1mim][NTf_2] is 5/95.

The rheology measurement was also conducted under UV irradiation, a much more higher gelation temperature was observed at 134.1 ℃ while T_g is 128.4 ℃ in the dark as shown in **Figure 6**. Clearly, the temperature for starting aggregation in *cis*-ILs as 6 ℃ higher than that in *trans*-ILs due to the improved affinity by *cis*-ILs to

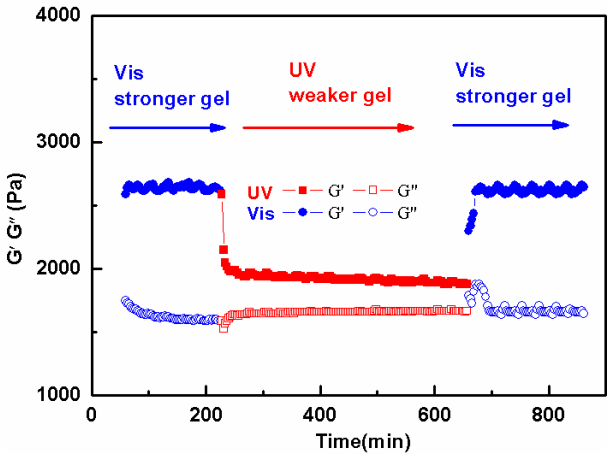

Figure 7. Photoinduced self-assembly of 30 wt% BMB in the ionic liquid mixture at 128 ℃ by illuminations of Vis-UV-Vis. And the weight ratio of [Azo][NTf_2]/[C_1mim][NTf_2] was 10/90.

PBnMA. At a higher temperature, above 140 ºC, the value of G′ in *trans*- and *cis*-IL are similar because *cis*-azobenzene cannot survive even with a higher UV intensity.

The photo controllable gelation behavior dependent on light was demonstrated in **Figure 7**. Due to azobenzene isomerization is extremely sensitive to the light from the circumstance at a higher temperature, a higher UV intensity light was used. Here we demonstrated a photo controllable stronger/weaker gel transitions based on an azobenzene ionic liquid. As is seen in **Figure 7,** G′ and G" responded to UV source very fast in 3 minutes with the sudden decreasing values and again reformed the stronger gel in 20 minutes upon visible light. Herein, such a desired responsive speed is obtained, perhaps due to the higher aggregation temperature compared with glass temperatures. The operation temperature (128 ºC) is far away from glass temperature of PBnMA (38 ºC), and PMMA. Therefore, the block polymers either in cores or shells perhaps are possible to reconstruct the polymer architecture switched by ILs. Also, higher molecular weights of PBnMA segments in the cores could be retained at such a higher temperature perhaps, even in *cis*-IL[13]. Another possible reason is the swelling of the cores tuned by affinity change between polymers and IL mixtures. Much more detailed research should be studied in future.

5.4 Small-angle X-ray scattering experiments

Small-angle X-ray scattering experiments were performed on the 20% sample using Anton Parr SAXSess mc^2 instrument. The capillary was purchased from TOHO and the diameter is 1.5mm. The sample was flam-sealed before conducting measurements under vacuum on a TCS120 sample holder with a precise temperature control from -30 to 120 ºC.

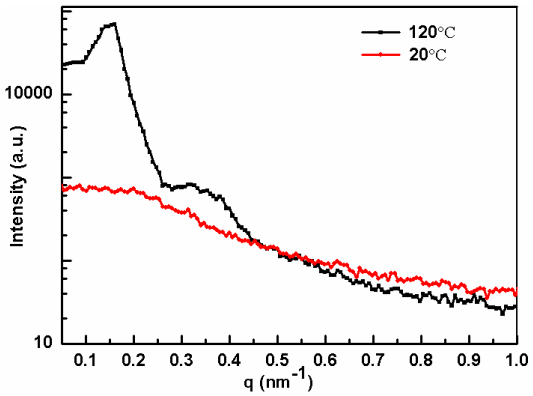

Figure 8. SAXS data of 20 wt% BMB in the ionic liquid mixture at 20 and 120 ºC on heating process. And the weight ratio of [Azo][NTf_2]/[C_1mim][NTf_2] was 5/95.

We have conducted small-angle X-ray scattering (SAXS) experiments for the ion gel containing 20 wt% BMB in ionic liquid mixture. **Figure 8** shows SAXS data of 20 wt% BMB/ILs composites at 120ºC. The 20 wt% BMB solution showed a distinct first form factor minimum at q = 0.28 nm^{-1}. The PBnMA core radius (R_c) can be calculated as 15.8 nm from the relationship of $qR_c = 4.49$ for hard spheres [14-16]. The aggregation number (N_{agg}) of 378 was estimated from the R_c and the density of PBnMA, ρ is1.179 g/cm^3. But this value suggests the cores are swollen by ionic liquid [17]. The peaks suggest the PBnMA sphere aggregations were packed as face-centered cubic structure [18-22]. We can also estimate the average distance between two neighboring PBnMA domains is 31.5 nm by assuming the formation of simple cubic lattice ($d = 2\pi/q^*$) from the first Bragg peak maximum. The value is reasonable judging from R_h and R_c of BMB micelle (70 nm from dynamic light scattering measurements). The structure of BMB is less compact than the PMP systems, perhaps higher LCST temperature over the glass temperature, resulting rubbery cores.

5.5 Conclusions

Poly(benzyl methacrylate)-b-poly(methyl methacrylate)-b-poly(benzyl methacrylate) (BMB) was designed and synthesized via well-established ATRP using poly(methyl methacrylate) (PMMA) as a macroinitiator, where the A blocks are LCST segment, PBnMA, while B midblock is PMMA, totally compatible with the ionic liquid mixtures. In a diluted polymer solution, the hydrodynamic radius R_h value is below 10 nm, unimer state, in consistent with individual BMB polymer chain with a total molecular weight around 10 kDa at lower temperatures. But R_h increases significantly in *trans*-ILs at 110 ºC, suggesting that the BMB triblock copolymer self-assembles into micelles with PBnMA cores surrounded. Similar behavior has been observed in *cis*-ILs and micellization temperature (120 ºC) is higher than 110 ºC in *trans*-ILs. In this the temperature range, photoinduced micellization occurred owing that aggregating behaviors of the A blocks dependent on photoisomerization of azobenzene IL. At a modest concentration of polymer solutions, the A blocks associate into micellar cross-linkers, and the B blocks provide bridging connections between micelles, forming a polymeric network. Meanwhile, two different gelation temperatures based on isomerization of azobenzene ILs were obtained and in this temperature range, so was the photoinduced gelation transitions. It is noticeable that photoresponsive behavior is just opposite to the PMP polymer system, while the only difference in two systems is just a small structural difference,

alkyl chain length between esters and aromatic rings (n=1 or 2).

5.6 References

[1] Shusharina N P, Nyrkova I A, Khokhlov A R. *Macromolecules* **1996**, 29, 3167.
[2] Mazer N A, Carey M C, Kwasnick R F, et al. *Biochemistry* **1979**, 18,3064.
[3] Maitra A. *J. Phys. Chem.* **1984**, 88, 5122.
[4] Kumbhakar M, Nath S, Mukherjee T, et al. *J. Chem. Phys.* **2004**, 121, 6026.
[5] Nagarajan R, Ganesh K. *J. Chem. Phys.* **1989**, 90, 5843.
[6] He Y, Lodge T P. *Chem. Commun.* **2007**, 26, 2732.
[7] He Y, Boswell P G, Bühlmann P, et al. *J. Phys. Chem. B.* **2007**, 111, 4645.
[8] He Y, Lodge T P. *Macromolecules* **2008**, 41, 167.
[9] Lei Y, Lodge T P. *Soft Matter*. **2012**, 8, 2110.
[10] Ueno K, Inaba A, Ueki T, et al. *Langmuir* **2010**, 26, 18031.
[11] Ma X, Usui R, Kitazawa Y, et al. *Polymer* **2015**, 78, 42.
[12] Chang R, An H, Li X, et al. *Poly.Chem.* **2017**, 8, 1263.
[13] Imaizumi S, Kokubo H, Watanabe M. Macromolecules, **2011**, 45, 401.
[14] Liu Y, Nie H, Bansil R, et al. *Physical Review E* **2006**, 73, 061803.
[15] Laurati M, Stellbrink J, Lund R, et al. *Physical Review E* **2007**, 76, 041503.
[16] Boon N, Schurtenberger P. *Phys. Chem. Chem. Phys.* **2017**. DOI: 10.1039/C7CP02434G.
[17] Kitazawa Y, Ueki T, McIntosh L D, et al. *Macromolecules* **2016**, 49, 1414.
[18] Daniel C, Hamley I W, Mingvanish W, et al. *Macromolecules* **2000**, 33, 2163.
[19] Hamley I W, Pople J A, Diat O. *Colloid Polym. Sci.* **1998**, 276, 446.
[20] Hamley I W, Pople J A, Fairclough J P A, et al. *J. Chem. Phys.* **1998**, 108, 6929.
[21] Hamley I W, Mortensen K, Yu G E, et al. *Macromolecules* **1998**, 31, 6958.
[22] Huang Y, Chen H L, Hashimoto T. *Macromolecules* **2003**, 36, 764.

Chapter Six

Concluding remarks and future directions

6 Concluding remarks and future directions

In this paper, we developed a novel photo/thermal responsive system based on photoswitchable ionic liquid rather than azobenzene-based polymer. Aazobenzene ionic liquid newly synthesized by covalently connecting to common imidazolium cation as a molecular trigger can drive the self-assembling of LCST polymers, resulting photoinduced unimer-micelle and sol-gel transitions. It is discovered that tiny modification of the polymer structure can impart the photoresponsive LCST behaviors, that is PBnMA shows a lower clouding temperature in *trans*-ILs while PPhEtMA with a longer alkyl chain length between ester and benzyl ring shows a lower clouding temperature in *cis*-ILs. Such a small structural difference can induce opposite photoresponsive behaviors. Through NMR measurement, two different chemical shifts of [C_1mim] cation under UV irradiation were obtained, indicated a photoresponsive solvation interaction. It is assumed that polarity change by isomerization of azobenzene influences the affinity between ILs and polymers. *Cis*-ILs prefer to interact with PBnMA rather than PPhEtMA, while *trans*-ILs prefers PPhEtMA (IL-phobic) owing to the IL-phobic according to "*like dissolve like*" theory.

By further being introducing these LCST polymers into ABA triblock copolymers as endblocks, LCST segments can attribute to theromoresponsive *unimer-micelle* and *sol-gel* transitions in common ILs. Photoresponsive *unimer-micelle* and *sol-gel* transitions were achieved by adding small amount of azobenzene ionic liquid. By SAXS measurements, we have investigated the morphology of both polymers in ionic liquid mixtures and both polymer solutions shows faced-centered cubic morphology when LCST occurred.

Currently, light as an external stimulus to process materials has been evoke intense interest, for its contactless manner, less toxic, precise control and environment friendly. Reported light processing materials are mainly directly based on photochromic reactions of azobenzene compounds, such as photoswitchable glass temperature transitions. Herein, a new concept to make material soft or hard was proposed in the research, that is, photoresponsive ionic liquid as a solvent can trigger the self-assembly of thermoresponsive triblock copolymers. This novel method is supposed to be suitable for the other thermoresponsive polymer systems either in ionic liquids or aqueous phase or other organic solutions. Meanwhile, due to a very limited amount of azobenzene ionic liquid addition, it gives rise to process a much

thicker film regarding the intrinsic property of light absorption from azobenzene.

In polymer science, it offers a novel method that using functionalized ionic liquids at the molecular level can trigger a macroscopic response with a mechanically tunable gelation process. Also, azobenzene ionic liquid worked as a molecular machine, “a nanoswitch” can induce different self-assembling behaviors of the polymer based on a small difference, which makes the system much more interesting.

Publish lists

1. **Caihong Wang**, Kei Hashimoto, Jiaheng Zhang, Yumi Kobayashi, Hisashi Kokubo, Masayoshi Watanabe. Micellization/demicellization self-assembly change of ABA triblock copolymers induced by a photoswitchable ionic liquid with a small molecular trigger. Macromolecules, **2017**, 50, 5377.

2. **Caihong Wang**, Xiaofeng Ma, Yuzo Kitazawa, Yumi Kobayashi, Shiguo Zhang, Hisashi Kokubo, Masayoshi Watanabe. From Macromolecular to Small-Molecular Triggers: Facile Method toward Photoinduced LCST Phase Behavior of Thermoresponsive Polymers in Mixed Ionic Liquids Containing an Azobenzene Moiety. *Macromol. Rapid Commun*. **2016**, 37, 1960.